



MOSCOW CENTER
FOR DIAGNOSTICS & TELEMEDICINE

ISSN 2712-8490 (Print)
ISSN 2712-8962 (Online)

DIGITAL DIAGNOSTICS

A peer-reviewed scientific medical journal

3 Volume 2 Issue



2022



ECO • VECTOR

<https://journals.eco-vector.com/DD>

УЧРЕДИТЕЛИ

- ГБУЗ «Научно-практический клинический центр диагностики и телемедицинских технологий ДЗМ»
- ООО «Эко-Вектор»

Свидетельство о регистрации СМИ ПИ
№ ФС 77 - 74099 от 19.10.2018.

ИЗДАТЕЛЬ

ООО «Эко-Вектор»

Адрес: 191186, г. Санкт-Петербург,
Аптекарский переулок, д. 3, литера А,
помещение 1Н
E-mail: info@eco-vector.com
WEB: <https://eco-vector.com>

РЕКЛАМА

Отдел рекламы
Тел.: +7 495 308 83 89
E-mail: adv@eco-vector.com

РЕДАКЦИЯ

Зав. редакцией

Елена Андреевна Филиппова
E-mail: ddjournal@eco-vector.com
Тел: +7 (965) 012 70 72
Адрес: 127051, г. Москва, ул. Петровка,
д. 24, стр. 1

ПОДПИСКА

Подписка на печатную версию через
интернет:
www.journals.eco-vector.com/
www.akc.ru
www.pressa-rf.ru

OPEN ACCESS

В электронном виде журнал
распространяется бесплатно —
в режиме немедленного открытого доступа

ИНДЕКСАЦИЯ

- РИНЦ
- Google Scholar
- Ulrich's International Periodicals Directory
- WorldCat

Оригинал-макет

подготовлен в издательстве «Эко-Вектор».
Литературный редактор: *М.Н. Шошина*
Корректор: *М.Н. Шошина*
Вёрстка: *Ф.А. Игнащенко*
Обложка: *Е.Д. Бугаенко*

Сдано в набор 07.07.2022.
Подписано в печать 13.07.2022. Формат 60 × 88%.
Печать офсетная. Печ. л. 8,75. Усл. печ. л. 8,14.
Уч.-изд. л. 4,8. Тираж 5000 экз. Заказ № 2-4661-IV.
Цена свободная.

Отпечатано в ООО «Типография Фурсова».
196105, Санкт-Петербург, ул. Благодатная, 69.
Тел.: +7 (812) 646-33-77



© ООО «Эко-Вектор», 2022

ISSN 2712-8490 (Print)
ISSN 2712-8962 (Online)

Digital Diagnostics

Том 3 | Выпуск 2 | 2022

ЕЖЕКВАРТАЛЬНЫЙ РЕЦЕНЗИРУЕМЫЙ НАУЧНЫЙ
МЕДИЦИНСКИЙ ЖУРНАЛ

Главный редактор

Синицын Валентин Евгеньевич, д.м.н., профессор (Москва, Россия)
ORCID: 0000-0002-5649-2193

Заместитель главного редактора

Юрий Александрович Васильев, к.м.н., (Москва, Россия)
ORCID: 0000-0002-0208-5218

Научный редактор

Березовская Татьяна Павловна, д.м.н., профессор (Обнинск, Россия)
ORCID: 0000-0002-3549-4499

Редакционная коллегия

Андрейченко А.Е., к.ф.-м.н. (Москва, Россия)
ORCID: 0000-0001-6359-0763
Berlin L., профессор (Иллинойс, США)
ORCID: 0000-0002-0717-0307
Беляев М.Г., к.ф.-м.н. (Москва, Россия)
ORCID: 0000-0001-9906-6453
Bisdas S., MBBS, MD, PhD (Лондон, Великобритания)
ORCID: 0000-0001-9930-5549
Гомболевский В.А., к.м.н. (Москва, Россия)
ORCID: 0000-0003-1816-1315
Frija G., профессор (Париж, Франция)
ORCID: 0000-0003-0415-0586
Guglielmi G., MD, профессор (Фоджа, Италия)
ORCID: 0000-0002-4325-8330
Holodny A., д.м.н. (Нью-Йорк, США)
ORCID: 0000-0002-1159-2705
Li H., MD, профессор (Пекин, КНР)
Кульберг Н.С., к.ф.-м.н., (Москва, Россия)
ORCID: 0000-0001-7046-7157
Mannelli L., MD (Нью-Йорк, США)
ORCID: 0000-0002-9102-4176
Мокиенко О.А., к.м.н. (Москва, Россия)
ORCID: 0000-0002-7826-5135
Морозов С.П., д.м.н., профессор (Москва, Россия)
ORCID: 0000-0001-6545-6170
Neri E., д.м.н. (Пиза, Италия)
ORCID: 0000-0001-7950-4559
Van Ooijen P., к.м.н. (Гронинген, Нидерланды)
ORCID: 0000-0002-8995-1210
Oudkerk M., профессор (Гронинген, Нидерланды)
ORCID: 0000-0003-2800-4110
Ros P.R., MD, MPH, PhD, профессор (Нью-Йорк, США)
ORCID: 0000-0003-3974-0797
Rovira A., профессор (Барселона, Испания)
ORCID: 0000-0002-2132-6750
Решетников Р.В., к.ф.-м.н., (Москва, Россия)
ORCID: 0000-0002-9661-0254
Румянцев П.О., д.м.н. (Москва, Россия)
ORCID: 0000-0002-7721-634X

Редакционный совет

Аншелес А.А., д.м.н. (Москва, Россия)
ORCID: 0000-0002-2675-3276
Арутюнов Г.П., д.м.н. (Москва, Россия)
ORCID: 0000-0002-6645-2515
Белевский А.С., д.м.н., профессор (Москва, Россия)
ORCID: 0000-0001-6050-724X
Васильева Е.Ю., д.м.н., профессор (Москва, Россия)
ORCID: 0000-0003-4111-0874
Гехт А.Б., д.м.н., профессор (Москва, Россия)
ORCID: 0000-0002-1170-6127
Кобякова О.С., д.м.н., профессор (Москва, Россия)
ORCID: 0000-0003-0098-1403
Кремнева Е.И., к.м.н. (Москва, Россия)
ORCID: 0000-0001-9396-6063
Петриков С.С., д.м.н., профессор (Москва, Россия)
ORCID: 0000-0003-3292-8789
Проценко Д.Н., к.м.н. (Москва, Россия)
ORCID: 0000-0002-5166-3280
Хатьков И.Е., д.м.н., профессор (Москва, Россия)
ORCID: 0000-0002-4088-8118

Редакция не несет ответственности за содержание рекламных материалов.
Точка зрения авторов может не совпадать с мнением редакции. К публикации
принимаются только статьи, подготовленные в соответствии с правилами для
авторов. Направляя статью в редакцию, авторы принимают условия договора
публикации. С правилами для авторов и договором публикации можно ознакомиться на сайте: <https://journals.eco-vector.com/DD/>. Полное
или частичное воспроизведение материалов, опубликованных в журнале,
допускается только с письменного разрешения издателя — издательства
«Эко-Вектор».



FOUNDERS

- Moscow Center for Diagnostics and Telemedicine
- Eco-Vector

PUBLISHER

Eco-Vector

Address: 3 liter A, 1H, Aptekarsky pereulok,
191186, Saint Petersburg Russian Federation
E-mail: info@eco-vector.com
WEB: <https://eco-vector.com>

ADVERTISE

Adv. department

Phone: +7 (495) 308 83 89
E-mail: adv@eco-vector.com

EDITORIAL

Executive editor

Elena A. Philippova
E-mail: ddjournal@eco-vector.com
Phone: +7 (965) 012 70 72

SUBSCRIPTION

For print version:
www.journals.eco-vector.com/

PUBLICATION ETHICS

Journal's ethic policies are based on:

- ICMJE
- COPE
- ORE
- CSE
- EASE

OPEN ACCESS

Immediate Open Access is mandatory for all published articles

INDEXATION

- Russian Science Citation Index
- Google Scholar
- Ulrich's International Periodicals Directory
- WorldCat

TYPESET

complete in Eco-Vector
Copyeditor: *M.N. Shoshina*
Proofreader: *M.N. Shoshina*
Layout editor: *Ph. Ignashchenko*
Cover: *E. Bugaenko*



© Eco-Vector, 2022

ISSN 2712-8490 (Print)
ISSN 2712-8962 (Online)

Digital Diagnostics

Volume 3 | Issue 2 | 2022

QUARTERLY PEER-REVIEW MEDICAL JOURNAL

EDITOR-IN-CHIEF

Valentin E. Sinitsyn, MD, Dr.Sci. (Med), Professor (Moscow, Russia)
ORCID: 0000-0002-5649-2193

DEPUTY EDITOR-IN-CHIEF

Yurii A. Vasilev, MD, Cand.Sci. (Med) (Moscow, Russia)
ORCID: 0000-0002-0208-5218

SCIENTIFIC EDITOR

Tatiana P. Berezovskaya MD, Dr.Sci. (Med.), Professor (Obninsk, Russia)
ORCID: 0000-0002-3549-4499

EDITORIAL BOARD

A.E. Andreychenko, PhD (Moscow, Russia)
ORCID: 0000-0001-6359-0763
L. Berlin, Professor (Illinois, United States)
ORCID: 0000-0002-0717-0307
M.G. Belyaev, Cand.Sci. (Phys-Math), Assistant Professor (Moscow, Russia)
ORCID: 0000-0001-9906-6453
S. Bisdas, MBBS, MD, PhD (London, United Kingdom)
ORCID: 0000-0001-9930-5549
V.A. Gomboleviskiy, MD, Dr.Sci. (Med) (Moscow, Russia)
ORCID: 0000-0003-1816-1315
G. Frija, Professor (Paris, France)
ORCID: 0000-0003-0415-0586
G. Guglielmi, MD, Professor (Foggia, Italy)
ORCID: 0000-0002-4325-8330
A. Holodny, MD (New-York, United States)
ORCID: 0000-0002-1159-2705
H. Li, MD, Professor (Beijing, China)
N.S. Kul'berg, Cand.Sci. (Phys-Math) (Moscow, Russia)
ORCID: 0000-0001-7046-7157
L. Mannelli, MD (New-York, United States)
ORCID: 0000-0002-9102-4176
O.A. Mokienco, MD, Cand.Sci. (Med) (Moscow, Russia)
ORCID: 0000-0002-7826-5135
S.P. Morozov, MD, Dr.Sci. (Med), Professor (Moscow, Russia)
ORCID: 0000-0001-6545-6170
E. Neri, MD, Associate Professor (Pisa, Italy)
ORCID: 0000-0001-7950-4559
P. van Ooijen, PhD, Assoc. Professor (Groningen, Netherlands)
ORCID: 0000-0002-8995-1210
M. Oudkerk, Professor (Groningen, Netherlands)
ORCID: 0000-0003-2800-4110
P.R. Ros, MD, MPH, PhD, Professor (New-York, United States)
ORCID: 0000-0003-3974-0797
A. Rovira, Professor (Barcelona, Spain)
ORCID: 0000-0002-2132-6750
R.V. Reshetnikov, Cand.Sci. (Phys-Math) (Moscow, Russia)
ORCID: 0000-0002-9661-0254
P.O. Romyantsev, MD, Dr.Sci. (Med) (Moscow, Russia)
ORCID: 0000-0002-7721-634X

EDITORIAL COUNCIL

A.A. Ansheles, MD, Dr.Sci. (Med) (Moscow, Russia)
ORCID: 0000-0002-2675-3276
G.P. Arutyunov, MD, Dr.Sci. (Med) (Moscow, Russia)
ORCID: 0000-0002-6645-2515
A.S. Belevskiy, MD, Dr.Sci. (Med), Professor (Moscow, Russia)
ORCID: 0000-0001-6050-724X
E.Y. Vasilieva, MD, Dr.Sci. (Med), Professor (Moscow, Russia)
ORCID: 0000-0003-4111-0874
A.B. Gekht, MD, Dr.Sci. (Med), Professor (Moscow, Russia)
ORCID: 0000-0002-1170-6127
O.S. Kobayakova, MD, Dr.Sci. (Med), Professor (Moscow, Russia)
ORCID: 0000-0003-0098-1403
E.I. Kremneva, MD, Cand.Sci. (Med) (Moscow, Russia)
ORCID: 0000-0001-9396-6063
S.S. Petrikov, MD, Dr.Sci. (Med), Professor (Moscow, Russia)
ORCID: 0000-0003-3292-8789
D.N. Protzenko, MD, Cand.Sci. (Med) (Moscow, Russia)
ORCID: 0000-0002-5166-3280
I.E. Khatkov, MD, Dr.Sci. (Med), Professor (Moscow, Russia)
ORCID: 0000-0002-4088-8118

The editors are not responsible for the content of advertising materials. The point of view of the authors may not coincide with the opinion of the editors. Only articles prepared in accordance with the guidelines are accepted for publication. By sending the article to the editor, the authors accept the terms of the public offer agreement. The guidelines for authors and the public offer agreement can be found on the website: <https://journals.eco-vector.com/DD/>. Full or partial reproduction of materials published in the journal is allowed only with the written permission of the publisher — the Eco-Vector publishing house.



CONTENTS

ORIGINAL STUDY ARTICLES

Salvatore Masala, Adriano Lacchè, Chiara Zini, Domenico Mannatrizio, Stefano Marcia, Matteo Bellini, Giuseppe Guglielmi

Safety and efficacy of percutaneous vesselplasty (Vessel-X) in the treatment of symptomatic thoracolumbar vertebral fractures 98

Ivan A. Blokhin, Anna P. Gonchar, Maria R. Kodenko, Alexander V. Solovov, Victor A. Gombolevskiy, Roman V. Reshetnikov

Impact of body mass index on the reliability of the CT0–4 grading system: a comparison of computed tomography protocols 108

REVIEWS

Anastasiya V. Yusupova, Einar S. Yusupov

Left atrial longitudinal strain analysis in diagnostic of cardiotoxicity 119

TECHNICAL REPORTS

Kirill M. Arzamasov, Tatiana M. Bobrovskaya, Viktor A. Dragovoz

Streaming technology: from games to tele-ultrasound 131

CASE REPORTS

Domenico Mannatrizio, Giacomo Fascia, Giuseppe Guglielmi

“Superior Pectus Carinatum” (Currarino–Silverman Syndrome) in a 66-year-old woman: a case report 141

Pavel B. Gelezhe, Kristina M. Goryacheva

Computer tomography of uro-lymphatic fistulas associated with renal colic 149

LATTERS TO THE EDITOR

Olga I. Pchelintseva, Olga V. Omelyanskaya

Features of conducting ethical review of research on artificial intelligence systems on the basis of the research and practical clinical center for diagnostics and telemedicine technologies of the Moscow Health Care Department, Moscow, Russian Federation 156

СОДЕРЖАНИЕ

ОРИГИНАЛЬНЫЕ ИССЛЕДОВАНИЯ

S. Masala, A. Lacchè, Ch. Zini, D. Mannatrizio, S. Marcia, M. Bellini, G. Guglielmi

Безопасность и эффективность чрескожной сосудопластики с применением устройства Vessel-X при лечении симптоматичных переломов грудных и поясничных позвонков 98

И.А. Блохин, А.П. Гончар, М.Р. Коденко, А.В. Соловьев, В.А. Гомболевский, Р.В. Решетников

Влияние индекса массы тела на надёжность шкалы КТ 0–4: сравнение протоколов компьютерной томографии 108

НАУЧНЫЕ ОБЗОРЫ

А.В. Юсупова, Э.С. Юсупов

Оценка показателей глобальной продольной деформации левого предсердия в диагностике кардиотоксичности 119

ТЕХНИЧЕСКИЕ ОТЧЁТЫ

К.М. Арзамасов, Т.М. Бобровская, В.А. Дроговоз

Стриминговые технологии: из игровой индустрии в телеультразвуковые исследования 131

КЛИНИЧЕСКИЕ СЛУЧАИ

D. Mannatrizio, G. Fascia, G. Guglielmi

Килевидная деформация грудной клетки по «верхнему» типу (синдром Куррарино–Сильвермана): клинический случай 141

П.Б. Гележе, К.М. Горячева

Уролимфатические фистулы, выявленные по данным компьютерной томографии на фоне почечной колики 149

ПИСЬМА В РЕДАКЦИЮ

О.И. Пчелинцева, О.В. Омелянская

Об особенностях этической экспертизы в исследованиях с применением технологий и систем искусственного интеллекта на базе Государственного бюджетного учреждения здравоохранения города Москвы «Научно-практический клинический центр диагностики и телемедицинских технологий Департамента здравоохранения города Москвы» (ГБУЗ НПКЦ ДиТ ДЗМ). 156

DOI: <https://doi.org/10.17816/DD88685>

Безопасность и эффективность чрескожной сосудопластики с применением устройства Vessel-X при лечении симптоматических переломов грудных и поясничных позвонков

S. Masala¹, A. Lacchè¹, Ch. Zini², D. Mannatrizio³, S. Marcia⁴, M. Bellini⁵, G. Guglielmi⁶¹ Department of Diagnostic Imaging and Interventional Radiology, General Hospital, University of Rome, Рим, Италия² USL Tuscany centre: Azienda USL Toscana centro, Тоскана, Италия³ Department of Clinical and Experimental Medicine, Foggia University School of Medicine, Фоджа, Италия⁴ ASSL Cagliari, Radiology PO SS Trinità, Сардиния, Италия⁵ Policlinico Santa Maria alle Scotte: Azienda Ospedaliera Universitaria Senese, Италия⁶ University of Foggia, Фоджа, Италия

АННОТАЦИЯ

Цель — оценить результаты клинических и рентгенологических исследований в отношении безопасности и эффективности устройства Vessel-X (Dragon Crown Medical Co., Ltd Shandong, Китай), применяемого для лечения симптоматических переломов позвонков с повреждением и без повреждения задней стенки позвонка и/или обеих замыкательных пластинок.

Материалы и методы. Ретроспективно обследовано 66 пациентов, перенёсших 92 хирургических вмешательства в связи с симптоматическими переломами тел позвонков в период с 19 марта по сентябрь 2020 г. Все переломы были разделены на 2 подгруппы: сложные (36 переломов с повреждением задней стенки и/или обеих замыкательных пластинок позвонков) и простые (все остальные). Результаты лечения оценивали по числовой рейтинговой шкале (Numerical rating scale, NRS) и индексу нетрудоспособности Освестри (Oswestry disability index, ODI) за день до хирургического вмешательства и через 1, 6 и 12 мес наблюдения. Восстановление высоты позвонков также оценивали путём сравнения рентгенологических снимков до и после вмешательства.

Результаты. Всего пролечено 92 позвонка (58 поясничных и 34 грудных), в 24 случаях — с помощью многоуровневых процедур. Частота технического успеха составила 100%, выявлен лишь один случай бессимптомной паравертебральной утечки цемента. В обеих подгруппах отмечалась достоверная статистическая разница между показателями NRS и ODI в дооперационный период и через 1, 6 и 12 мес наблюдения ($p < 0,05$), а также в отношении высоты позвонков при сравнении данных до и после операции ($p < 0,05$). Достоверно значимой разницы в отношении восстановления высоты позвонков среди сложных и простых переломов не наблюдалось.

Заключение. Сосудопластика — безопасный и эффективный метод лечения простых и сложных болезненных переломов позвонков, обеспечивающий значительное уменьшение симптоматики, отличный контроль утечки цемента и надлежащее восстановление высоты позвонков.

Ключевые слова: сосудопластика; остеопластика; переломы позвонков; утечка цемента; восстановление высоты позвоночника.

Как цитировать

Masala S., Lacchè A., Zini Ch., Mannatrizio D., Marcia S., Bellini M., Guglielmi G. Безопасность и эффективность чрескожной сосудопластики с применением устройства Vessel-X при лечении симптоматических переломов грудных и поясничных позвонков // *Digital Diagnostics*. 2022. Т. 3, № 2. С. 98–107. DOI: <https://doi.org/10.17816/DD88685>

DOI: <https://doi.org/10.17816/DD88685>

Safety and efficacy of percutaneous vesselplasty (Vessel-X) in the treatment of symptomatic thoracolumbar vertebral fractures

Salvatore Masala¹, Adriano Lacchè¹, Chiara Zini², Domenico Mannatrizio³, Stefano Marcia⁴, Matteo Bellini⁵, Giuseppe Guglielmi⁶

¹ Department of Diagnostic Imaging and Interventional Radiology, General Hospital, University of Rome, Rome, Italy

² USL Tuscany centre: Azienda USL Toscana centro, Toscana, Italy

³ Department of Clinical and Experimental Medicine, Foggia University School of Medicine, Foggia, Italy

⁴ ASSL Cagliari, Radiology PO SS Trinità, Italy

⁵ Policlinico Santa Maria alle Scotte: Azienda Ospedaliera Universitaria Senese, Italy

⁶ University of Foggia, Foggia, Italy

ABSTRACT

AIMS: to assess radiological and clinical outcomes, in terms of safety and efficacy, of symptomatic vertebral fractures with and without posterior wall and/or both endplates involvement, treated with vesselplasty technique (Vessel-X, Dragon Crown Medical Co., Ltd Shandong, China).

MATERIALS AND METHODS: We retrospectively evaluated 66 patients who underwent 92 vesselplasty procedures, performed for the treatment of symptomatic vertebral body fractures from March 19 to September 2020. We divided the fractures in two subgroups: 36 vertebral fractures with posterior wall and/or both endplates involvement, which we defined complex, while all the others were defined simple. Numerical Rating Scale (NRS) and Oswestry Disability Index (ODI) values has been registered 1 day before the procedure and at 1, 6 and 12 months follow-up. We also evaluated vertebral height restoration by comparing pre-interventional with post-interventional imaging.

RESULTS: 92 vertebrae were treated (58 lumbar, 34 thoracic), with 24 multilevel procedures. We observed a technical success rate of 100%, without major complications; a single case of asymptomatic paravertebral cement leak was reported. Both simple and complex subgroups registered a significative statistical difference in NRS and ODI between preoperative and at 1, 6 and 12 months ($p < 0.05$). A significant statistical difference was demonstrated in vertebral height comparing pre-operative and post-operative data ($p < 0.05$). No significant difference in vertebral height restoration was observed between simple and complex vertebral fractures groups.

CONCLUSIONS: Vesselplasty represents a safe and effective technique for the treatment of both simple and complex painful vertebral fractures, granting a significant reduction of symptoms, excellent cement leakage control and proper vertebral height restoration.

Keywords: vesselplasty; osteoplasty; vertebral fractures; cement leakage; vertebral height restoration.

To cite this article

Masala S, Lacchè A, Zini Ch, Mannatrizio D, Marcia S, Bellini M, Guglielmi G. Safety and efficacy of percutaneous vesselplasty (Vessel-X) in the treatment of symptomatic thoracolumbar vertebral fractures. *Digital Diagnostics*. 2022;3(2):98–107. DOI: <https://doi.org/10.17816/DD88685>

Received: 18.11.2021

Accepted: 10.05.2022

Published: 21.06.2022

DOI: <https://doi.org/10.17816/DD88685>

使用Vessel-X设备进行经皮血管成形术治疗有症状的胸腰椎骨折的安全性和有效性

Salvatore Masala¹, Adriano Lacchè¹, Chiara Zini², Domenico Mannatrizio³, Stefano Marcia⁴, Matteo Bellini⁵, Giuseppe Guglielmi⁶

¹ Department of Diagnostic Imaging and Interventional Radiology, General Hospital, University of Rome, Rome, Italy

² USL Tuscany centre: Azienda USL Toscana centro, Toscana, Italy

³ Department of Clinical and Experimental Medicine, Foggia University School of Medicine, Foggia, Italy

⁴ ASSL Cagliari, Radiology PO SS Trinità, Italy

⁵ Policlinico Santa Maria alle Scotte: Azienda Ospedaliera Universitaria Senese, Italy

⁶ University of Foggia, Foggia, Italy

简评

目的。评估有关Vessel-X设备（中国山东冠龙医疗用品有限公司）安全性和有效性的临床和放射学研究结果，该设备用于治疗有和没有椎体后壁和/或两个终板损伤的症状性脊椎骨折。

材料与方法。对2020年3月19日至9月期间因症状性椎体骨折而接受92次手术干预的共66名患者进行了回顾性检查。所有骨折均分为2个亚组：“复杂”（36处骨折，后壁和/或椎骨的两个终板受损）和“简单”（所有其他）。

在手术前一天和随访1、6和12个月后，使用数字评分量表(NRS)和Oswestry功能障碍指数(ODI)评估治疗结果。椎体高度恢复(VHR)也是通过比较干预前后的X光片来评估的。

结果。共有92块椎骨（58块腰椎和34块胸椎）使用24次多级手术进行了治疗。技术成功率为100%，仅发现无症状椎旁骨水泥渗漏1例。在两个亚组中，术前和随访1、6和12个月后NRS和ODI之间存在可靠的统计差异（ $p < 0.05$ ），在比较手术前后的数据时，椎体高度也是如此（ $p < 0.05$ ）。复杂骨折与单纯骨折的椎体高度恢复差异无统计学意义。

结论。血管成形术是治疗简单和复杂疼痛性椎体骨折的一种安全有效的治疗方法，可以明显减轻症状，确保良好的骨水泥渗漏的控制，并适当恢复椎体高度。

关键词：血管成形术；骨整形术；椎骨骨折；水泥泄漏；恢复脊柱高度。

To cite this article

Masala S, Lacchè A, Zini Ch, Mannatrizio D, Marcia S, Bellini M, Guglielmi G. 使用Vessel-X设备进行经皮血管成形术治疗有症状的胸腰椎骨折的安全性和有效性. *Digital Diagnostics*. 2022;3(2):98–107. DOI: <https://doi.org/10.17816/DD88685>

收到: 18.11.2021

接受: 10.05.2022

发布日期: 21.06.2022

INTRODUCTION

In the last decades, a significant increase has been observed in the number of vertebral augmentation procedures (VAP) for the treatment of vertebral fractures (VFs), with the development of more advanced techniques. All these interventions cause excellent results, with reduced complication rates and a better cost–benefit ratio compared to open surgical procedures [1–3].

The VAP term comprises several treatment options that can be subdivided into simple percutaneous vertebroplasty (PVP), percutaneous kyphoplasty (PKP), and percutaneous implant techniques (PIT) [4], which all aim to reduce and possibly eliminate pain symptoms by fracture consolidation and, whenever is possible, to restore parapsychological vertebral body height (VBH) by injecting bone-filling material (BFM) under image guidance [4].

Although BFM injection is thoroughly monitored via fluoroscopy imaging, it can leak outside the vertebrae into the adjacent spaces in 7%–30% of VAPs [5–7].

A correlation between high volume injections of BFM and its leakage has been demonstrated; the presence of cortical bone defects of the vertebra represents an additional risk factor for the occurrence of this complication. Moreover, to prevent an undesired BFM leakage in the epidural space with potentially serious complications, several studies excluded patients with posterior wall defects [8].

Many devices have been developed during the last years to reduce the incidence of this complication; therefore, our retrospective study aimed to share our experiences in using the vesselplasty technique (Vessel-X, Dragon Crown Medical Co., Ltd Shandong, China), a dedicated PIT with a container made of polyethylene terephthalate (PET), a non-stretchable material with 100- μ m porosity, to restore the VBH and prevent BFM leakage. Furthermore, when the pressure inside the container is greater than the surrounding resistance, BFM starts to interdigitate through the pores equally in all directions, without concentrating in the locus of minor resistance of the vertebral body (Fig. 1).

METHODS AND MATERIALS

Study design

A retrospective single-center study on a relatively small sample size.

Patients

In our study, 66 patients (16 males and 50 females, with a mean age of 73.1 year) with 92 painful dorsolumbar vertebral body fractures who were resistant to conservative management were included in the study; among them, 56 were associated with severe osteoporosis, 4 with multiple myeloma, 2 with metastatic breast cancer, and 4 were traumatic.

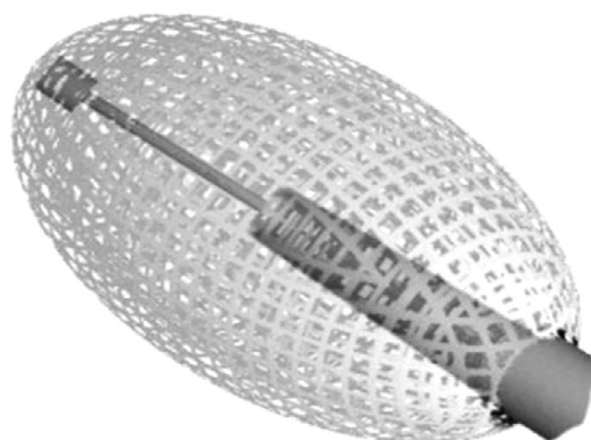


Fig. 1. Vessel-X device, made of a mesh of Polyethylene Terephthalate (PET), a non-stretchable material that has a porosity of 100- μ m.

Patients with active infection, a fracture, or an abnormal vertebral body that is not causing pain or clinical problem; with very old fractures, coagulopathy, spinal cord or nerve impingement causing radicular pain, osteoblastic metastasis, and bone metastasis that extended to the epidural space; and who already underwent other VAP were excluded.

Patients with endplate interruption and/or posterior wall defect documented with magnetic resonance (MR) and/or computed tomography (CT) were classified to the “complex” subgroup, which had VFs related to osteoporosis (N = 19), traumatic fracture (N = 3), multiple myeloma (N = 2), and metastatic breast cancer (N = 2).

A total of 24 patients underwent a multilevel procedure in the same intervention (3 levels, N = 2; 2 levels, N = 22).

The numerical rating scale (NRS) score and Oswestry disability index (ODI) have been evaluated 1 day before the procedure and at 1, 6, and 12 months after.

MRI follow-up was performed at 1, 6, and 12 months, whereas CT was performed at 1 and 12 months post-intervention.

Imaging analysis

Preoperative VBH was obtained by measuring anterior, central, and posterior heights with MRI and/or CT; postoperative VBH was calculated immediately after the Vessel-X implantation with fluoroscopic images and at 1, 6, and 12 months post-intervention with MRI and at 1 and 12 months with CT.

Vertebral height restoration (VHR) was calculated by measuring the difference between pre- and postoperative height, with control measurement of the adjacent untreated vertebral bodies as a reference.

Procedure

Procedures have been performed in our dedicated angiosuite under local anesthesia and ongoing antibiotic prophylaxis based on CIRSE guidelines [4].

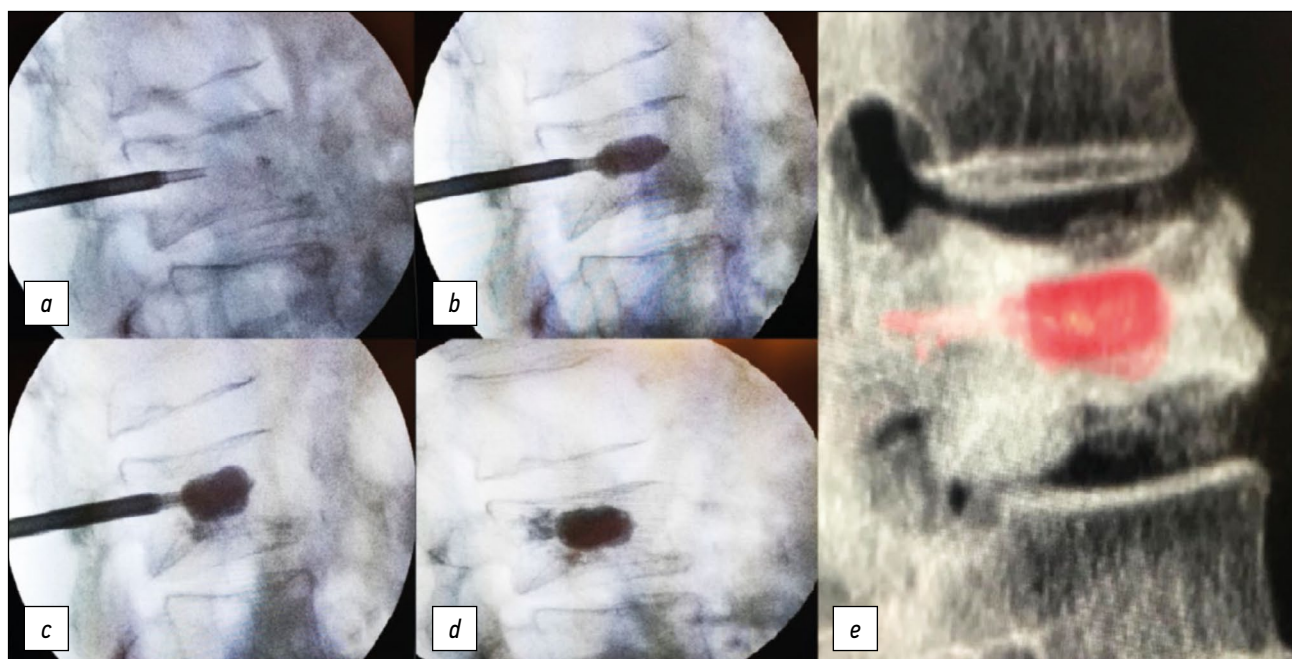


Fig. 2. (a–d): Intraoperative positioning of Vessel-X device. BMF starts to spread out of the PET container only after it reached its maximum size. (e): VR reconstruction of Vessel-X.

The patient was placed in the prone position, and, under fluoroscopic guidance, the target vertebra was centered and the arc rotated to display the chosen transpedicular path. Then, the trocar, a spinal needle of 8-G with a variable length of 90–150 mm was advanced until it reached the vertebral body.

The target position lies immediately after the posterior wall in lateral projection and toward the midline in A–P projection and at midway between the two endplates.

Vessel-X has two dimensions and we chose which one to use in the preoperative based on the vertebral size. Then, it was positioned and filled with BFM (mean quantity = 3.3 ± 0.8 mL/vertebra). BFM is a high viscosity acrylic-based radiopaque bone cement.

After injecting BFM, Vessel-X loses its tubular shape in favor of a cylindrical conformation until a predefined size is reached.

The BFM maximum pressure inside the container, before it starts to spread outside, is associated with the relative resistance of the surrounding bone density, which is different between fresh and old fractures or young and osteoporotic bone. Once this pressure is reached, it starts to penetrate the micropores interdigitating between the trabecular spaces and stabilizing the container with the subsequent lifting of vertebral endplates.

Technical success was defined as the correct placement and implant of the Vessel-X (Fig. 2).

Ethical statement

Formal consent is not required for this type of study.

Statistical analysis

NRS and ODI were presented as descriptive statistics, such as the mean, standard deviation, median, and

interquartile range, before and at 1-, 6-, and 12-months follow-up.

To detect statistically significant changes in NRS and ODI in the post-treatment period and to compare the results with the pre-treatment period, both paired t-test and Wilcoxon matched-paired signed-rank test were used.

The null hypothesis of no difference between pre- and post-treatment was then assumed for each series of scores.

All analyses were performed using Matlab (The MathWorks Inc., Natick, MA, USA).

RESULTS

A total of 92 vertebrae have been treated (58 lumbar and 34 thoracic; range, D5–L5) using Vessel-X with a technical success rate of 100%.

The bipedicular approach was the preferred method at lumbar levels, whereas the monopedicular approach was performed in the thoracic vertebrae.

A multilevel procedure was performed in 24 patients (3 levels in 2; 2 levels in 22).

No major complication occurred; a single case of asymptomatic paravertebral leak in a L1 traumatic complex fracture without involving the spinal canal or nerve roots was observed in both MRI and CT control at 1 month.

No new fractures in the adjacent vertebral bodies were reported during the 12-month follow-up period.

In 10 patients with pathological and traumatic fractures, MRI scan at 6 and 12 months confirmed the absence of bone marrow edema in the target vertebra and the adjacent ones.

We observed a significant decrease in ODI values from a preoperative mean of 73.2 ± 7.9 to the mean values of

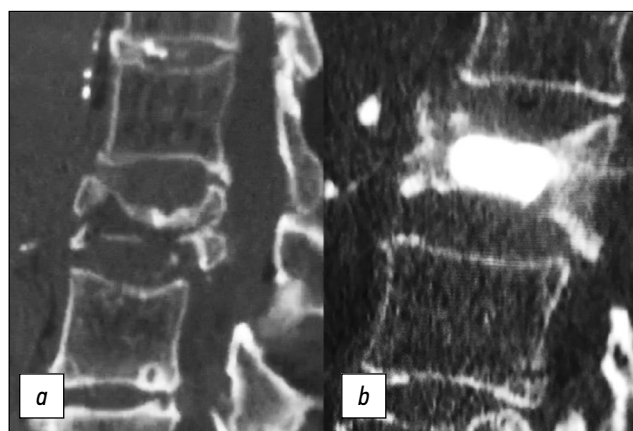


Fig. 3. (a): CT scan: Sagittal reconstruction of a complex vertebral fracture. (b): Post-operative CT control. Vessel-X is perfectly placed without BFM leakage.

14.1±3.3, 13.8±3.6, and 14.0±2.9 at 1-, 6-, and 12-months follow-up, respectively ($p < 0.05$) (Fig. 3).

The preoperative mean NRS of 7.3±1.2 dropped to 1.8±1.3, 2.1±0.8, and 1.7±1.0 at 1, 6, and 12 months ($p < 0.05$). (Fig. 4)

No statistically significant difference was observed in the two VF subgroups based on standard deviation.

The mean preoperative anterior VBH was 11.3±2.2 (range 7–15) mm and increased to 14.0±1.7 (range 10–19) mm at post-procedure ($p < 0.05$).

The mean preoperative central VBH was 11.9±2.5 (range 6–17) mm and increased to 16.1±1.8 mm at post-procedure ($p < 0.05$).

Mean preoperative posterior VBH was 16.4±2.5 (range 10–22) mm and increased to 19.5±1.6 (range 23–16) mm at post-procedure ($p < 0.05$).

No statistically significant differences were observed based on VHR between the simple and complex VF subgroups.

In VBs treated with bilateral access, the distribution of BFM was more homogeneous than in the monopedicular

approach. However, no difference was observed in VBH restoration between bipedicular and monopedicular groups.

DISCUSSION

One of the main complications of VAP is represented by undesired cement leakage outside the target vertebral body. A large meta-analysis conducted by Zhan Y. et al. showed an incidence rate of cement leakage of 54.7% and 18.4% for percutaneous vertebroplasty and percutaneous balloon kyphoplasty, respectively [9].

To reduce the risk of cement leakage, many devices have been developed including the Vessel-X. In our study, short-term follow-up results are promising; the complete technical success with just a single case of asymptomatic cement leakage (1.08%) indicates that vesselplasty is a safe and effective technique for VF treatment, including those with endplates and/or posterior wall interruption highly at risk for adverse events. No clinically significant side effects, infection, or neural damages were observed.

Additionally, intradiscal cement leak has been shown to increase the risk of subsequent new fractures of the adjacent vertebral bodies [10–16]; in our study, no intradiscal cement leak occurred and no subsequent fracture has been demonstrated at the 12-month follow-up. We believe this is related to Vessel-X properties of a controlled BFM distribution due to a homogeneous spread through its mesh pores, in contrast to other PIT devices in which the cement expansion privileges the weakest areas of the fracture, causing leakage [17, 18].

Beyond complication prevention, vesselplasty has shown excellent clinical results, supported by the significant reduction in NRS and ODI values during follow-up evaluations.

Bipedicular injection of BFM is reported to provide better results based on VB stiffness restoration, albeit no significant

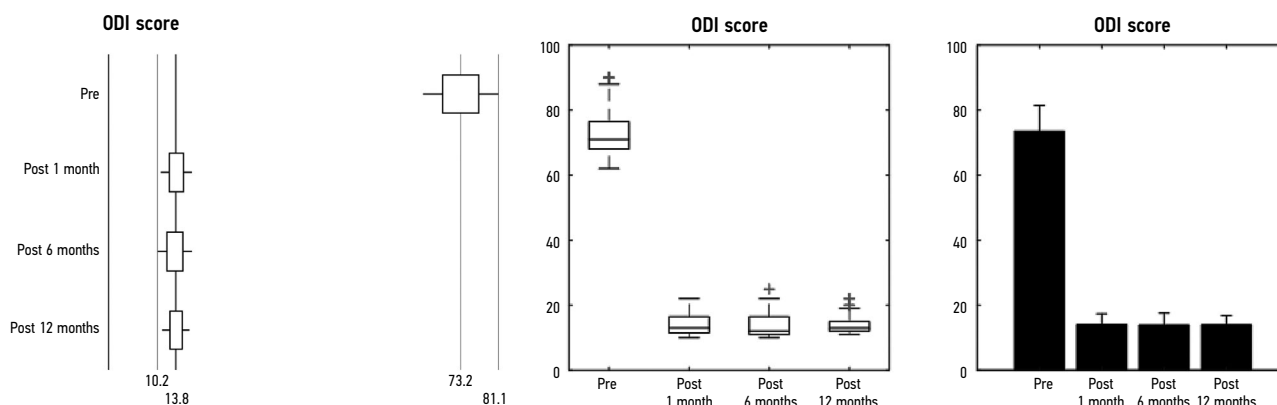


Fig. 4. The index is expressed in percentage points and ranges from 0% to 100%, with the lower limit related to the absence of disability and the upper limit to the maximum degree of disability (patients are bed-bound).

At pretreatment, the median ODI score was 78% (25th percentile, 70.5%; 75th percentile, 84%); no outliers were identified.

At 1 month post-treatment, the median ODI score was 14% (25th percentile, 12.7%; 75th percentile, 17%); no outliers were identified.

At 6 months post-procedure, the median ODI score was 13% (25th percentile, 12%; 75th percentile, 16%); no outliers were identified.

At 12 months post-procedure, the median ODI score was 13% (25th percentile, 12.4%; 75th percentile, 16%); no outliers were identified.

The mean ODI scores decreased from 73.2±7.9 to 14.1±3.3 at 1 month and 13.8±3.6 at 6 months ($p < 0.001$).

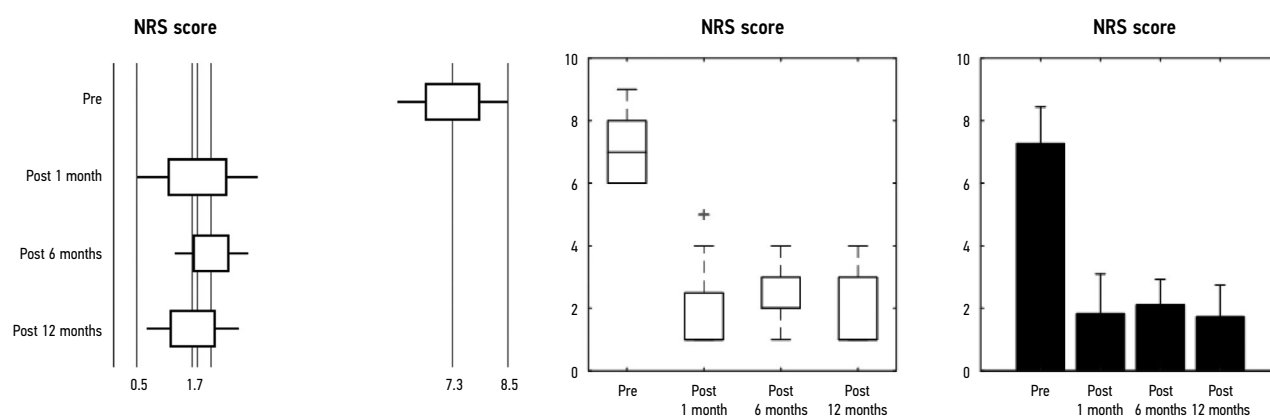


Fig. 5. At pretreatment, NRS scores were mostly concentrated on the upper limits of the scale (median, 8; 25th percentile, 7; and 75th percentile, 8). The distribution of NRS scores in the post-treatment survey at 1 month (median, 2; 25th percentile, 2; and 75th percentile, 3) at 6 months (median, 2; 25th percentile, 2; and 75th percentile, 3), and 12 months (median, 2; 25th percentile, 2; and 75th percentile, 3); no outlier was identified. The mean NRS score was 7.3 ± 1.2 at pre-procedure and decreased to 1.8 ± 1.3 at 1 month, 2.1 ± 0.8 at 6 months, and 1.7 ± 1.0 at 12 months ($p < 0.001$).

difference in VB strength, due to the greater volume of BFM applied and the symmetric distribution [18]. When possible, we opted for a monopedicular access at the thoracic level and a bipedicular for lumbar procedures, mainly for the higher axial load forces at this level, in which we believed that a greater quantity of BFM was required. As for VHR, no significant difference was observed between the two approaches.

Regarding VHR, stability at post-treatment represents an important target. Several studies have shown that after percutaneous kyphoplasty, an important reduction in VBH routinely occurs, probably due to an inhomogeneous BFM distribution. PKP procedure requires balloon inflation inside the VB and successive withdrawal to allow cement injection of cement, causing a partial collapse of the vertebral body, resulting in negative effects on height restoration [5,17,18].

Conversely, this event is more common in standard PVP when the fracture remains unstable. In this case, a new PVP intervention is advocated; however, it must be noted that the risk of undesired cement leakage is greatly increased [9, 19–22].

In our series, we did not observe any perceivable difference in VBH between the procedure final control and follow-up assessment, suggesting how the Vessel-X device offers good support for the fractured vertebral body preventing its collapse.

Furthermore, vesselplasty guarantees shorter exposure time to ionizing radiation, as for the first 2 mL of injected BFM, no fluoroscopic control is required. Then, a fluoroscopy examination is necessary for every 0.25 mL of BFM injected until the desired VBH is reached [17].

Limitations

Our study presents some limitations: it is a retrospective single-center study and on relatively small sample size.

However, our results are encouraging and, if confirmed, would allow patients with exclusion criteria like interrupted posterior wall to be treated.

CONCLUSION

Vesselplasty technique using Vessel-X may be considered an effective and safe option for the treatment of standard and complex VFs.

Due to its design, Vessel-X guarantees optimal control of BFM distribution with a reduced rate of cement leakage and shorter fluoroscopy time compared to PVP and PKP procedures.

Vessel-X has also shown good clinical results with a significant reduction of NRS and ODI values post-treatment.

However, to further validate these results, prospective randomized trials are necessary.

ADDITIONAL INFORMATION

Funding source. This study was not supported by any external sources of funding.

Competing interests. The authors declare that they have no competing interests.

Authors' contribution. All authors made a substantial contribution to the conception of the work, acquisition, analysis, interpretation of data for the work, drafting and revising the work, final approval of the version to be published and agree to be accountable for all aspects of the work. S. Masala — conception of the work, drafting and revising the work; A. Lacchè — acquisition, analysis, interpretation of data for the work; Ch. Zini — analysis, interpretation of data for the work; D. Mannatrizio — drafting and revising the work; S. Marcia — interpretation of data for the work; M. Bellini, G. Guglielmi — drafting and revising the work.

REFERENCES

1. Kushchayev SV, Wiener PC, Teytelboym OM, et al. Percutaneous vertebroplasty: a history of procedure, technology, culture, specialty, and economics. *Neuroimaging Clin N Am*. 2019;29(4):481–494. doi: 10.1016/j.nic.2019.07.011
2. Bornemann R, Koch EM, Wollny M, Pflugmacher R. Treatment options for vertebral fractures an overview of different philosophies and techniques for vertebral augmentation. *Eur J Orthop Surg Traumatol*. 2014;24(Suppl 1):S131–143. doi: 10.1007/s00590-013-1257-3
3. Flors L, Lonjedo E, Leiva-Salinas C, et al. Vesselplasty: a new technical approach to treat symptomatic vertebral compression fractures. *AJR Am J Roentgenol*. 2009;193(1):218–226. doi: 10.2214/AJR.08.1503
4. Tsoumakidou G, Too CW, Koch G, et al. CIRSE guidelines on percutaneous vertebral augmentation. *Cardiovasc Intervent Radiol*. 2017;40(3):331–342. doi: 10.1007/s00270-017-1574-8
5. Filippidis DK, Marcia S, Masala S, et al. Percutaneous vertebroplasty and kyphoplasty: current status, new developments and old controversies. *Cardiovasc Intervent Radiol*. 2017;40(12):1815–1823. doi: 10.1007/s00270-017-1779-x
6. Diel P, Röder C, Perler G, et al. Radiographic and safety details of vertebral body stenting: results from a multicenter chart review. *BMC Musculoskelet Disord*. 2013;14:233. doi: 10.1186/1471-2474-14-233
7. Vanni D, Galzio R, Kazakova A, et al. Third-generation percutaneous vertebral augmentation systems. *J Spine Surg*. 2016;2(1):13–20. doi: 10.21037/jss.2016.02.01
8. Anselmetti GC, Manca A, Marcia S, et al. Vertebral augmentation with nitinol endoprosthesis: clinical experience in 40 patients with 1-year follow-up. *Cardiovasc Intervent Radiol*. 2014;37(1):193–202. doi: 10.1007/s00270-013-0623-1
9. Zhan Y, Jiang J, Liao H, et al. Risk factors for cement leakage after vertebroplasty or kyphoplasty: a meta-analysis of published evidence. *World Neurosurg*. 2017;101:633–642. doi: 10.1016/j.wneu.2017.01.124
10. Tempesta V, Cannata G, Ferraro G, et al. The new Vessel-X kyphoplasty for vertebral compression fractures: 2-year follow-up of 136 levels. Las Vegas: American Academy of Orthopaedic Surgeons Annual Meeting; 2009.
11. McCall T, Cole C, Dailey A. Vertebroplasty and kyphoplasty: a comparative review of efficacy and adverse events. *Curr Rev Musculoskelet Med*. 2008;1:17–23. doi: 10.1007/s12178-007-9013-0
12. Mroz TE, Yamashita T, Davros WJ, Lieberman IH. Radiation exposure to the surgeon and the patient during kyphoplasty. *J Spinal Disord Tech*. 2008;21(2):96–100. doi: 10.1097/BSD.0b013e31805fe9e1
13. Ruiz Santiago F, Santiago Chinchilla A, Guzmán Álvarez L, et al. Comparative review of vertebroplasty and kyphoplasty. *World J Radiol*. 2014;6(6):329–343. doi: 10.4329/wjr.v6.i6.329
14. Hiwatashi A, Yoshiura T, Yamashita K, et al. Morphologic change in vertebral body after percutaneous vertebroplasty: follow-up with MDCT. *AJR Am J Roentgenol*. 2010;195:W207–W212. doi: 10.2214/AJR.10.4195
15. Grohs JG, Matzner M, Trieb K, Krepler P. Minimal invasive stabilization of osteoporotic vertebral fractures: a prospective nonrandomized comparison of vertebroplasty and balloon kyphoplasty. *J Spinal Disord Tech*. 2005;18(3):238–242.
16. Lin EP, Ekholm S, Hiwatashi A, Westesson PL. Vertebroplasty: cement leakage into the disc increases the risk of new fracture of adjacent vertebral body. *AJNR Am J Neuroradiol*. 2004;25(2):175–180.
17. Bambang D. Vesselplasty: a novel concept of percutaneous treatment for stabilization and height restoration of vertebral compression fractures. *J Musculoskelet Res*. 2008;11(2):71–79. doi: 10.1142/s0218957708001985
18. Zheng Z, Luk KD, Kuang G, et al. Vertebral augmentation with a novel Vessel-X bone void filling container system and bioactive bone cement. *Spine (Phila Pa 1976)*. 2007;32(19):2076–2082. doi: 10.1097/BRS.0b013e3181453f64
19. Carlier RY, Gordji H, Mompoin DM, et al. Osteoporotic vertebral collapse: percutaneous vertebroplasty and local kyphosis correction. *Radiology*. 2004;233(3):891–898. doi: 10.1148/radiol.2333030400
20. Chen WJ, Kao YH, Yang SC, et al. Impact of cement leakage into disks on the development of adjacent vertebral compression fractures. *J Spinal Disord Tech*. 2010;23(1):35–39. doi: 10.1097/BSD.0b013e3181981843
21. Komemushi A, Tanigawa N, Kariya S, et al. Percutaneous vertebroplasty for osteoporotic compression fracture: multivariate study of predictors of new vertebral body fracture. *Cardiovasc Intervent Radiol*. 2006;29(4):580–585. doi: 10.1007/s00270-005-0138-5
22. Guarnieri G, Masala S, Muto M. Update of vertebral cementoplasty in porotic patients. *Interv Neuroradiol*. 2015;21(3):372–380. doi: 10.1177/1591019915582364

СПИСОК ЛИТЕРАТУРЫ

1. Kushchayev S.V., Wiener P.C., Teytelboym O.M., et al. Percutaneous vertebroplasty: a history of procedure, technology, culture, specialty, and economics // *Neuroimaging Clin N Am*. 2019. Vol. 29, N 4. P. 481–494. doi: 10.1016/j.nic.2019.07.011
2. Bornemann R., Koch E.M., Wollny M., Pflugmacher R. Treatment options for vertebral fractures an overview of different philosophies and techniques for vertebral augmentation // *Eur J Orthop Surg Traumatol*. 2014. Vol. 24, Suppl 1. P. S131–143. doi: 10.1007/s00590-013-1257-3
3. Flors L., Lonjedo E., Leiva-Salinas C., et al. Vesselplasty: a new technical approach to treat symptomatic vertebral compression fractures // *AJR Am J Roentgenol*. 2009. Vol. 193, N 1. P. 218–226. doi: 10.2214/AJR.08.1503
4. Tsoumakidou G., Too C.W., Koch G., et al. CIRSE guidelines on percutaneous vertebral augmentation // *Cardiovasc Intervent Radiol*. 2017. Vol. 40, N 3. P. 331–342. doi: 10.1007/s00270-017-1574-8
5. Filippidis D.K., Marcia S., Masala S., et al. Percutaneous vertebroplasty and kyphoplasty: current status, new developments and old controversies // *Cardiovasc Intervent Radiol*. 2017. Vol. 40, N 12. P. 1815–1823. doi: 10.1007/s00270-017-1779-x
6. Diel P., Röder C., Perler G., et al. Radiographic and safety details of vertebral body stenting: results from a multicenter chart review // *BMC Musculoskelet Disord*. 2013. Vol. 14. P. 233. doi: 10.1186/1471-2474-14-233
7. Vanni D., Galzio R., Kazakova A., et al. Third-generation percutaneous vertebral augmentation systems // *J Spine Surg*. 2016. Vol. 2, N 1. P. 13–20. doi: 10.21037/jss.2016.02.01

8. Anselmetti G.C., Manca A., Marcia S., et al. Vertebral augmentation with nitinol endoprosthesis: clinical experience in 40 patients with 1-year follow-up // *Cardiovasc Intervent Radiol*. 2014. Vol. 37, N 1. P. 193–202. doi: 10.1007/s00270-013-0623-1
9. Zhan Y., Jiang J., Liao H., et al. Risk factors for cement leakage after vertebroplasty or kyphoplasty: a meta-analysis of published evidence // *World Neurosurg*. 2017. Vol. 101. P. 633–642. doi: 10.1016/j.wneu.2017.01.124
10. Tempesta V., Cannata G., Ferraro G., et al. The new vessel-x kyphoplasty for vertebral compression fractures: 2-year follow-up of 136 levels. Las Vegas: American Academy of Orthopaedic Surgeons Annual Meeting; 2009.
11. McCall T., Cole C., Dailey A. Vertebroplasty and kyphoplasty: a comparative review of efficacy and adverse events // *Curr Rev Musculoskelet Med*. 2008. Vol. 1. P. 17–23. doi: 10.1007/s12178-007-9013-0
12. Mroz T.E., Yamashita T., Davros W.J., Lieberman I.H. Radiation exposure to the surgeon and the patient during kyphoplasty // *J Spinal Disord Tech*. 2008. Vol. 21, N 2. P. 96–100. doi: 10.1097/BSD.0b013e31805fe9e1
13. Ruiz S.F., Santiago C.A., Guzmán Á.L., et al. Comparative review of vertebroplasty and kyphoplasty // *World J Radiol*. 2014. Vol. 6, N 6. P. 329–343. doi: 10.4329/wjr.v6.i6.329
14. Hiwatashi A., Yoshiura T., Yamashita K., et al. Morphologic change in vertebral body after percutaneous vertebroplasty: follow-up with MDCT // *AJR Am J Roentgenol*. 2010. Vol. 195. P. W207–W212. doi: 10.2214/AJR.10.4195
15. Grohs J.G., Matzner M., Trieb K., Krepler P. Minimal invasive stabilization of osteoporotic vertebral fractures: a prospective non-randomized comparison of vertebroplasty and balloon kyphoplasty // *J Spinal Disord Tech*. 2005. Vol. 18, N 3. P. 238–242.
16. Lin E.P., Ekholm S., Hiwatashi A., Westesson P.L. Vertebroplasty: cement leakage into the disc increases the risk of new fracture of adjacent vertebral body // *AJNR Am J Neuroradiol*. 2004. Vol. 25, N 2. P. 175–180.
17. Bambang D. Vesselplasty: a novel concept of percutaneous treatment for stabilization and height restoration of vertebral compression fractures // *J Musculoskeletal Res*. 2008. Vol. 11, N 2. P. 71–79. doi: 10.1142/s0218957708001985
18. Zheng Z., Luk K.D., Kuang G., et al. Vertebral augmentation with a novel Vessel-X bone void filling container system and bioactive bone cement // *Spine (Phila Pa 1976)*. 2007. Vol. 32, N 19. P. 2076–2082. doi: 10.1097/BRS.0b013e3181453f64
19. Carlier R.Y., Gordji H., Mompoin D.M., et al. Osteoporotic vertebral collapse: percutaneous vertebroplasty and local kyphosis correction // *Radiology*. 2004. Vol. 233, N 3. P. 891–898. doi: 10.1148/radiol.2333030400
20. Chen W.J., Kao Y.H., Yang S.C., et al. Impact of cement leakage into disks on the development of adjacent vertebral compression fractures // *J Spinal Disord Tech*. 2010. Vol. 23, N 1. P. 35–39. doi: 10.1097/BSD.0b013e3181981843
21. Komemushi A., Tanigawa N., Kariya S., et al. Percutaneous vertebroplasty for osteoporotic compression fracture: multivariate study of predictors of new vertebral body fracture // *Cardiovasc Intervent Radiol*. 2006. Vol. 29, N 4. P. 580–585. doi: 10.1007/s00270-005-0138-5
22. Guarnieri G., Masala S., Muto M. Update of vertebral cementoplasty in porotic patients // *Interv Neuroradiol*. 2015. Vol. 21, N 3. P. 372–380. doi: 10.1177/1591019915582364

AUTHORS' INFO

* **Guseppe Guglielmi**, MD, Professor;

address: Viale L. Pinto 1, 71121 Foggia, Italy;

ORCID: <http://orcid.org/0000-0002-4325-8330>;

e-mail: giuseppe.guglielmi@unifg.it

Salvatore Masala, MD; ORCID: 0000-0003-0032-7970;

e-mail salva.masala@tiscali.it

Adriano Lacchè, MD; ORCID: 000-0003-1782-8624;

e-mail adrianolacche@gmail.com

Chiara Zini, MD; ORCID: 0000-0003-3456-4106;

e-mail zini.chiara@gmail.com

Domenico Mannatrizio, MD; ORCID: 0000-0003-3365-7132;

e-mail dr.mannatrizio@gmail.com

Stefano Marcia, MD; ORCID: 0000-0002-2118-9864;

e-mail stemarcia@gmail.com

Matteo Bellini, MD; ORCID: 0000-0002-1704-6246;

e-mail matteo.bellini@icloud.com

05 ABTOPAX

* **Guglielmi G.**, MD, Professor;

адрес: Viale L. Pinto 1, 71121 Foggia, Italy;

ORCID: <http://orcid.org/0000-0002-4325-8330>;

e-mail: giuseppe.guglielmi@unifg.it

Masala S., MD; ORCID: 0000-0003-0032-7970;

e-mail salva.masala@tiscali.it

Lacchè A., MD; ORCID: 000-0003-1782-8624;

e-mail adrianolacche@gmail.com

Zini Ch., MD; ORCID: 0000-0003-3456-4106;

e-mail zini.chiara@gmail.com

Mannatrizio D., MD; ORCID: 0000-0003-3365-7132;

e-mail dr.mannatrizio@gmail.com

Marcia S., MD; ORCID: 0000-0002-2118-9864;

e-mail stemarcia@gmail.com

Bellini M., MD; ORCID: 0000-0002-1704-6246;

e-mail matteo.bellini@icloud.com

* Corresponding author / Автор, ответственный за переписку

DOI: <https://doi.org/10.17816/DD104358>

Влияние индекса массы тела на надёжность шкалы КТ 0–4: сравнение протоколов компьютерной томографии

И.А. Блохин¹, А.П. Гончар¹, М.Р. Коденко^{1,2}, А.В. Соловьев¹, В.А. Гомболевский³, Р.В. Решетников^{1,4}

¹ Научно-практический клинический центр диагностики и телемедицинских технологий, Москва, Российская Федерация

² Московский государственный технический университет имени Н.Э. Баумана (национальный исследовательский университет), Москва, Российская Федерация

³ Институт искусственного интеллекта (AIRI), Москва, Российская Федерация

⁴ Первый Московский государственный медицинский университет имени И.М. Сеченова (Сеченовский Университет), Москва, Российская Федерация

АННОТАЦИЯ

Обоснование. Из-за повышения частоты использования компьютерной томографии органов грудной клетки в борьбе с COVID-19 возникла необходимость применения низкодозной компьютерной томографии для снижения дозовой нагрузки на организм пациента при сохранении диагностической ценности исследования. При этом данных о влиянии индекса массы тела пациента на точность низкодозной компьютерно-томографической диагностики у пациентов с COVID-19 в опубликованной литературе не обнаружено.

Цель — оценить влияние индекса массы тела пациента на уровень согласия между врачами-рентгенологами при интерпретации стандартной и низкодозной компьютерной томографии органов грудной клетки при COVID-19-ассоциированной пневмонии по визуальной полуколичественной шкале КТ 0–4.

Материалы и методы. Ретроспективное многоцентровое исследование, в котором каждому из участников в рамках одного визита было последовательно выполнено два исследования органов грудной клетки по стандартному и низкодозному протоколу. Интерпретация стандартной и низкодозной компьютерной томографии органов грудной клетки с лёгочным и мягкотканым кернелами проводилась по визуальной полуколичественной шкале КТ 0–4. Данные для каждого протокола были сгруппированы по значению индекса массы тела (пороговое значение для патологии было принято равным 25 кг/м²). Согласие рассчитывали на основе бинарной и взвешенной классификаций. Оценку наличия статистически значимых различий средних для полученных групп проводили методом однофакторного дисперсионного анализа ANOVA.

Результаты. Из общего количества пациентов ($n=231$) 230 соответствовали установленным критериям включения в исследование. Эксперты обработали по 4 исследования стандартной и низкодозной компьютерной томографии с лёгочным и мягкотканым кернелами для каждого пациента. Доля пациентов с нормальным весом составила 31% (71 человек), медиана индекса массы тела для выборки равна 27,5 (18,3; 48,3) кг/м². Статистически значимых различий при межгрупповом попарном сравнении не выявлено ни для бинарной, ни для взвешенной классификации (p -value 0,09 и 0,12 соответственно). Группа пациентов с избыточным весом была дополнительно разделена по степеням ожирения, однако результаты исследования оказались инвариантны к такому делению (статистически значимых различий нет: для максимально различных по индексу массы тела групп «норма» и «ожирение 3-й степени» p -value 0,17).

Заключение. Индекс массы тела пациента не влияет на интерпретацию стандартной и низкодозной компьютерной томографии органов грудной клетки при COVID-19 по визуальной полуколичественной шкале КТ 0–4.

Ключевые слова: индекс массы тела; согласие между экспертами; компьютерная томография; низкодозная компьютерная томография; COVID-19.

Как цитировать

Блохин И.А., Гончар А.П., Коденко М.Р., Соловьев А.В., Гомболевский В.А., Решетников Р.В. Влияние индекса массы тела на надёжность шкалы КТ 0–4: сравнение протоколов компьютерной томографии // *Digital Diagnostics*. 2022. Т. 3, № 2. С. 108–118. DOI: <https://doi.org/10.17816/DD104358>

DOI: <https://doi.org/10.17816/DD104358>

Impact of body mass index on the reliability of the CT0–4 grading system: a comparison of computed tomography protocols

Ivan A. Blokhin¹, Anna P. Gonchar¹, Maria R. Kodenko^{1,2}, Alexander V. Solovev¹, Victor A. Gomboleviskiy³, Roman V. Reshetnikov^{1,4}

¹ Moscow Center for Diagnostics and Telemedicine, Moscow, Russian Federation

² Bauman Moscow State Technical University, Moscow, Russian Federation

³ Artificial Intelligence Research Institute, Moscow, Russian Federation

⁴ The First Sechenov Moscow State Medical University (Sechenov University), Moscow, Russian Federation

ABSTRACT

BACKGROUND: The increased frequency of chest computed tomography utilization in the fight against COVID-19 has made usage of low-dose computed tomography necessary to reduce the radiation dose while preserving diagnostic quality. However, in the published literature, there were no data on the effect of body mass index on low-dose computed tomography accuracy in patients with COVID-19.

AIM: To assess the effect of patient body mass index on the level of agreement between radiologists interpreting standard-dose computed tomography and low-dose computed tomography in COVID-19-associated pneumonia using visual semiquantitative CT 0–4 scale.

MATERIALS AND METHODS: In this retrospective multicenter study, each participant underwent two consecutive chest scans at a single visit using standard-dose and low-dose protocols. Standard-dose and low-dose computed tomography with pulmonary and soft tissue kernels were interpreted using a visual semiquantitative CT 0–4 grading system. Data for each protocol were grouped by body mass index value (threshold value for pathology was equal to 25 kg/m²). Agreement was calculated based on binary and weighted classifications. One-way ANOVA analysis of variance was used to assess the presence of statistically significant differences in the mean for the groups.

RESULTS: Two hundred thirty patients met the established inclusion criteria for the study. The experts processed 4 studies for each patient: standard-dose and low-dose computed tomography with pulmonary and soft tissue kernels. The proportion of normal-weight patients was 31% (71 subjects), and the sample's median body mass index was 27.5 (18.3; 48.3) kg/m². There were no statistically significant differences in intergroup pairwise comparisons for both the binary and weighted classifications (*p* values were 0.09 and 0.12, respectively). The group of overweight patients was further subdivided according to the degrees of obesity; however, the results were invariant to this division (no statistically significant differences: for the most different body mass index groups "normal" and "3rd degree obesity" *p*-value 0.17).

CONCLUSION: Body mass index does not affect chest standard-dose and low-dose computed tomography interpretation in COVID-19 using the visual semiquantitative CT 0–4 grading system.

Keywords: Body mass index; Reproducibility of findings; X-ray computed tomography; SARS-CoV-2 infection.

To cite this article

Blokhin IA, Gonchar AP, Kodenko MR, Solovev AV, Gomboleviskiy VA, Reshetnikov RV. Impact of body mass index on the reliability of the CT0–4 grading system: a comparison of computed tomography protocols. *Digital Diagnostics*. 2022;3(2):108–118. DOI: <https://doi.org/10.17816/DD104358>

Received: 02.03.2022

Accepted: 26.05.2022

Published: 08.06.2022

DOI: <https://doi.org/10.17816/DD104358>

体重指数对CT 0-4量表可靠性的影响： 计算机断层扫描协议的比较

Ivan A. Blokhin¹, Anna P. Gonchar¹, Maria R. Kodenko^{1,2}, Alexander V. Solovov¹,
Victor A. Gombolevskiy³, Roman V. Reshetnikov^{1,4}

¹ Moscow Center for Diagnostics and Telemedicine, Moscow, Russian Federation

² Bauman Moscow State Technical University, Moscow, Russian Federation

³ Artificial Intelligence Research Institute, Moscow, Russian Federation

⁴ The First Sechenov Moscow State Medical University (Sechenov University), Moscow, Russian Federation

简评

论证。由于在对抗COVID-19的过程中使用胸部计算机断层扫描的频率越来越高，因此有必要应用低剂量计算机断层扫描(LDCT)来减少患者身体的剂量负荷，同时保持研究的诊断价值。然而，在已发表的文献中未发现有关患者体重指数对COVID-19患者LDCT诊断准确性影响的数据。

目的是评估患者的BMI对放射科医生在解释COVID-19相关肺炎的标准和低剂量胸部CT扫描时在0-4视觉半定量CT评分上的一致程度的影响。

材料与方法。一项回顾性多中心研究，其中在一次访问时每位参与者接受了两次连续的胸部检查，使用标准和低剂量方案。对标准和低剂量胸部CT扫描的肺部和软组织核素的解释是以视觉半定量的CT 0-4尺度进行的。每个方案的数据根据体重指数的值进行分组（病理学阈值等于公斤/平方米²）。协议是根据二元和加权分类计算的。通过方差单因素方差分析来评估各组平均值之间是否存在统计学上的显著差异。

结果。在患者总数（n=231）中，230人符合确立的研究纳入标准。专家为每位患者处理了4项标准和低剂量计算机断层扫描研究，包括肺和软组织卷积核。体重正常的患者比例为31%（71人），样本的中位体重指数中位为27.5（18.3；48.3）公斤/平方米。无论是二元分类还是加权分类，组间配对比较未发现统计学上的显著差异（p值分别为0.09和0.12）。超重患者组根据肥胖程度进一步划分，但研究结果对这种划分是不变的（没有统计学上的显著差异：身体质量参数最大不同组别»正常»和»3度肥胖»的p值为0.17）。

结论。患者的体重指数不影响在0-4的视觉半定量CT等级上对COVID-19胸部标准和低剂量计算机断层扫描的解释。

关键词：体重指数；专家之间的协议；CT扫描；低剂量计算机断层扫描；新冠肺炎。

To cite this article

Blokhin IA, Gonchar AP, Kodenko MR, Solovov AV, Gombolevskiy VA, Reshetnikov RV. 体重指数对CT 0-4量表可靠性的影响：计算机断层扫描协议的比较. *Digital Diagnostics*. 2022;3(2):108-118. DOI: <https://doi.org/10.17816/DD104358>

收到: 02.03.2022

接受: 26.05.2022

发布日期: 08.06.2022

BACKGROUND

Computed tomography of the chest (chest CT) plays a unique role in the diagnosis of coronavirus disease 2019 (COVID-19) [1]. A visual semi-quantitative scale of pulmonary parenchyma damage (CT 0–4) is currently used to assess the severity and predict the course of COVID-19-associated pneumonia [2]. Considering the increased frequency of CT use in patients with COVID-19, a low-dose computed tomography (LDCT) must reduce the radiation dose while maintaining the diagnostic value of this method [3]. An LDCT is proved not to be associated with DNA damage. In contrast, a standard-dose CT was associated with an increase in DNA double-strand breaks and chromosome aberrations [4].

A high body mass index (BMI) is known to be one of the factors of an unfavorable COVID-19 infection course [5]. However, a chest LDCT has limited application in patients with BMI >35 kg/m² [6]. A. Manowitz et al. reported previously [7] that in patients with high BMI, radiation exposure from abdominal CT could be reduced without diagnostic quality impairment. N.S. Paul et al. [8] assessed the effect of obesity on the coronary CT-angiography effectiveness and noted a strong correlation between BMI and image noise in both men ($r = 0.66$) and women ($r = 0.85$) with increased body weight. The authors concluded that when reducing radiation exposure, patient's BMI should be considered. However, at the time of preparing this article, no data about the impact of BMI on LDCT accuracy in COVID-19 patients could be found in the literature.

This study aimed to evaluate the effect of a patient's BMI on the reliability of standard-dose and low-dose chest CT findings in COVID-19-associated pneumonia and the accuracy of their interpretation by different radiologists using a visual semi-quantitative scale CT 0–4.

Null hypothesis

A BMI does not affect an inter-rater agreement rate when assessing the severity of COVID-19-associated pneumonia with standard-dose and low-dose chest CT using a CT 0–4 scale.

MATERIALS AND METHODS

Study design

A retrospective study was conducted using materials that were obtained in the previous prospective multicenter study, "LDCT in COVID-19 Pneumonia: a Prospective Moscow Study" (registered in ClinicalTrials.gov under NCT04379531 on April 25, 2020) [9].

Eligibility criteria

Inclusion criteria. Patients aged ≥18 yr who received treatment in two state outpatient clinics in Moscow for suspected COVID-19-associated pneumonia and symptoms of acute respiratory viral infection.

Exclusion criteria. Patients with incomplete data (height, weight, and BMI); pregnant and lactating women; patients with foreign bodies in the area to be scanned.

Conditions of the study

Each patient underwent two consecutive chest CT scans during a single visit (using standard-dose and low-dose protocol). CT findings were analyzed by 10 radiologists with 3 to 25 yr of experience, who were trained in the interpretation of COVID-19-associated pneumonia. Modified FAnTom software was used to provide online access to anonymized data for an assessment of the disease severity using the CT 0–4 scale [9, 10]. Radiologists were randomly assigned with CT and LDCT scans reconstructed using lung and soft tissue kernels with each study independently and blindly interpreted by two specialists.

Study duration

Data from chest CT and LDCT were collected from May 6 to May 22, 2020.

Description of medical interventions

A 64-slice CT scanner (Aquilion 64, Canon, Japan) was used to perform a chest CT scan without using any iterative reconstruction algorithms. Two chest CT protocols were employed: a standard-dose protocol provided by the manufacturer and a previously developed low-dose protocol for COVID-19.

For chest CT, the current is automatically adjusted over the entire scan length within the range of 40–500 mA as long as the noise level for 5.0 mm slices is 10 (standard deviation).

For chest LDCT, the current is automatically adjusted over the entire scan length in the range of 10–500 mA as long as the noise level for 5.0 mm slices is 36 (standard deviation).

Additional CT parameters (the same for CT and LDCT) are voltage (120 kV), rotation time (0.5 s), direction (outward, from the legs to the head), XY modulation (enabled), collimation (64 × 0.5 mm), and helix pitch (53.0). Scanning was performed at peak inspiratory depth. The average scanning time was 6 s (depending on individual body features). Examinations were performed without any contrast enhancement.

Image reconstruction parameters were the same for standard-dose CT and LDCT: matrix 512 × 512; D-FOV 350 mm; scanning length 300 mm; reconstruction core (kernel) FC51 (pulmonary kernel) and FC07 (soft tissue kernel); slice thickness 1.0 mm; increment 1.0 mm.

Primary study outcome

This study evaluated the impact of BMI on the quality of chest LDCT interpretation in patients with COVID-19-associated pneumonia. A standard-dose CT protocol was used as a comparison method. The results were interpreted using a visual semi-quantitative CT 0–4 scale.

Ethical review

This paper is based on a study from the Independent Ethics Committee of the Moscow Regional Branch of the Russian Society of Roentgenologists and Radiologists with approval no. 03/2020. All patients signed informed voluntary consent.

Statistical analysis

The inter-rater agreement rate for each patient was assessed by formulas (1) and (2) for the following protocols:

- standard-dose CT with lung kernel (reconstruction filter) FC51 (Sharp CT);
- standard-dose CT with soft tissue kernel (reconstruction filter) FC07 (Soft CT);
- low-dose CT with lung kernel (reconstruction filter) FC51 (Sharp LDCT);
- low-dose CT with soft tissue kernel (reconstruction filter) FC07 (Soft LDCT).

Data for each protocol were divided into two BMI groups: normal BMI ($<25 \text{ kg/m}^2$) and overweight BMI ($\geq 25 \text{ kg/m}^2$) [11]. The inter-rater agreement rate for each subgroup was reported as the mean value with standard deviation.

Data were processed using R, version 4.0.4, dplyr, ggplot2, and irr packages [12].

The agreement rate was calculated as a percentage based on the absolute difference between the scores of two raters:

$$|\Delta| = |\text{rater1} - \text{rater2}| \quad (1).$$

Disagreements were interpreted in two ways:

1. Binary classification, which was not sensitive to numerical difference between scores (Δ). If there was no difference between the scores of two raters ($|\Delta| = 0$), the agreement rate was 100%. If there was any difference between scores ($|\Delta| \neq 0$), the agreement rate was equal to 0%.
2. A weighted classification considered a numerical differences between the scores of two raters (Δ), as well as a threshold percentage of lung damage, which was used as the reason for hospital admission:

$$\text{Agreement rate} = (1 - |\frac{\Delta}{\Delta_{\max}}|) \times 100, \quad (2)$$

where Δ is the difference between raters' scores for the current study according to formula (1); Δ_{\max} is the maximum possible score difference ($\Delta_{\max} = 4$, four categories of CT 0–4 scores). In this study, the weighted agreement score was a discrete value and ranged from 0% to 100% with increments of 25%. Agreement rates of 0%, 25%, 50%, 75%, and 100% corresponded to differences in four, three, two, and one categories and complete agreement, respectively.

Statistically significant differences in means for the groups obtained were assessed by one-way analysis of variance (ANOVA) [13]. First, the quality of variances of the study groups were statistically analyzed using the Levene test [14]. Next, ANOVA was performed for the equality of means, considering data on the equality of variances. The agreement rate between radiologists was a dependent

variable. A BMI (binary classification, normal weight, and overweight) and CT protocol (Sharp CT, Soft CT, Sharp LDCT, and Soft LDCT) were used as independent variables. A retrospective analysis using Tukey's honestly significant difference (HSD) test was performed to determine numerical p -values for inter-subgroup differences, [15]. A statistical significance level of 0.05 was used for all comparisons.

RESULTS

The total number of patients selected was 231, and 230 of them were included in the study (one patient had no BMI data). In the selected cohort, 55.6% were women. The mean age of patients was 47 ± 15 yr. For each patient, CT and LDCT findings were obtained and reconstructed using pulmonary and soft tissue kernels.

The main descriptive statistics for the whole population were as follows: range (18.3; 48.3) kg/m^2 ; median 27.5 kg/m^2 , mean $27.9 \pm 5.6 \text{ kg/m}^2$; distribution did not correspond to a normal one (p -value ≤ 0.01), the asymmetry coefficient was 0.9 (significant right-sided asymmetry).

The following are patient categories by BMI: non-overweight (BMI $< 25 \text{ kg/m}^2$), 31% (71); overweight (BMI $\geq 25 \text{ kg/m}^2$), 69% (159).

Using the Sharp LDCT protocol, the highest agreement rate for patients with normal BMI was obtained: 83.5% and 92.8% for binary and weighted classifications, respectively (Figure 1; Table 1). The Soft LDCT protocol had the lowest agreement rate for patients with normal BMI: 64.9% and 86.9% for binary and weighted classifications, respectively.

For overweight patients, the highest inter-rater agreement rate was recorded for Sharp CT (71.2% and 88.4% for binary and weighted classifications, respectively). The lowest agreement rate for this group of patients was observed when using the Soft CT protocol: 64.4% and 86.4% for binary and weighted classifications, respectively (Figure 1 and Table 1).

The greatest difference in the homogeneity of interpretations between normal weight and overweight patients was observed using the Sharp LDCT protocol (the mean difference 16.1% and 4.5% for binary and weighted classifications, respectively). The least heterogeneous interpretation was recorded when using Sharp CT and Soft LDCT protocols. The mean difference did not exceed 1% for any of the classifications (Figure 1 and Table 1).

ANOVA

A one-way ANOVA was performed to analyze differences between interpretations of radiologists based on BMI, scanning, and reconstruction protocol. This analysis demonstrated no statistically significant differences between the mean agreement rates for normal weight and overweight groups and for all four protocols using both binary classification ($p = 0.13$ for protocol and $p = 0.18$ for BMI) and weighted classification ($p = 0.18$ and $p = 0.14$, respectively).

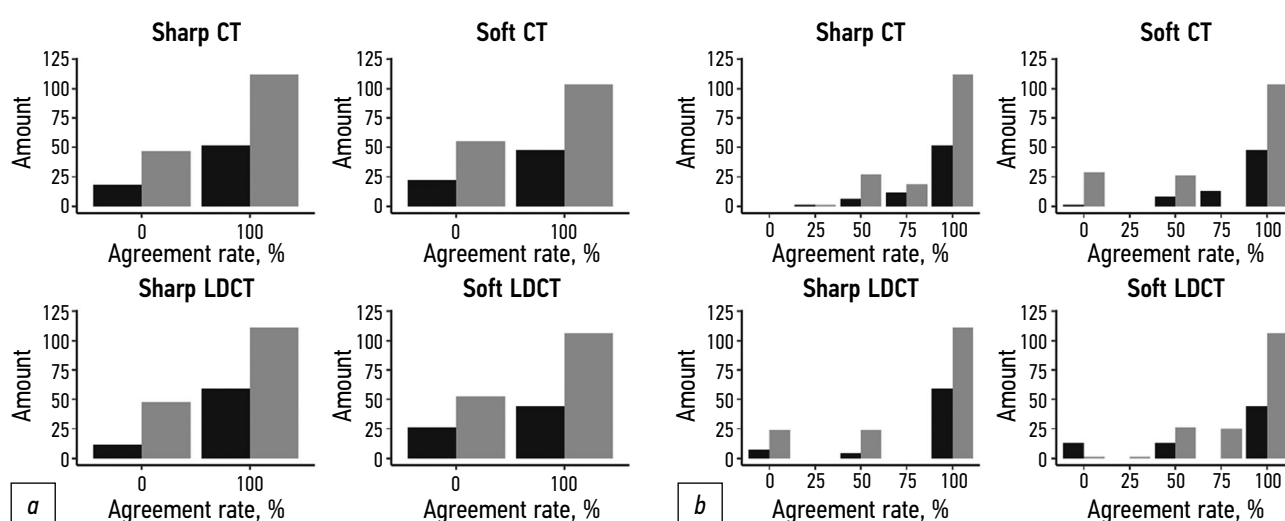


Fig. 1. An inter-rater agreement diagram for binary (a) and weighted (b) classifications by body mass index (gray: overweight group, black: normal weight group).

Table 1. Numerical inter-rater agreement values (%) for binary (light gray) and weighted (dark gray) classifications

Value	Sharp CT		Soft CT		Sharp LDCT		Soft LDCT	
	Normal	Overweight	Normal	Overweight	Normal	Overweight	Normal	Overweight
Mean	72.2	71.2	69.1	64.4	83.5	67.4	64.9	65.9
SD	45.1	45.4	46.5	48.1	37.3	47.0	48.0	47.6
Mean	89.4	88.4	88.4	86.4	92.8	88.3	86.9	86.4
SD	18.7	19.6	19.8	19.9	16.9	18.4	19.5	21.3

In addition to comparing mean agreement rates, we evaluated the variability of raters' scores depending on BMI and imaging method. With the Levene test, differences in binary and weighted classifications allow to accept the hypothesis about the equal variances in study groups.

Subgroup differences were evaluated using post hoc analysis with a Tukey's HSD test (Figure 2). For all compared pairs, 95% confidence intervals included "0" for both binary (Figure 2a) and weighted (Figure 2b) classifications. This indicates no statistically significant differences in radiologist interpretations for different BMI groups and imaging methods.

For binary classification, the minimum p -value was 0.22 for comparing Sharp LCDT in normal weight patients and Soft CT in overweight patients; the minimum p -value for one protocol was 0.65 (Sharp LDCT). For weighted classification, the minimum p -value was 0.08, and the minimum p -value for each protocol was 0.36 in similar groups.

An additional ROC-analysis (receiver operating characteristic) of study groups allowed to determine the optimal BMI threshold for predicting the level of compliance, equal to 26.24 kg/m². For this threshold, repeated ANOVA confirmed that there were no statistically significant differences in variances (p -values were 0.13 and 0.09 for binary classification and 0.18 and 0.12 for weighted classification for protocol and BMI, respectively) and means (p -values were similar) of study groups for each protocol. For both classification types, the minimum p -value was recorded

for comparing normal weight and overweight groups using the Sharp LDCT protocol, which was 0.65 and 0.15 for binary and weighted classifications, respectively.

An additional analysis was performed using the "overweight," "class 1 obesity," "class 2 obesity," and "class 3 obesity" groups in consideration of the original population to "overweight" (BMI of [25; 30] kg/m²). For all protocols, the analysis showed no statistically significant differences for both types of classifications (the minimal p -value was recorded for "normal weight" and "class 1 obesity" groups, and it was 0.09 and 0.08 for binary and weighted classifications, respectively). For "normal weight" and "class 3 obesity" groups with the largest BMI difference, p -value was 0.17.

Additionally, a series of studies was analyzed with inter-rater CT 0–4 disagreements in more than one category. There were 26 series identified. After reviewing each case, these disagreements may be divided into two groups.

The first group consisted of 15 series (58%), for which both raters confirmed the presence of COVID-19-associated abnormalities (CT1 and higher score) but have disagreements regarding the degree of lung tissue damage. This may be due to the preferred scanning plane (axial, frontal, or sagittal) and direction (apices to diaphragm or diaphragm to apices), as well as to the presence of manifestations of different temporal stages of viral pneumonia, for example, simultaneously "frosted glass" and "cobblestone pavement." Since COVID-19

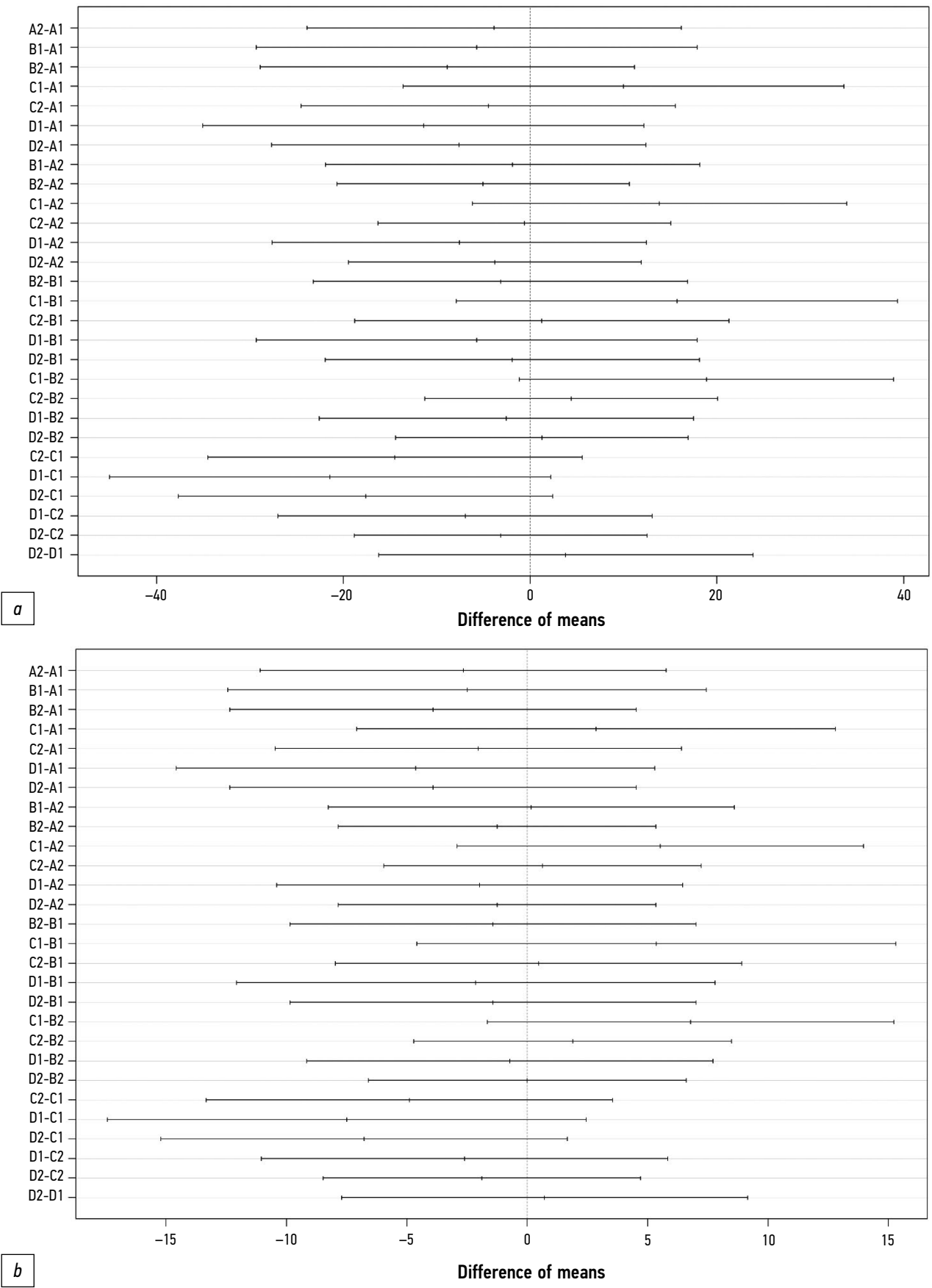


Fig. 2. A post-post-hoc analysis of our hypothesis for the similarity of means: (a) binary classification; (b) normalized classification (Sharp CT, Soft CT, Sharp LDCT, and Soft LDCT protocols are coded with A, B, C, and D, respectively; the normal weight group is coded with “1”; the overweight group is coded with “2”).

pneumonia is more severe in basal lung regions, axial sliding from the diaphragm to apices can lead to an upward bias for the severity of abnormalities assessed by the rater with higher CT 0–4 score. Use of sagittal multiply or 3D reconstructions allows to “capture” these abnormalities immediately, reducing the risk of overestimating the lesion severity. Inter-rater disagreements in the first group suggested the significant effect of human factor in visual assessment of the disease severity as well as the need to study the capabilities of systems for automatic lung parenchyma densitometry.

The second group consisted of 11 series (42%), for which one of the raters did not confirm the presence of COVID-19-associated abnormalities (CT0 score). This was related to false positive cases (hypostatic changes in the basal parts of lungs with a high a priori probability of infection) as well as the fact that the CT 0–4 classification does not provide a way to express the probability of COVID-19 origin of these abnormalities. In the second group, inter-rater differences highlight the value of a joint application of CO-RADS and CT 0–4 classifications.

DISCUSSION

This study evaluated the agreement rate for assessments of chest CT and LDCT by different radiologists using a CT 0–4 scale, depending on weight and reconstruction kernel in patients with COVID-19-associated pneumonia. A comparative analysis showed no statistically significant differences. Sizes of samples compared needed to be balanced by BMI groups, so patients were divided into two classes by BMI (“normal weight” and “overweight”), which could affect the interpretation of results. An additional analysis, however, revealed the invariant qualitative result (“no statistically significant differences were found”) for the “obesity” category. Given the limitations of this study, we can conclude that BMI does not have any significant effect on the agreement rate when assessing the lung damage using a CT 0–4 scale. Therefore, the scanning protocol can be selected regardless of the patient’s BMI.

Our study provides us with the additional justification for choosing the lowest possible radiation dose for patients with COVID-19, because the increased BMI has no impact on the diagnostic quality of images when using the CT 0–4 scale, so the kernel can be selected solely at the discretion of a radiologist.

In 2016, T. Kubo et al. [16] compared the diagnostic capabilities of LDCT (50 mAc) and CT (150 mAc) for the routine chest examination. Three radiologists independently analyzed 118 2-mm image series (two series for each patient in the sample) and assessed abnormalities, such as emphysema, frosted glass, reticular changes, micronodules, bronchiectasis, honeycomb lung, nodules (>5 mm), aortic aneurysm, coronary artery calcification, pericardial and pleural effusions, pleural thickening, mediastinal masses, and enlarged lymph nodes. According to the authors’ conclusion,

which is consistent with our data, the LDCT protocol can be used in the routine radiological practice.

CT scans are said to be of lower quality (with lower signal-to-noise ratio) when using the low-dose protocol compared with standard-dose CT [17]. Therefore, additional methods should be used to improve the scanning quality, especially in patients with increased body weight. One of such methods is using iterative reconstructions [18].

D.A. Filatova et al. [19] compared CT and LDCT of the chest in patients with COVID-19, using iterative reconstructions. The sample size was 151 patients. No significant losses of diagnostic information during the chest LDCT were revealed compared with the standard-dose CT, so the chest LDCT can be used in routine practice for the diagnosis of COVID-19 [19], and this confirmed our results. The aforementioned study, however, did not evaluate the effect of BMI on the scanning quality, unlike our study.

Moreover, the method using effective radiation doses <0.3 mSv and iterative reconstructions has limitations for patients with interstitial pneumonia/emphysema and BMI >25 kg/m² [20].

Study limitations

Our study has some limitations. Only one model of CT scanner was used. The recommended protocols for other models and manufacturers may differ from those used by us. To interpret findings, only the subjective assessment of radiologists using a CT 0–4 scale was used. Our conclusions are based on the analysis of the sample, without grouping by the degree of obesity. As shown, however, the qualitative outcome was invariant for this parameter.

CONCLUSION

Therefore, considering the above limitations, we can conclude that there are no significant effects of BMI on the interpretation of the chest CT and LDCT in patients with COVID-19 using a visual semi-quantitative CT 0–4 scale.

ADDITIONAL INFORMATION

Funding source. This study was not supported by any external sources of funding.

Competing interests. The authors declare that they have no competing interests.

Authors’ contribution. All authors confirm that they meet the international ICMJE criteria for authorship (all authors made substantial contributions to the concept development, conducting the research and preparation of the article, and read and approved the final version before publication). The largest contributions were as follows: I.A. Blokhin — concept and study design, data analysis, manuscript preparation; A.P. Gonchar — manuscript preparation; M.R. Kodenko — data collection and processing, data analysis, manuscript preparation; A.V. Solovev, A.V. Gombolevskiy — manuscript preparation; R.V. Reshetnikov — research concept and design, manuscript preparation.

REFERENCES

1. Islam N, Ebrahimzadeh S, Salameh JP, et al. Thoracic imaging tests for the diagnosis of COVID-19. *Cochrane Database Syst Rev*. 2021;3(3):CD013639. doi: 10.1002/14651858.CD013639.pub4
2. Morozov SP, Chernina VY, Blokhin IA, Gomboleviskiy V. Chest computed tomography for outcome prediction in laboratory-confirmed COVID-19: a retrospective analysis of 38,051 cases. *Digital Diagnostics*. 2020;1(1):27–36. doi: 10.17816/DD46791
3. Prasad KN, Cole WC, Haase GM. Radiation protection in humans: extending the concept of as low as reasonably achievable (ALARA) from dose to biological damage. *BJR*. 2004;77(914):97–99. doi: 10.1259/bjr/88081058
4. Sakane H, Ishida M, Shi L, et al. Biological effects of low-dose chest CT on chromosomal DNA. *Radiol*. 2020;295(2):439–445. doi: 10.1148/radiol.2020190389
5. Du Y, Lv Y, Zha W, et al. Association of body mass index (BMI) with critical COVID-19 and in-hospital mortality: a dose-response meta-analysis. *Metabolism*. 2021;117:154373. doi: 10.1016/j.metabol.2020.154373
6. Ohana M, Ludes C, Schaal M, et al. Quel avenir pour la radiographie thoracique face au scanner ultra-low dose? *Revue Pneumologie Clinique*. 2017;73(1):3–12. doi: 10.1016/j.pneumo.2016.09.007
7. Manowitz A, Sedlar M, Griffon M, et al. Use of BMI guidelines and individual dose tracking to minimize radiation exposure from low-dose helical chest CT scanning in a lung cancer screening program. *Academ Radiol*. 2012;19(1):84–88. doi: 10.1016/j.acra.2011.09.015
8. Paul NS, Kashani H, Odedra D, et al. The influence of chest wall tissue composition in determining image noise during cardiac CT. *Am J Roentgenol*. 2011;197(6):1328–1334. doi: 10.2214/AJR.11.6816
9. Blokhin I, Gomboleviskiy V, Chernina V, et al. Inter-observer agreement between low-dose and standard-dose CT with soft and sharp convolution kernels in COVID-19 pneumonia. *J Clin Med*. 2022;11(3):669. doi: 10.3390/jcm11030669
10. Morozov SP, Gomboleviskiy VA, Elizarov AB, et al. A simplified cluster model and a tool adapted for collaborative labeling of lung cancer CT scans. *Computer Methods Programs Biomed*. 2021;206:106111. doi: 10.1016/j.cmpb.2021.106111
11. Powell-Wiley TM, Poirier P, Burke LE, et al. Obesity and cardiovascular disease: a scientific statement from the American Heart Association. *Circulation*. 2021;143(21):e984–e1010. doi: 10.1161/CIR.0000000000000973
12. The R Foundation. The R Project for Statistical Computing [Internet]. Available from: <https://www.r-project.org/>. Accessed: 15.03.2022.
13. Fisher RA. XXI. —On the dominance ratio. *Proceedings Royal Soc Edinburgh*. 1923;42:321–341. doi: 10.1017/S0370164600023993
14. Levene H. Robust tests for equality of variances. In: Olkin I, Ghurye S, Hoeffding W, et al. Contributions to probability and statistics: essays in honor of harold hotelling. Stanford University Press; 1961. P. 279–292.
15. Mosteller F. Data analysis and regression: a second course in statistics. Addison-Wesley Pub. Co., Boston; 1977. 588 p.
16. Kubo T, Ohno Y, Nishino M, et al. Low dose chest CT protocol (50 mas) as a routine protocol for comprehensive assessment of intrathoracic abnormality. *Eur J Radiol Open*. 2016;3:86–94. doi: 10.1016/j.ejro.2016.04.001
17. Silin AY, Gruzdev IS, Morozov SP. The influence of model iterative reconstruction on the image quality in standard and low-dose computer tomography of the chest. Experimental study. *J Clin Pract*. 2020;11(4):49–54. doi: 10.17816/clinpract34900
18. Zhu Z, Ming ZX, Feng ZY, et al. Feasibility study of using gemstone spectral imaging (GSI) and adaptive statistical iterative reconstruction (ASIR) for reducing radiation and iodine contrast dose in abdominal CT patients with high BMI values. *PLOS ONE*. 2015;10(6):e0129201. doi: 10.1371/journal.pone.0129201
19. Filatova DA, Sinitsin VE, Mershina EA. Opportunities to reduce the radiation exposure during computed tomography to assess the changes in the lungs in patients with COVID-19: use of adaptive statistical iterative reconstruction. *Digital Diagnostics*. 2021;2(2):94–104. doi: 10.17816/DD62477
20. Lee SW, Kim Y, Shim SS, et al. Image quality assessment of ultra-low dose chest CT using sinogram-affirmed iterative reconstruction. *Eur Radiol*. 2014;24(4):817–826. doi: 10.1007/s00330-013-3090-9

СПИСОК ЛИТЕРАТУРЫ

1. Islam N., Ebrahimzadeh S., Salameh J.P., et al. Thoracic imaging tests for the diagnosis of COVID-19 // *Cochrane Database Syst Rev*. 2020. Vol. 3, N 3. P. CD013639. doi: 10.1002/14651858.CD013639.pub4
2. Morozov S.P., Chernina V.Y., Blokhin I.A., Gomboleviskiy V. Chest computed tomography for outcome prediction in laboratory-confirmed COVID-19: a retrospective analysis of 38,051 cases // *Digital Diagnostics*. 2020. Vol. 1, N 1. P. 27–36. doi: 10.17816/DD46791
3. Prasad K.N., Cole W.C., Haase G.M. Radiation protection in humans: extending the concept of as low as reasonably achievable (ALARA) from dose to biological damage // *Br J Radiol*. 2004. Vol. 77, N 914. P. 97–99. doi: 10.1259/bjr/88081058
4. Sakane H., Ishida M., Shi L., et al. Biological effects of low-dose chest CT on chromosomal DNA // *Radiol*. 2020. Vol. 295, N 2. P. 439–445. doi: 10.1148/radiol.2020190389
5. Du Y., Lv Y., Zha W., et al. Association of body mass index (BMI) with critical COVID-19 and in-hospital mortality: a dose-response meta-analysis // *Metabolism*. 2021. Vol. 117. P. 154373. doi: 10.1016/j.metabol.2020.154373
6. Ohana M., Ludes C., Schaal M., et al. Quel avenir pour la radiographie thoracique face au scanner ultra-low dose? // *Revue Pneumologie Clinique*. 2017. Vol. 73, N 1. P. 3–12. doi: 10.1016/j.pneumo.2016.09.007
7. Manowitz A., Sedlar M., Griffon M., et al. Use of BMI guidelines and individual dose tracking to minimize radiation exposure from low-dose helical chest CT scanning in a lung cancer screening program // *Academ Radiol*. 2012. Vol. 19, N 1. P. 84–88. doi: 10.1016/j.acra.2011.09.015
8. Paul N.S., Kashani H., Odedra D., et al. The influence of chest wall tissue composition in determining image noise during cardiac CT // *Am J Roentgenol*. 2011. Vol. 197, N 6. P. 1328–1334.
9. Blokhin I., Gomboleviskiy V., Chernina V., et al. Inter-observer agreement between low-dose and standard-dose CT with soft and

sharp convolution kernels in COVID-19 pneumonia // *J Clin Med*. 2022. Vol. 11, N 3. P. 669. doi: 10.3390/jcm11030669

10. Morozov S.P., Gomboleviskiy V.A., Elizarov A.B., et al. A simplified cluster model and a tool adapted for collaborative labeling of lung cancer CT scans // *Computer Methods Programs Biomed*. 2021. Vol. 206. P. 106111. doi: 10.1016/j.cmpb.2021.106111

11. Powell-Wiley T.M., Poirier P., Burke L.E., et al. Obesity and cardiovascular disease: a scientific statement from the American Heart Association // *Circulation*. 2021. Vol. 143, N 21. P. e984–e1010. doi: 10.1161/CIR.0000000000000973

12. The R Foundation. The R Project for Statistical Computing [интернет]. Режим доступа: <https://www.r-project.org/>. Дата обращения: 15.03.2022.

13. Fisher R.A. XXI. — On the dominance ratio // *Proceedings Royal Soc Edinburgh*. 1923. Vol. 42. P. 321–341. doi: 10.1017/S0370164600023993

14. Levene H. Robust tests for equality of variances // Olkin I., Ghurye S., Hoefding W., et al. Contributions to probability and statistics: essays in honor of harold hotelling. Stanford University Press, 1961. P. 279–292.

15. Mosteller F. Data analysis and regression: a second course in statistics. Addison-Wesley Pub. Co., Boston, 1977. 588 p.

16. Kubo T., Ohno Y., Nishino M., et al.; iLEAD Study Group. Low dose chest CT protocol (50 mAs) as a routine protocol for comprehensive assessment of intrathoracic abnormality // *Eur J Radiol Open*. 2016. Vol. 3. P. 86–94. doi: 10.1016/j.ejro.2016.04.001

17. Silin A.Y., Gruzdev I.S., Morozov S.P. The influence of model iterative reconstruction on the image quality in standard and low-dose computer tomography of the chest. Experimental study // *J Clin Pract*. 2020. Vol. 11, N 4. P. 49–54. doi: 10.17816/clinpract34900

18. Zhu Z., Ming Z.X., Feng Z.Y., et al. Feasibility study of using gemstone spectral imaging (GSI) and adaptive statistical iterative reconstruction (ASIR) for reducing radiation and iodine contrast dose in abdominal CT patients with high BMI values // *PLoS One*. 2015. Vol. 10, N 6. P. e0129201. doi: 10.1371/journal.pone.0129201

19. Filatova D.A., Sinitsin V.E., Mershina E.A. Opportunities to reduce the radiation exposure during computed tomography to assess the changes in the lungs in patients with COVID-19: use of adaptive statistical iterative reconstruction // *Digital Diagnostics*. 2021. Vol. 2, N 2. P. 94–104.

20. Lee S.W., Kim Y., Shim S.S., et al. Image quality assessment of ultra-low dose chest CT using sinogram-affirmed iterative reconstruction // *Eur Radiol*. 2014. Vol. 24, N 4. P. 817–826. doi: 10.1007/s00330-013-3090-9

AUTHORS' INFO

* Ivan A. Blokhin, MD;

address: Petrovka st. 24 bld, 1, Moscow, 127051, Russia;
ORCID: <https://orcid.org/0000-0002-2681-9378>;
eLibrary SPIN: 3306-1387; e-mail: i.blokhin@npcmr.ru

Anna P. Gonchar, MD;

ORCID: <https://orcid.org/0000-0001-5161-6540>;
eLibrary SPIN: 3513-9531; e-mail: a.gonchar@npcmr.ru

Maria R. Kodenko,

ORCID: <https://orcid.org/0000-0002-0166-3768>;
eLibrary SPIN: 5789-0319; e-mail: m.kodenko@npcmr.ru

Alexander V. Solovev, MD;

ORCID: <https://orcid.org/0000-0003-4485-2638>;
eLibrary SPIN: 9654-4005; e-mail: a.solovev@npcmr.ru

Victor A. Gomboleviskiy, MD, Cand. Sci. (Med.);

ORCID: <https://orcid.org/0000-0003-1816-1315>;
eLibrary SPIN: 6810-3279; e-mail: g_victor@mail.ru

Roman V. Reshetnikov, Cand. Sci. (Phys.-Math.);

ORCID: <https://orcid.org/0000-0002-9661-0254>;
eLibrary SPIN: 8592-0558; e-mail: reshetnikov@fbb.msu.ru

ОБ АВТОРАХ

* Блохин Иван Андреевич;

адрес: Россия, 127051, Москва, ул. Петровка, д. 24, стр. 1;
ORCID: <https://orcid.org/0000-0002-2681-9378>;
eLibrary SPIN: 3306-1387; e-mail: i.blokhin@npcmr.ru

Гончар Анна Павловна;

ORCID: <https://orcid.org/0000-0001-5161-6540>;
eLibrary SPIN: 3513-9531; e-mail: a.gonchar@npcmr.ru

Коденко Мария Романовна;

ORCID: <https://orcid.org/0000-0002-0166-3768>;
eLibrary SPIN: 5789-0319; e-mail: m.kodenko@npcmr.ru

Соловьев Александр Владимирович;

ORCID: <https://orcid.org/0000-0003-4485-2638>;
eLibrary SPIN: 9654-4005; e-mail: a.solovev@npcmr.ru

Гомболеviskiy Виктор Александрович, к.м.н.;

ORCID: <https://orcid.org/0000-0003-1816-1315>;
eLibrary SPIN: 6810-3279; e-mail: g_victor@mail.ru

Решетников Роман Владимирович, к.ф.-м.н.;

ORCID: <https://orcid.org/0000-0002-9661-0254>;
eLibrary SPIN: 8592-0558; e-mail: reshetnikov@fbb.msu.ru

* Corresponding author / Автор, ответственный за переписку

DOI: <https://doi.org/10.17816/DD108243>

Оценка показателей глобальной продольной деформации левого предсердия в диагностике кардиотоксичности

А.В. Юсупова¹, Э.С. Юсупов²¹ Клиническая больница Святителя Луки, Санкт-Петербург, Российская Федерация² Северо-Западный окружной научно-клинический центр имени Л.Г. Соколова, Санкт-Петербург, Российская Федерация

АННОТАЦИЯ

Широкий спектр крайне эффективных химиотерапевтических препаратов обладает негативным влиянием на сердечно-сосудистую систему, нивелируя успехи онкологического лечения. В связи с этим ранняя диагностика кардиотоксичности имеет крайне важное значение, позволяя вовремя применять профилактические и лечебные мероприятия.

Определение фракции выброса левого желудочка с помощью эхокардиографии — базовый неинвазивный инструментальный метод оценки сердечной функции и главный ориентир в вопросах диагностики сердечной дисфункции на фоне химиотерапии. Однако при субклиническом поражении показатель долго может оставаться нормальным, а также иметь выраженную межоператорскую вариабельность и зависимость от объемной нагрузки. Специалисты постоянно находятся в поиске оптимальных эхокардиографических параметров, позволяющих диагностировать сердечную дисфункцию на ранних стадиях. Анализ глобальной продольной деформации левого предсердия представляется перспективным методом для данных целей. Большое количество накопленных данных позволяет говорить о том, что левое предсердие является не просто камерой-кондуитом, а отражает давление наполнения левого желудочка, являясь чувствительным маркером его систолической и диастолической дисфункции.

В обзоре представлен анализ имеющихся на настоящий момент исследований по применению методики оценки глобальной продольной деформации левого предсердия в диагностике сердечной дисфункции на фоне применения кардиотоксичных препаратов.

Ключевые слова: левое предсердие; кардиоонкология; кардиотоксичность; стрейн; эхокардиография; сердечная дисфункция; антрациклины.

Как цитировать

Юсупова А.В., Юсупов Э.С. Оценка показателей глобальной продольной деформации левого предсердия в диагностике кардиотоксичности // *Digital Diagnostics*. 2022. Т. 3, № 2. С. 119–130. DOI: <https://doi.org/10.17816/DD108243>

DOI: <https://doi.org/10.17816/DD108243>

Left atrial longitudinal strain analysis in diagnostic of cardiotoxicity

Anastasiya V. Yusupova¹, Einar S. Yusupov²

¹ Clinical Hospital of St. Luke, Saint-Petersburg, Russian Federation

² North-Western District Scientific and Clinical Center named after L.G. Sokolov, Saint Petersburg, Russian Federation

ABSTRACT

A wide range of extremely effective chemotherapy drugs has a negative effect on the cardiovascular system, leveling oncological treatment success. Early diagnosis of cardiotoxicity is very important, allowing timely application of preventive and therapeutic measures. Left ventricular ejection fraction evaluation using echocardiography is the basic non-invasive instrumental method to assess cardiac function and the main guideline in cardiac dysfunction diagnosis during chemotherapy. However, if dysfunction is subclinical, the ejection fraction can remain normal for a long time, and also has a pronounced inter-operator variability and dependence on volumetric load. Specialists are constantly in search of optimal echocardiographic parameters that allow early-stage cardiac dysfunction diagnosis. Analysis of the global longitudinal deformation of the left atrium seems to be a promising method for these purposes. A large amount of accumulated data suggests that the left atrium is not just a conduit chamber, but a reflection of the filling pressure of the left ventricle, being a sensitive marker of its systolic and diastolic dysfunction. This review presents an analysis of currently available studies on applying the methodology for assessing global longitudinal deformation of the left atrium in cardiac dysfunction diagnosis in the use of cardiotoxic drugs.

Keywords: left atrial function; transthoracic echocardiography; cardiotoxic agent; left ventricular dysfunction; anthracycline.

To cite this article

Yusupova AV, Yusupov ES. Left atrial longitudinal strain analysis in diagnostic of cardiotoxicity. *Digital Diagnostics*. 2022;3(2):119–130.

DOI: <https://doi.org/10.17816/DD108243>

Received: 26.05.2022

Accepted: 16.06.2022

Published: 27.06.2022

DOI: <https://doi.org/10.17816/DD108243>

左心房整体长轴应变参数在心脏毒性诊断中的评价

Anastasiya V. Yusupova¹, Einar S. Yusupov²

¹ Clinical Hospital of St. Luke, Saint-Petersburg, Russian Federation

² North-Western District Scientific and Clinical Center named after L.G. Sokolov, Saint Petersburg, Russian Federation

简评

一系列极其有效的化疗药物对心血管系统有负面影响，从而找平了癌症治疗的成功。因此，心脏毒性的早期诊断非常重要，可以及时采取预防和治疗措施。

使用超声心动图测定左心室射血分数是评估心脏功能的基本无创仪器方法，也是化疗期间诊断心功能不全的主要指南。然而，在亚临床病变中，该指数可能在很长一段时间内保持正常，并且还具有明显的操作者间变异性和对体积负荷的依赖性。专家们一直在寻找最佳的超声心动图参数，以便在早期阶段诊断出心功能失调。左心房整体长轴应变的分析似乎是对于这些目的的有前途的方法。大量积累的数据表明，左心房不仅仅是一个导管，而是反映了左心室的充盈压力，是其收缩和舒张功能障碍的敏感标志。

本综述分析了目前关于使用心脏毒性药物诊断心脏功能障碍的左心房整体长轴应变的现有研究。

关键词：左心房；心脏肿瘤学；心脏毒性；心肌劳损；超声心动图；心功能不全；葱环类药物

To cite this article

Yusupova AV, Yusupov ES. 左心房整体长轴应变参数在心脏毒性诊断中的评价. *Digital Diagnostics*. 2022;3(2):119–130.

DOI: <https://doi.org/10.17816/DD108243>

收到: 26.05.2022

接受: 16.06.2022

发布日期: 27.06.2022

INTRODUCTION

Advances in modern oncology care have significantly increased the survival of cancer patients over recent decades. New chemotherapy drugs continue to be actively developed and introduced into clinical practice. The methods for detecting and diagnosing early cancer are improving. However, the short-term and long-term side effects of chemotherapy, such as death from heart and vascular diseases, have a significant effect on cancer mortality [1]. According to epidemiological studies, in patients successfully treated for cancer, the risk of cancer recurrence is eventually outweighed by the risk of cardiovascular diseases and their complications [2]. Cardiovascular mortality in childhood cancer survivors increases significantly after the age of 60 yr, which indicates a delayed effect of both the disease itself and treatment consequences [3]. Therefore, this patient population is the increasing focus of general practitioners and cardiologists. This is related to the general population aging as well as the fact that most cancer patients are in the age group of 65 yr and older [4]. As a result, both patients and healthcare systems have an increased burden, including financial [5].

It is now clear that this population requires a multidisciplinary approach. Cardio-oncology is a relatively new therapeutic area that focuses on patients receiving various types of cancer treatments that carry potential risks to the cardiovascular system. The systematic approach of this rapidly developing healthcare field is focused on screening, risk stratification, prevention, follow-up, and treatment of patients receiving chemotherapy and radiological treatment [6]. Cardiotoxicity is not limited to damage to the left ventricle (LV). It can be manifested by rhythm disturbances, damage to the pericardium and heart valves, coronary arteries, as well as arterial and pulmonary hypertension [7]. Simultaneously, some chemotherapy drugs cause rapid and early damage to the cardiovascular system, while side effects of other drugs appear only in many years [8]. Studies demonstrate the significance of the early detection of heart dysfunction (HD) signs, which in turn helps initiate timely treatment and prevent irreversible cardiac damage [9]. Echocardiography (Echo) plays a leading role in the diagnosis of this condition.

ECHOCARDIOGRAPHY FOR THE DIAGNOSIS OF CARDIOTOXICITY

Echocardiography is the basic diagnostic method in cardio-oncology. Measuring left ventricular ejection fraction (LVEF) using two-dimensional echocardiography remains one of the main tools in diagnosing cardiotoxicity signs and symptoms due to its availability and safety. It does, however, have some limitations, such as the inter-operator variability and the effect of image quality on the result. The ejection fraction (EF) is a volume-dependent parameter, and this often becomes critical for cancer patients, who are often hypovolemic due

to vomiting, diarrhea, and loss of appetite [10]. LVEF does not change until the complete exhaustion of compensation mechanisms and significant myocardial damage, which makes it difficult to diagnose early cardiotoxicity using only this parameter [11].

The two-dimensional speckle-tracking Echo with global longitudinal strain (GLS) evaluations of the LV improves the diagnosis of HD, including the subclinical form, by diagnosing even minimal changes in LV function [12]. However, this parameter is also dependent on preload [13]. The LV strain is well reproducible in serial measurements and can be useful in identifying risk groups for heart damage, watchful waiting, and early decision-making on the initiation of cardioprotective therapy [12, 14].

Currently, there is the concept of a strain-oriented strategy in oncological cardioprotection [15]. A randomized, controlled, multicenter study (Strain Surveillance of Chemotherapy for Improving Cardiovascular Outcomes) [10] was conducted from 2014 to 2019 and included 331 patients treated with anthracyclines. The results of this study were inconsistent. In the group of strain-oriented and conventional cardioprotective strategies, the EF was not statistically significantly different at the end of the study, so the primary endpoint was not reached. The subgroup sub-analysis revealed that LV strain-guided cardioprotective treatment significantly reduced a meaningful fall of LVEF to the abnormal range [16]. These results highlight the need for further research to determine whether the LV strain may be better than EF in identifying selected patient populations who would benefit from cardioprotective treatment to prevent cancer therapy-associated HD [10].

In 2021, the British Society of Echocardiography and the British Cardio-Oncology Society defined the following Echo criteria for cardiotoxicity: a decline in LVEF by >10% (absolute percentage points) from baseline to a value <50% (LVEF of 50 up to 54% is considered borderline and requires further information to decide if there is HD). When it comes to LV strain, a decline of <15% is considered abnormal, while only one episode of such decrease should be interpreted considering the whole clinical picture, as well as additional data, such as laboratory markers and results of other imaging techniques [17]. The authors of these guidelines emphasize that there are “grey zones” that can be seen in both the subclinical HF and normal condition, despite the integral Echo assessment of contractile function.

DIASTOLIC FUNCTION AND CARDIOTOXICITY

The measurement of diastolic function is also recommended in patients receiving cardiotoxic treatment, but its prognostic role is still unclear. Diastolic dysfunction, which is characterized by increased LV filling pressure, significantly increased the risk of cardiovascular events in the general population [18]. Studies in cancer patients demonstrate

inconsistent results and are often limited by a small sample size and a high heterogeneity of chemotherapy regimens.

The meta-analysis by M. Nagiub et al. [19] studied the predictive ability of diastolic parameters in the detection of doxorubicin-induced cardiomyopathy and showed that Doppler parameters E ($p = 0.003$), E/A ratio ($p < 0.0001$), lateral e' ($p < 0.005$), and s' ($p = 0.01$) were significantly associated with the systolic function worsening in this group of patients over a long follow-up period. However, the authors highlighted that only 4 of the 17 studies included in the meta-analysis were optimally designed and had all serial diastolic measurements.

A prospective study by J.N. Upshaw et al. ($n = 362$) [20] also studied changes in diastolic parameters during treatment with anthracyclines with/without trastuzumab. Study participants demonstrated a persistent diastolic function deterioration with decrease in the E/A ratio, lateral and septal e' velocity, and increase in the E/e' ratio E/e' ($p < 0.01$) by Month 6. The abnormal diastolic function was observed in 60% of cases after 1 yr, 70% after 2 yr, and 80% after 3 yr. The impaired function was associated with a subsequent decrease in LVEF and progressive longitudinal deformity of the LV. The authors concluded that comprehensive breast cancer therapy is associated with a moderate persistent deterioration in diastolic function with a low risk of the subsequent HD.

A meta-analysis of 13 studies ($n = 892$) by R.I. Mincu et al. [21] demonstrated that in patients without pre-existing heart disease who received anthracyclines, treatment had a modest effect on the E/A ratio ($p < 0.001$) with no change in e' and E/e' . The authors of this meta-analysis point to multiple limitations of studies and their heterogeneity with the high risk of bias, so randomized trials are required with large samples using new echocardiographic parameters (such as diastolic strain).

The aforementioned studies of diastolic function in patients receiving cardiotoxic treatment indicate the need for more careful monitoring of cancer patients and identifying an abnormal diastolic profile. Further research is also needed.

To sum up, we can say that there are still some questions, gaps, and “grey zones” related to the echocardiographic diagnosis of HD associated with the use of cardiotoxic drugs with a focus on its early signs, which should be detected to prevent irreversible myocardial damage.

LEFT ATRIUM FUNCTION AND CARDIOTOXICITY

Cardiac imaging professionals are constantly looking for available reproducible techniques and parameters that can be routinely used in clinical practice for the consistent serial evaluation with minimal inter-operator variability and maximum angle- and volume-independence. It is important to note the growing interest of researchers in the function of the left atrium (LA). Large studies have demonstrated

an independent predictive value of LA size in patients with heart failure, so this parameter can be considered a possible global prognostic indicator of the population [22, 23]. After developing the invasive techniques, such as 3D and speckle tracking Echo, it became clear that the LA is not just a conduit chamber for filling the LV. The close dynamic relationship between the LV and the LA makes it a kind of mirror reflecting the function of the LV and modulates its filling pressure through the reservoir, conduit, and contractile phases [24, 25]. The LA adapts to changes in the LV compliance by changing its own function and mechanics [26]. Over the past decade, there has been a rapid increase in publications on using speckle-tracking Echo for LA strain assessment. These data are used to assess both diastolic and atrial functions [27, 28]. The method demonstrates a good correlation with computed tomography and magnetic resonance imaging of the heart as well as with invasive measurements [29–31]. Although the deformation of the LA is not completely independent of the preload, its conditions appear to have less effect on the deformation of the LA than on its volume [32]. Simultaneously, different phases of LA contraction have some specific characteristics. For example, reservoir and contractile functions decrease until the symptoms of heart failure occur, the LA dilates, and non-invasive LV filling pressure increases, which allows to diagnose the diastolic dysfunction at the preclinical stage [33]. Evidence has been obtained during the past 10 yr in favor of using changes in parameters of the GLS of the LA as the only marker of LV diastolic dysfunction [28, 34]. We can say that LA deformity, indicating LV compliance, can be used as a significant indicator of LA dysfunction and an early marker of diastolic dysfunction when general echocardiographic parameters are still normal [35]. A meta-analysis by F. Pathan et al. [36], which included 30 studies (with 2,038 healthy volunteers), demonstrated the following normal levels of global longitudinal LA strain parameters: reservoir strain (ϵ_R) 39% (95% confidence interval (CI) 38–41), contractile strain (ϵ_{CT}) 18% (95% CI 16–19), and conduit strain (ϵ_{CD}) 23% (95% CI 21–25).

In cardio-oncological imaging, the LA function remained unstudied for a long time, since the focus was completely shifted to the LV. Its function (volume) was indirectly evaluated by examination of diastolic function. In recent years, the LA strain analysis has attracted the close attention of specialists involved in the diagnosis of cardiotoxicity.

The very first study of LA strain and cardiotoxicity was conducted in 2013 by I. Monteet al. [37] in a small sample of patients with multiple sclerosis ($n = 20$) treated with mitoxantrone. This prospective study showed a decrease in the global LA strain by the end of treatment (10 months vs. 0 months: 15.2 ± 12.5 vs. 20.2 ± 11.1 , $p < 0.05$). Cardiotoxic anthracycline drugs and epidermal growth factor inhibitors were the main focus of the subsequent studies, but other groups have also been studied. For example, the study by A. Sonagliani et al. [38] included patients ($n = 28$) receiving

bevacizumab (an inhibitor of the biological activity of vascular endothelial growth factor) for bowel cancer. Echo was performed before the start of treatment, then after 3 and 6 months with measuring positive and negative LA strain (ϵ CD and ϵ CT). After 6 months, no statistically significant changes in the parameters were observed. In subgroups of patients developing cardiotoxicity-associated HD, it was found that in patients with HD, basal echocardiographic characteristics indicating increased LV filling pressure were statistically significantly higher, including a higher E/e' ratio ($p = 0.01$) and lower baseline ϵ CD ($p = 0.007$). Accordingly, the observed changes could be predictors of HD. Similar data were obtained in a prospective study by J. Meloche et al. ($n = 51$) [39]: In nine patients who achieved the cardiotoxicity criteria, treatment with anthracyclines and trastuzumab was associated with a lower basal ϵ R ($50.0\% \pm 9.6\%$ vs. $45.6\% \pm 4.9\%$, $p = 0.058$) and ϵ CT ($30.1\% \pm 8.0\%$ vs. $24.3\% \pm 4.6\%$, $p = 0.008$). Of them, seven demonstrated an increase in ϵ CT, probably due to compensating the reduced LV function. At all phases of treatment, this group of patients showed an early decrease in LA function: ϵ CT by Month 3 (29.5 ± 7.6 vs. 27 ± 8.5 , $p = 0.008$), ϵ R ($49.7\% \pm 8.8\%$ vs. $44.4\% \pm 10.4\%$, $p < 0.001$), and ϵ CT ($20.2\% \pm 4.6\%$ vs. $17.3\% \pm 5.3\%$, $p < 0.001$) by Month 6.

R. Emerson et al. ($n = 51$) [40], M. Laufer-Perl et al. ($n = 40$) [41], S. Moustafa et al. ($n = 68$) [42], J. and Moreno et al. ($n = 52$) [43] showed a statistically significant decrease in LA strain during anthracycline therapy with or without the addition of trastuzumab. E. Setti et al. ($n = 64$) [44] found that ϵ R and LA volumes can predict the EF trend during 6 months of trastuzumab treatment.

In contrast, S. Moustafa et al. ($n = 56$) [45] and Y. Anqi et al. ($n = 40$) [46] found no differences in parameters of LA function associated with chemotherapy. In the first study [45], this can be explained by using a tyrosine kinase inhibitor as a study drug, which does not have a direct toxic effect on the heart muscle and has rather toxic effects on vessels. In the second study [46], authors pointed out that anthracyclines were administered in low doses, although the decrease in LVEF ($p < 0.05$) and LV strain ($p < 0.05$) reached statistical significance. A.T. Timóteo et al. [47] ($n = 77$) also did not find any difference in the LA deformity. The most significant declining trend was observed in ϵ CT, and this is consistent with the data of J. Meloche et al. [39] and M. Laufer-Perl et al. [41]. A retrospective study by H. Park et al. ($n = 72$) [48] included patients already treated with anthracyclines. They were subsequently divided into those who developed ($n = 13$) and did not develop ($n = 59$) HD. Basal echocardiographic findings were the same. At the end of chemotherapy, LV strain ($p = 0.002$) and ϵ R ($p < 0.001$) decreased statistically significantly in both groups. In ROC analysis, 11.7% was the optimal ϵ R reduction for predicting future HD, with sensitivity and specificity superior to LV strain. D. di Lisi et al. [49] ($n = 102$) assessed LA strain, and they were the first who determined index of LA stiffness (a new potential predictive

index, which is the E/e' to ϵ R ratio). None of the patients developed clinical signs of HD. However, 53% of the patients had subclinical dysfunction, so they were divided into two groups (with and without dysfunction). In both groups, an early increase in the index of LA stiffness ($p < 0.0001$) and a decrease in ϵ R ($p < 0.0001$) were observed. The authors concluded that these parameters could detect the early subclinical HD more accurately than the LV strain [49], and their conclusions are consistent with the findings of H. Park et al. [48].

Two cross-sectional studies should be mentioned, which evaluated long-term effects of anthracycline therapy on LA function in childhood cancer survivors. VW Li et al. ($n = 26$) [50] included men who received anthracycline treatment in childhood (time without chemotherapy 14.2 ± 5.4 yr), and they were compared with age-matched healthy people. Cancer patients had statistically significantly lower maximum ($p = 0.009$) and minimum ($p = 0.017$) values of LA volume and ϵ CT ($p = 0.011$). The authors suggested that LA remodeling, which is characterized by a decrease in its contractile function, was caused by LA fibrosis which was induced by anthracycline treatment in childhood.

R.W. Loar et al. [51] compared two groups of sex- and age-matched patients: cancer patients without chemotherapy for more than 1 yr ($n = 45$) and healthy individuals ($n = 45$). In the first group, there were statistically significantly lower ϵ R values ($p = 0.04$) compared with controls. The sub-analysis identified 11 patients as the lowest quartile with the lowest ϵ R values. In this group, all patients were statistically significantly older than the patients in top three quartiles ($p = 0.001$), who had no changes in diastolic function and LA strain, regardless of the duration of chemotherapy and doses of anthracyclines. Therefore, age was the only independent predictor of decreased LA function after cancer therapy ($p < 0.001$). A retrospective observational study by NR Patel et al. [52] showed the opposite results: Of 55 children, only those under 12 yr old had statistically significant differences in LA strain before/after chemotherapy ($p = 0.01$). As a result, the long-term effects of ongoing treatment on LA function have yet to be established, and this will require long-term observational studies.

In conclusion, we would like to present some data from a retrospective study by M. Tadic et al. ($n = 92$) [53], which showed a decrease in reservoir and conduit functions of the LA ($p < 0.001$) in cancer patients before the initiation of chemotherapy compared with a control group with comparable characteristics. The authors suggested that cancer itself may be associated with a decrease in LA function, regardless of other characteristics, and consider several hypotheses and potential mechanisms for this relationship, such as inflammation, activation of biohormonal systems, circulation of vasoactive peptides and cytokines, prevalence of smoking in this group, and disease-related changes in lifestyle (in particular, decreased activity).

To sum up, it can be noted that many studies predominantly involve women, whose initial population-based values of LA strain are higher than those of men [54]. The LA strain measurement itself has the following advantages: This is an angle-independent technique; visualization of the LA in the four-chamber position is less susceptible to lung lobe interference; and image artifacts and reverberation occur less frequently [55]. However, this method also has some limitations: The LA is a thin-walled chamber, which makes it difficult to trace the endocardium. Additionally, researchers often “cut off” the projection of the LA, shortening its longitudinal size. Remember that the dependence of the parameter on the frame rate and preload (but less than that of the LV and EF strain). Moreover, special software is required. However, simplicity and prognostic and diagnostic value of this method make it a useful tool for cardio-oncologists.

It is necessary to establish in which cases the serial measurement of the LA strain will provide the greatest advantage and complement echocardiographic findings: when used for the diagnosis of early subclinical cardiotoxicity or delayed effects of chemotherapy or for deciding on the initiation of therapy and monitoring its effectiveness. Answering these questions will require prospective controlled studies in large patient populations.

The active development of new chemotherapeutic drugs provides cardio-oncologists with new challenges. For example, an irreversible tyrosine kinase inhibitor ibrutinib is associated with a high incidence of atrial fibrillation. A recent study by A. Singh et al. [56] showed a good predictive value of LA strain in this population of patients.

REFERENCES

- Herrmann J, Lerman A, Sandhu NP, et al. Evaluation and management of patients with heart disease and cancer: cardio-oncology. *Mayo Clin Proc.* 2014;89(9):1287. doi: 10.1016/J.MAYOCP.2014.05.013
- Okwuosa TM, Anzevino S, Rao R. Cardiovascular disease in cancer survivors. *Postgrad Med J.* 2017;93(1096):82–90. doi: 10.1136/POSTGRADMEDJ-2016-134417
- Fidler MM, Reulen RC, Henson K, et al. Population-based long-term cardiac-specific mortality among 34 489 five-year survivors of childhood cancer in Great Britain. *Circulation.* 2017;135(10):951–963. doi: 10.1161/CIRCULATIONAHA.116.024811
- Miller KD, Nogueira L, Mariotto AB, et al. Cancer treatment and survivorship statistics, 2019. *CA Cancer J Clin.* 2019;69(5):363–385. doi: 10.3322/CAAC.21565
- Valero-Elizondo J, Chouairi F, Khera R, et al. Atherosclerotic cardiovascular disease, cancer, and financial toxicity among adults in the United States. *JACC CardioOncology.* 2021;3(2):236–246. doi: 10.1016/J.JACCAO.2021.02.006
- Tajiri K, Aonuma K, Sekine I. Cardio-oncology: a multidisciplinary approach for detection, prevention and management of cardiac dysfunction in cancer patients. *JJCO Japanese J Clin Oncol.* 2017;47(8):678–682. doi: 10.1093/jjco/hyx068
- Chang HM, Moudgil R, Scarabelli T, et al. Cardiovascular complications of cancer therapy: best practices in diagnosis, prevention, and management: part 1. *J Am Coll Cardiol.* 2017;70(20):2536–2551. doi: 10.1016/j.jacc.2017.09.1096
- Armstrong GT, Ross JD. Late cardiotoxicity in aging adult survivors of childhood cancer. *Prog Pediatr Cardiol.* 2014;36(1-2):19. doi: 10.1016/J.PPEDCARD.2014.09.003
- Lati G, Heck SL, Ree AH, et al. Prevention of cardiac dysfunction during adjuvant breast cancer therapy (PRADA): a 2×2 factorial, randomized, placebo-controlled, double-blind clinical trial of candesartan and metoprolol. *Eur Heart J.* 2016;37(21):1671–1680. doi: 10.1093/eurheartj/ehw022
- Lopez-Mattei JC, Hassan S. The SUCCOUR trial: a cardiovascular imager’s perspective — American College of Cardiology [Electronic resource]. Available from: <https://www.acc.org/latest-in-cardiology/articles/2021/04/16/13/09/the-succour-trial>. Accessed: 15.02.2022.
- Laufer-Perl M, Gilon D, Kapusta L, Iakobishvili Z. The role of speckle strain echocardiography in the diagnosis of early subclinical cardiac injury in cancer patients — is there more than just left ventricle global longitudinal strain? *J Clin Med.* 2021;10(1):154. doi: 10.3390/JCM10010154

Study limitations

In conclusion, limitations of the review should be noted. Most studies reported have small patient populations and are retrospective. In terms of chemotherapy regimens, they are quite heterogeneous. Some patients receive radiation therapy for the thoracic area, which may contribute to changes in echocardiographic parameters.

CONCLUSION

Therefore, currently available studies suggest the potential value of assessing LA deformity in patients receiving chemotherapy with a cardiotoxic effect.

The potential of Echo needs further research. The assessment of LA strain appears to be a promising and useful method in cardio-oncology.

ADDITIONAL INFORMATION

Funding source. This article was not supported by any external sources of funding.

Competing interests. The authors declare that they have no competing interests.

Authors’ contribution. A.V. Yusupova — review idea, literature review, collection and analysis of literary sources; E.S. Yusupov — literature review, collection and analysis of literary sources. All authors made a substantial contribution to the conception of the work, acquisition, analysis, interpretation of data for the work, drafting and revising the work, final approval of the version to be published and agree to be accountable for all aspects of the work.

12. Laufer-Pearl M, Arnold JH, Mor L, et al. The association of reduced global longitudinal strain with cancer therapy-related cardiac dysfunction among patients receiving cancer therapy. *Clin Res Cardiol.* 2020;109(2):255–262. doi: 10.1007/S00392-019-01508-9
13. Choi JO, Shin DH, Cho SW, et al. Effect of preload on left ventricular longitudinal strain by 2D speckle tracking. *Echocardiography.* 2008;25(8):873–879. doi: 10.1111/j.1540-8175.2008.00707.x
14. Santoro C, Arpino G, Esposito R, et al. 2D and 3D strain for detection of subclinical anthracycline cardiotoxicity in breast cancer patients: a balance with feasibility. *Eur Heart J Cardiovasc Imaging.* 2017;18(8):930–936. doi: 10.1093/ehjci/jex033
15. Santoro C, Esposito R, Lembo M, et al. Strain-oriented strategy for guiding cardioprotection initiation of breast cancer patients experiencing cardiac dysfunction. *Eur Heart J Cardiovasc Imaging.* 2019;20(12):1345–1352. doi: 10.1093/ehjci/jez194
16. Thavendiranathan P, Negishi T, Somers E, et al. Strain-guided management of potentially cardiotoxic cancer therapy. *J Am Coll Cardiol.* 2021;77(4):392–401. doi: 10.1016/j.jacc.2020.11.020
17. Dobson R, Ghosh AK, Ky B, et al. BSE and BCOS guideline for transthoracic echocardiographic assessment of adult cancer patients receiving anthracyclines and/or trastuzumab. *JACC CardioOncology.* 2021;3(1):1–16. doi: 10.1016/J.JACCAO.2021.01.011
18. Kuznetsova T, Thijs L, Knez J, et al. Prognostic value of left ventricular diastolic dysfunction in a general population. *J Am Hear Assoc Cardiovasc Cerebrovasc Dis.* 2014;3(3):e000789. doi: 10.1161/JAHA.114.000789
19. Nagiub M, Nixon JV, Kontos MC. Ability of nonstrain diastolic parameters to predict doxorubicin-induced cardiomyopathy: a systematic review with meta-analysis. *Cardiol Rev.* 2018;26(1):29–34. doi: 10.1097/CRD.0000000000000161
20. Upshaw JN, Finkelman B, Hubbard RA, et al. Comprehensive assessment of changes in left ventricular diastolic function with contemporary breast cancer therapy. *JACC Cardiovasc Imaging.* 2020;13(1):198–210. doi: 10.1016/J.JCMG.2019.07.018
21. Mincu RI, Lampe LF, Mahabadi AA, et al. Left ventricular diastolic function following anthracycline-based chemotherapy in patients with breast cancer without previous cardiac disease — a meta-analysis. *J Clin Med.* 2021;10(17):3890. doi: 10.3390/JCM10173890
22. Rossi A, Temporelli PL, Quintana M, et al. Independent relationship of left atrial size and mortality in patients with heart failure: an individual patient meta-analysis of longitudinal data (MeRGE Heart Failure). *Eur J Heart Fail.* 2009;11(10):929–936. doi: 10.1093/EURJHF/HFP112
23. Benjamin E, D'Agostino R, Belanger A. Left atrial size and the risk of stroke and death. The Framingham Heart Study. *Circulation.* 1995;92(4):835–841. doi: 10.1161/01.CIR.92.4.835
24. Thomas L, Marwick HT, Popescu AB, et al. Left atrial structure and function, and left ventricular diastolic dysfunction: JACC state of the art review. *J Am Coll Cardiol.* 2019;73(15):1961–1977. doi: 10.1016/J.JACC.2019.01.059
25. Serezhina EK, Obrezan AG. Significance of the echocardiographic evaluation of left atrial myocardial strain for early diagnosis of heart failure with preserved ejection fraction. *Kardiologija.* 2021;61(8):68–75. (In Russ). doi: 10.18087/cardio.2021.8.n1418
26. Kebed KY, Addetia K, Lang RM. Importance of the left atrium: more than a bystander? *Heart Fail Clin.* 2019;15(2):191–204. doi: 10.1016/j.hfc.2018.12.001
27. Litwin SE. Left atrial strain: a single parameter for assessing the dark side of the cardiac cycle? *JACC Cardiovasc Imaging.* 2020;13(10):2114–2116. doi: 10.1016/j.jcmg.2020.07.037
28. Alekhin MN, Kalinin AO. Diastolic function of the left ventricle: the meaning of left atrium longitudinal strain. *Ultrasound Funct Diagnostics.* 2020;(3):91–104. (In Russ). doi: 10.24835/1607-0771-2020-3-91-104
29. Szilveszter B, Nagy AI, Vattay B, et al. Left ventricular and atrial strain imaging with cardiac computed tomography: validation against echocardiography. *J Cardiovasc Comput Tomogr.* 2020;14(4):363–369. doi: 10.1016/j.jcct.2019.12.004
30. Kim J, Yum B, Palumbo MC, et al. Left atrial strain impairment precedes geometric remodeling as a marker of post-myocardial infarction diastolic dysfunction. *JACC Cardiovasc Imaging.* 2020;13(10):2099–2113. doi: 10.1016/j.jcmg.2020.05.041
31. Pathan F, Zainal Abidin HA, Vo QH, et al. Left atrial strain: a multi-modality, multi-vendor comparison study. *Eur Heart J Cardiovasc Imaging.* 2021;22(1):102–110. doi: 10.1093/ehjci/jez303
32. Genovese D, Singh A, Volpato V, et al. Load dependency of left atrial strain in normal subjects. *J Am Soc Echocardiogr.* 2018;31(11):1221–1228. doi: 10.1016/j.echo.2018.07.016
33. Brecht A, Oertelt-Prigione S, Seeland U, et al. Left Atrial function in preclinical diastolic dysfunction: two-dimensional speckle-tracking echocardiography — derived results from the BEFRI trial. *J Am Soc Echocardiogr.* 2016;29(8):750–758. doi: 10.1016/j.echo.2016.03.013
34. Lundberg A, Johnson J, Hage C, et al. Left atrial strain improves estimation of filling pressures in heart failure: a simultaneous echocardiographic and invasive haemodynamic study. *Clin Res Cardiol.* 2019;108:703–715. doi: 10.1007/s00392-018-1399-8
35. Mandoli GE, Sisti N, Mondillo S, et al. Left atrial strain in left ventricular diastolic dysfunction: have we finally found the missing piece of the puzzle? *Heart Fail Rev.* 2020;25(3):409–417. doi: 10.1007/s10741-019-09889-9
36. Pathan F, D'Elia N, Nolan MT, et al. Normal ranges of left atrial strain by speckle-tracking echocardiography: a systematic review and meta-analysis. *J Am Soc Echocardiogr.* 2017;30(1):59–70.e8. doi: 10.1016/j.echo.2016.09.007
37. Monte I, Bottari V, Buccheri S, et al. Chemotherapy-induced cardiotoxicity: subclinical cardiac dysfunction evidence using speckle tracking echocardiography. *J Cardiovasc Echogr.* 2013;23(1):33–38. doi: 10.4103/2211-4122.117983
38. Sonagliani A, Albini A, Fossile E, et al. Speckle-tracking echocardiography for cardioncological evaluation in bevacizumab-treated colorectal cancer patients. *Cardiovasc Toxicol.* 2020;20(6):581–592. doi: 10.1007/s12012-020-09583-5
39. Meloche J, Nolan M, Amir E, et al. Temporal changes in left atrial function in women with HER2+ breast cancer receiving sequential anthracyclines and trastuzumab therapy. *J Am Coll Cardiol.* 2018;71(11):A1524. doi: 10.1016/s0735-1097(18)32065-5
40. Emerson P, Stefani L, Terluk A, et al. Left atrial strain analysis in breast cancer patients post anthracycline (AC). *Hear Lung Circ.* 2021;30:S196. doi: 10.1016/j.hlc.2021.06.225
41. Laufer-Pearl M, Arias O, Dorfman SS, et al. Left atrial strain changes in patients with breast cancer during anthracycline therapy. *Int J Cardiol.* 2021;330:238–244. doi: 10.1016/J.IJCARD.2021.02.013
42. Moustafa S, Murphy K, Nelluri BK, et al. Temporal trends of cardiac chambers function with trastuzumab in hu-

man epidermal growth factor receptor ii-positive breast cancer patients. *Echocardiography*. 2016;33(3):406–415. doi: 10.1111/echo.13087

43. Moreno J, García-Sáez JA, Clavero M, et al. Effect of breast cancer cardiotoxic drugs on left atrial myocardium mechanics. Searching for an early cardiotoxicity marker. *Int J Cardiol*. 2016;210:32–34. doi: 10.1016/j.ijcard.2016.02.093

44. Setti E, Dolci G, Bergamini C, et al. P2460 prospective evaluation of atrial function by 2D speckle tracking analysis in HER-2 positive breast cancer patients during Trastuzumab therapy. *Eur Heart J*. 2019;40(Suppl 1):2460. doi: 10.1093/eurheartj/ehz748.0792

45. Moustafa S, Ho TH, Shah P, et al. Predictors of Incipient dysfunction of all cardiac chambers after treatment of metastatic renal cell carcinoma by tyrosine kinase inhibitors. *J Clin Ultrasound*. 2016;44(4):221. doi: 10.1002/JCU.22333

46. Anqi Y, Yu Z, Mingjun X, et al. Use of echocardiography to monitor myocardial damage during anthracycline chemotherapy. *Echocardiography*. 2019;36(3):495–502. doi: 10.1111/echo.14252

47. Timóteo AT, Moura Branco L, Filipe F, et al. Cardiotoxicity in breast cancer treatment: What about left ventricular diastolic function and left atrial function? *Echocardiography*. 2019;36(10):1806–1813. doi: 10.1111/echo.14487

48. Park H, Kim KH, Kim HY, et al. Left atrial longitudinal strain as a predictor of cancer therapeutics-related cardiac dysfunction in patients with breast cancer. *Cardiovasc Ultrasound*. 2020;18(1):1–8. doi: 10.1186/S12947-020-00210-5

49. Di Lisi D, Cadeddu Dessalvi C, Manno G, et al. Left atrial strain and left atrial stiffness for early detection of cardiotoxicity in cancer patients. *Eur Heart J*. 2021;42(Suppl 1):2021. doi: 10.1093/eurheartj/ehab724.021

50. Li VW, Lai CT, Liu AP, et al. Left atrial mechanics and integrated calibrated backscatter in anthracycline-treated long-term survivors of childhood cancers. *Ultrasound Med Biol*. 2017;43(9):1897–1905. doi: 10.1016/j.ultrasmedbio.2017.05.017

51. Loar RW, Colquitt JL, Rainusso NC, et al. Assessing the left atrium of childhood cancer survivors. *Int J Cardiovasc Imaging*. 2021;37(1):155–162. doi: 10.1007/s10554-020-01970-x

52. Patel NR, Chyu CK, Satou GM, et al. Left atrial function in children and young adult cancer survivors treated with anthracyclines. *Echocardiography*. 2018;35(10):1649–1656. doi: 10.1111/echo.14100

53. Tadic M, Genger M, Cuspidi C, et al. Phasic left atrial function in cancer patients before initiation of anti-cancer therapy. *J Clin Med*. 2019;8(4):421. doi: 10.3390/JCM8040421

54. Liao JN, Chao TF, Kuo JY, et al. Age, sex, and blood pressure-related influences on reference values of left atrial deformation and mechanics from a large-scale asian population. *Circ Cardiovasc Imaging*. 2017;10(10):e006077. doi: 10.1161/CIRCIMAGING.116.006077

55. Cameli M, Mandoli GE, Loiacono F, et al. Left atrial strain: a new parameter for assessment of left ventricular filling pressure. *Heart Fail Rev*. 2016;21(1):65–76. doi: 10.1007/S10741-015-9520-9

56. Singh A, El Hangouche N, McGee K, et al. Utilizing left atrial strain to identify patients at risk for atrial fibrillation on ibrutinib. *Echocardiography*. 2021;38(1):81–88. doi: 10.1111/echo.14946

СПИСОК ЛИТЕРАТУРЫ

1. Herrmann J, Lerman A, Sandhu N.P., et al. Evaluation and management of patients with heart disease and cancer: cardio-oncology // Mayo Clin. Proc. 2014. Vol. 89, № 9. P. 1287. doi: 10.1016/J.MAYOCP.2014.05.013

2. Okwuosa T.M., Anzevino S., Rao R. Cardiovascular disease in cancer survivors // Postgrad Med J. 2017. Vol. 93, № 1096. P. 82–90. doi: 10.1136/POSTGRADMEDJ-2016-134417

3. Fidler M.M., Reulen R.C., Henson K., et al. Population-based long-term cardiac-specific mortality among 34 489 five-year survivors of childhood cancer in Great Britain // Circulation. 2017. Vol. 135, № 10. P. 951–963. doi: 10.1161/CIRCULATIONAHA.116.024811

4. Miller K.D., Nogueira L., Mariotto A.B., et al. Cancer treatment and survivorship statistics, 2019 // CA Cancer J Clin. 2019. Vol. 69, № 5. P. 363–385. doi: 10.3322/CAAC.21565

5. Valero-Elizondo J., Chouairi F., Khera R., et al. Atherosclerotic cardiovascular disease, cancer, and financial toxicity among adults in the United States // JACC CardioOncology. 2021. Vol. 3, № 2. P. 236–246. doi: 10.1016/J.JACCAO.2021.02.006

6. Tajiri K., Aonuma K., Sekine I. Cardio-oncology: a multidisciplinary approach for detection, prevention and management of cardiac dysfunction in cancer patients // JJCO Japanese J Clin Oncol. 2017. Vol. 47, № 8. P. 678–682. doi: 10.1093/jjco/hyx068

7. Chang H.M., Moudgil R., Scarabelli T., et al. Cardiovascular complications of cancer therapy: best practices in diagnosis, prevention, and management: part 1 // J Am College Cardiol. 2017. Vol. 70, № 20. P. 2536–2551. doi: 10.1016/j.jacc.2017.09.1096

8. Armstrong G.T., Ross J.D. Late Cardiotoxicity in aging adult survivors of childhood cancer // Prog Pediatr Cardiol. 2014. Vol. 36, № 1–2. P. 19. doi: 10.1016/J.PPEDCARD.2014.09.003

9. Lati G., Heck S.L., Ree A.H., et al. Prevention of cardiac dysfunction during adjuvant breast cancer therapy (PRADA): a 2x2 factorial, randomized, placebo-controlled, double-blind clinical trial of candesartan and metoprolol // Eur Heart J. 2016. Vol. 37, № 21. P. 1671–1680. doi: 10.1093/eurheartj/ehw022

10. Lopez-Mattei J.C., Hassan S. The SUCCOUR trial: a cardiovascular imager's perspective — American College of Cardiology [Electronic resource]. Режим доступа: <https://www.acc.org/latest-in-cardiology/articles/2021/04/16/13/09/the-succour-trial>. Дата обращения: 15.02.2022.

11. Laufer-Perl M., Gilon D., Kapusta L., et al. The role of speckle strain echocardiography in the diagnosis of early subclinical cardiac injury in cancer patients — is there more than just left ventricle global longitudinal strain? // J Clin Med. 2021. Vol. 10, № 1. P. 154. doi: 10.3390/JCM10010154

12. Laufer-Pearl M., Arnold J.H., Mor L., et al. The association of reduced global longitudinal strain with cancer therapy-related cardiac dysfunction among patients receiving cancer therapy // Clin Res Cardiol. 2020. Vol. 109, № 2. P. 255–262. doi: 10.1007/S00392-019-01508-9

13. Choi J.O., Shin D.H., Cho S.W., et al. Effect of preload on left ventricular longitudinal strain by 2D speckle tracking // Echocardiography. 2008. Vol. 25, № 8. P. 873–879. doi: 10.1111/j.1540-8175.2008.00707.x

14. Santoro C., Arpino G., Esposito R., et al. 2D and 3D strain for detection of subclinical anthracycline cardiotoxicity in breast cancer patients: a balance with feasibility // Eur Heart J Cardiovasc Imaging. 2017. Vol. 18, № 8. P. 930–936. doi: 10.1093/ehjci/jex033

15. Santoro C., Esposito R., Lembo M., et al. Strain-oriented strategy for guiding cardioprotection initiation of breast cancer patients experiencing cardiac dysfunction // Eur Heart

- J Cardiovasc Imaging. 2019. Vol. 20, № 12. P. 1345–1352. doi: 10.1093/ehjci/jez194
16. Thavendiranathan P., Negishi T., Somers E., et al. Strain-guided management of potentially cardiotoxic cancer therapy // *J Am Coll Cardiol*. 2021. Vol. 77, № 4. P. 392–401. doi: 10.1016/j.jacc.2020.11.020
 17. Dobson R., Ghosh A.K., Ky B., et al. BSE and BCOS guideline for transthoracic echocardiographic assessment of adult cancer patients receiving anthracyclines and/or trastuzumab // *JACC CardioOncology*. 2021. Vol. 3, № 1. P. 1–16. doi: 10.1016/J.JACCAO.2021.01.011
 18. Kuznetsova T., Thijs L., Knez J., et al. Prognostic value of left ventricular diastolic dysfunction in a general population // *J Am Hear Assoc Cardiovasc Cerebrovasc Dis*. 2014. Vol. 3, № 3. P. e000789. doi: 10.1161/JAHA.114.000789
 19. Nagiub M., Nixon J.V., Kontos M.C. Ability of nonstrain diastolic parameters to predict doxorubicin-induced cardiomyopathy: a systematic review with meta-analysis // *Cardiol Rev*. 2018. Vol. 26, № 1. P. 29–34. doi: 10.1097/CRD.0000000000000161
 20. Upshaw J.N., Finkelman B., Hubbard R.A., et al. Comprehensive assessment of changes in left ventricular diastolic function with contemporary breast cancer therapy // *JACC Cardiovasc*. 2020. Vol. 13, № 1. P. 198–210. doi: 10.1016/J.JCMG.2019.07.018
 21. Mincu R.I., Lampe L.F., Mahabadi A.A., et al. Left ventricular diastolic function following anthracycline-based chemotherapy in patients with breast cancer without previous cardiac disease — a meta-analysis // *J Clin Med*. 2021. Vol. 10, № 17. P. 3890. doi: 10.3390/JCM10173890
 22. Rossi A., Temporelli P.L., Quintana M., et al. Independent relationship of left atrial size and mortality in patients with heart failure: an individual patient meta-analysis of longitudinal data (MERGE Heart Failure) // *Eur J Heart Fail*. 2009. Vol. 11, № 10. P. 929–936. doi: 10.1093/EURJHF/HFP112
 23. Benjamin B., D'Agostino R., Belanger A., et al. Left atrial size and the risk of stroke and death. The Framingham Heart Study // *Circulation*. 1995. Vol. 92, № 4. P. 835–841. doi: 10.1161/01.CIR.92.4.835
 24. Thomas L., Marwick H.T., Popescu A.B., et al. Left atrial structure and function, and left ventricular diastolic dysfunction: JACC state of the art review // *J Am Coll Cardiol*. 2019. Vol. 73, № 15. P. 1961–1977. doi: 10.1016/J.JACC.2019.01.059
 25. Сережина Е.К., Обрезан А.Г. Значимость эхокардиографической оценки деформации миокарда левого предсердия в ранней диагностике сердечной недостаточности с сохраненной фракцией выброса // *Кардиология*. 2021. Т. 61, № 8. С. 68–75. doi: 10.18087/cardio.2021.8.n1418
 26. Kebed K.Y., Addetia K., Lang R.M. Importance of the left atrium: more than a bystander? // *Heart Failure Clinics*. 2019. Vol. 15, № 2. P. 191–204. doi: 10.1016/j.hfc.2018.12.001
 27. Litwin S.E. Left atrial strain: a single parameter for assessing the dark side of the cardiac cycle? // *JACC: Cardiovascular Imaging*. 2020. Vol. 13, № 10. P. 2114–2116. doi: 10.1016/j.jcmg.2020.07.037
 28. Алехин М.Н., Калинин А.О. Диастолическая функция левого желудочка: значение глобальной продольной деформации левого предсердия // *Ультразвуковая и функциональная диагностика*. 2020. № 3. P. 91–104. doi: 10.24835/1607-0771-2020-3-91-104
 29. Szilveszter B., Nagy A.I., Vattay B., et al. Left ventricular and atrial strain imaging with cardiac computed tomography: validation against echocardiography // *J Cardiovasc Comput Tomogr*. 2020. Vol. 14, № 4. P. 363–369. doi: 10.1016/j.jcct.2019.12.004
 30. Kim J., Yum B., Palumbo M.C., et al. Left atrial strain impairment precedes geometric remodeling as a marker of post-myocardial infarction diastolic dysfunction // *JACC Cardiovasc. Imaging*. 2020. Vol. 13, № 10. P. 2099–2113. doi: 10.1016/j.jcmg.2020.05.041
 31. Pathan F., Zainal Abidin H.A., Vo Q.H., et al. Left atrial strain: a multi-modality, multi-vendor comparison study // *Eur Heart J Cardiovasc*. 2021. Vol. 22, № 1. P. 102–110. doi: 10.1093/ehjci/jez303
 32. Genovese D., Singh A., Volpato V., et al. Load dependency of left atrial strain in normal subjects // *J Am Soc Echocardiogr*. 2018. Vol. 31, № 11. P. 1221–1228. doi: 10.1016/j.echo.2018.07.016
 33. Brecht A., Oertelt-Prigione S., Seeland U., et al. Left atrial function in preclinical diastolic dysfunction: two-dimensional speckle-tracking echocardiography — derived results from the BEFRI Trial // *J Am Soc Echocardiogr*. 2016. Vol. 29, № 8. P. 750–758. doi: 10.1016/j.echo.2016.03.013
 34. Lundberg A., Johnson J., Hage C., et al. Left atrial strain improves estimation of filling pressures in heart failure: a simultaneous echocardiographic and invasive haemodynamic study // *Clin Res Cardiol*. 2019. Vol. 108. P. 703–715. doi: 10.1007/s00392-018-1399-8
 35. Mandoli G.E., Sisti N., Mondillo S., et al. Left atrial strain in left ventricular diastolic dysfunction: have we finally found the missing piece of the puzzle? // *Heart Fail Rev*. 2020. Vol. 25, № 3. P. 409–417. doi: 10.1007/s10741-019-09889-9
 36. Pathan F., D'Elia N., Nolan M.T., et al. Normal ranges of left atrial strain by speckle-tracking echocardiography: a systematic review and meta-analysis // *J Am Soc Echocardiogr*. 2017. Vol. 30, № 1. P. 59–70.e8. doi: 10.1016/j.echo.2016.09.007
 37. Monte I., Bottari V., Buccheri S., et al. Chemotherapy-induced cardiotoxicity: subclinical cardiac dysfunction evidence using speckle tracking echocardiography // *J Cardiovasc Echogr*. 2013. Vol. 23, № 1. P. 33–38. doi: 10.4103/2211-4122.117983
 38. Sonaglioli A., Albin A., Fossile E., et al. Speckle-tracking echocardiography for cardioncological evaluation in bevacizumab-treated colorectal cancer patients // *Cardiovasc Toxicol*. 2020. Vol. 20, № 6. P. 581–592. doi: 10.1007/s12012-020-09583-5
 39. Meloche J., Nolan M., Amir E., et al. Temporal changes in left atrial function in women with HER2+ breast cancer receiving sequential anthracyclines and trastuzumab therapy // *J Am Coll Cardiol*. 2018. Vol. 71, № 11. P. A1524. doi: 10.1016/s0735-1097(18)32065-5
 40. Emerson P., Stefani L., Terluk A., et al. Left atrial strain analysis in breast cancer patients post anthracycline (AC) // *Hear Lung Circ*. 2021. Vol. 30. P. S196. doi: 10.1016/j.hlc.2021.06.225
 41. Laufer-Perl M., Arias O., Dorfman S.S., et al. Left atrial strain changes in patients with breast cancer during anthracycline therapy // *Int J Cardiol*. 2021. Vol. 330. P. 238–244. doi: 10.1016/J.IJCARD.2021.02.013
 42. Moustafa S., Murphy K., Nelluri B.K., et al. Temporal trends of cardiac chambers function with trastuzumab in human epidermal growth factor receptor ii-positive breast cancer patients // *Echocardiography*. 2016. Vol. 33, № 3. P. 406–415. doi: 10.1111/echo.13087
 43. Moreno J., García-Sáez J.A., Clavero M., et al. Effect of breast cancer cardiotoxic drugs on left atrial myocardium mechanics. Searching for an early cardiotoxicity marker // *Int J Cardiol*. 2016. Vol. 210. P. 32–34. doi: 10.1016/j.ijcard.2016.02.093
 44. Setti E., Dolci G., Bergamini C., et al. P2460 prospective evaluation of atrial function by 2D speckle tracking analysis in HER-2 positive breast cancer patients during Trastuzumab therapy // *Eur Heart J*. 2019. Vol. 40, Suppl. 1. P. 2460. doi: 10.1093/eurheartj/ehz748.0792

45. Moustafa S., Ho T.H., Shah P., et al. Predictors of incipient dysfunction of all cardiac chambers after treatment of metastatic renal cell carcinoma by tyrosine kinase inhibitors // *J Clin Ultrasound*. 2016. Vol. 44, № 4. P. 221. doi: 10.1002/JCU.22333
46. Anqi Y., Yu Z., Mingjun X., et al. Use of echocardiography to monitor myocardial damage during anthracycline chemotherapy // *Echocardiography*. 2019. Vol. 36, № 3. P. 495–502. doi: 10.1111/echo.14252
47. Timóteo A.T., Moura Branco L., Filipe F., et al. Cardiotoxicity in breast cancer treatment: what about left ventricular diastolic function and left atrial function? // *Echocardiography*. 2019. Vol. 36, № 10. P. 1806–1813. doi: 10.1111/echo.14487
48. Park H., Kim K.H., Kim H.Y., et al. Left atrial longitudinal strain as a predictor of cancer therapeutics-related cardiac dysfunction in patients with breast cancer // *BioMed Central*. 2020. Vol. 18, № 1. P. 1–8. doi: 10.1186/S12947-020-00210-5
49. Di Lisi D., Cadeddu Dessalvi C., Manno G., et al. Left atrial strain and left atrial stiffness for early detection of cardiotoxicity in cancer patients // *Eur Heart J*. 2021. Vol. 42, Suppl. 1. P. 2021. doi: 10.1093/eurheartj/ehab724.021
50. Li V.W., Lai C.T., Liu A.P., et al. Left atrial mechanics and integrated calibrated backscatter in anthracycline-treated long-term survivors of childhood cancers // *Ultrasound Med Biol*. 2017. Vol. 43, № 9. P. 1897–1905. doi: 10.1016/j.ultrasmedbio.2017.05.017
51. Loar R.W., Colquitt J.L., Rainusso N.C., et al. Assessing the left atrium of childhood cancer survivors // *Int J Cardiovasc*. 2021. Vol. 37, № 1. P. 155–162. doi: 10.1007/s10554-020-01970-x
52. Patel N.R., Chyu C.K., Satou G.M., et al. Left atrial function in children and young adult cancer survivors treated with anthracyclines // *Echocardiography*. 2018. Vol. 35, № 10. P. 1649–1656. doi: 10.1111/echo.14100
53. Tadic M., Genger M., Cuspidi C., et al. Phasic left atrial function in cancer patients before initiation of anti-cancer therapy // *J Clin Med*. 2019. Vol. 8. P. 421. doi: 10.3390/JCM8040421
54. Liao J.N., Chao T.F., Kuo J.Y., et al. Age, sex, and blood pressure-related influences on reference values of left atrial deformation and mechanics from a large-scale asian population // *Circ Cardiovasc Imaging*. 2017. Vol. 10, № 10. P. e006077. doi: 10.1161/CIRCIMAGING.116.006077
55. Cameli M., Mandoli G.E., Loiacono F., et al. Left atrial strain: a new parameter for assessment of left ventricular filling pressure // *Heart Fail Rev*. 2016. Vol. 21, № 1. P. 65–76. doi: 10.1007/S10741-015-9520-9
56. Singh A., El Hangouche N., McGee K., et al. Utilizing left atrial strain to identify patients at risk for atrial fibrillation on ibrutinib // *Echocardiography*. 2021. Vol. 38, № 1. P. 81–88. doi: 10.1111/echo.14946

AUTHORS' INFO

* Anastasiya V. Yusupova; MD;

address: 46 Chugunnaya street, Saint-Petersburg, 194044, Russia;
ORCID: <https://orcid.org/0000-0002-0763-0537>;
eLibrary SPIN: 1492-1947; e-mail: yusupova@lucaclinic.ru

Einar S. Yusupov, MD, Cand. Sci. (Med.);

ORCID: <https://orcid.org/0000-0002-4716-0314>;
eLibrary SPIN: 6632-4484; e-mail: usupov_as@mail.ru

ОБ АВТОРАХ

* Юсупова Анастасия Владимировна;

адрес: Россия, 194044, Санкт-Петербург, ул. Чугунная, д. 46;
ORCID: <https://orcid.org/0000-0002-0763-0537>;
eLibrary SPIN: 1492-1947; e-mail: yusupova@lucaclinic.ru

Юсупов Эйнар Салихович, к.м.н.;

ORCID: <https://orcid.org/0000-0002-4716-0314>;
eLibrary SPIN: 6632-4484; e-mail: usupov_as@mail.ru

* Corresponding author / Автор, ответственный за переписку

DOI: <https://doi.org/10.17816/DD100779>

Стриминговые технологии: из игровой индустрии в телеультразвуковые исследования

К.М. Арзамасов¹, Т.М. Бобровская¹, В.А. Дроговоз²¹ Научно-практический клинический центр диагностики и телемедицинских технологий, Москва, Российская Федерация² Научно-производственное объединение «РусБИТех», Москва, Российская Федерация

АННОТАЦИЯ

Обоснование. Стремительное развитие игровой индустрии привело к появлению многих технических средств и технологий с уникальными характеристиками. Одной из таких технологий, имеющих высокий потенциал к применению в медицинской диагностике, является стриминг (потокное онлайн-вещание). Подключив ультразвуковой сканер к системе видеозахвата, возможно существенно расширить функционал диагностического устройства.

Цель — изучить возможность применения достижений информационных технологий игровой индустрии в телемедицине на примере телеультразвуковых исследований.

Материалы и методы. В данном исследовании проводили запись ультразвукового видеоизображения при помощи системы видеозахвата, разработанной для геймеров. Видеоизображение получалось в ходе телеультразвукового исследования брахицефальных артерий в следующих режимах: серошкальный В-режим, цветное дуплексное картирование и импульсно-доплеровский режим. В режиме реального времени проводили трансляцию исследования на видеостриминговый сервис.

Результаты. Получены оптимальные показатели видеоизображения, а также определены минимально допустимые настройки видеостриминга для адекватной дистанционной оценки врачом-экспертом по ультразвуковому исследованию. Рекомендуется использовать на автоматизированном рабочем месте видеозахвата следующие настройки: видео 1280×720, 24 кадра в секунду, кодировщик H.264, битрейт не менее 350 Кбит/с.

Заключение. Использование технических и программных средств, разработанных для стриминга видеоигр, возможно для обеспечения телеультразвуковых исследований.

Ключевые слова: телемедицина; телеУЗИ; УЗИ; видеозахват; стриминг.

Как цитировать

Арзамасов К.М., Бобровская Т.М., Дроговоз В.А. Стриминговые технологии: из игровой индустрии в телеультразвуковые исследования // *Digital Diagnostics*. 2022. Т. 3, № 2. С. 131–140. DOI: <https://doi.org/10.17816/DD100779>

DOI: <https://doi.org/10.17816/DD100779>

Streaming technology: from games to tele-ultrasound

Kirill M. Arzamasov¹, Tatiana M. Bobrovskaya¹, Viktor A. Drogovoz²

¹ Moscow Center for Diagnostics and Telemedicine, Moscow, Russian Federation

² Scientific and Production Association "RusBITech", Moscow, Russian Federation

ABSTRACT

BACKGROUND: Due to the gaming industry's rapid development, a large number of technical tools and technologies with unique characteristics have emerged. One of these technologies, which can be potentially used in medical diagnostics, is streaming (online streaming). By connecting an ultrasound scanner to a video capture system, it is possible to significantly expand the diagnostic device's functionality.

AIM: To investigate the possibility of applying the gaming industry's information technology in telemedicine, like tele-ultrasound.

MATERIALS AND METHODS: In this study, an ultrasound video image was captured using a video capture system developed for gamers. The video was obtained during brachycephalic arteries ultrasound in the following modes: greyscale B-mode, color duplex, and pulse Doppler mode. The examination was broadcast to a video streaming service in real time.

RESULTS: An expert sonologist obtained optimal video image parameters and determined the minimum required video streaming settings for an adequate remote evaluation. The following video capture workstation settings are recommended: video, 1280×720; 24 fps; H.264 encoder; bitrate, at least 350 Kbps.

CONCLUSIONS: Using technical and software tools developed for video game streaming to provide tele-ultrasound is possible.

Keywords: telemedicine; tele-ultrasound; ultrasound; video capture; streaming.

To cite this article

Arzamasov KM, Bobrovskaya TM, Drogovoz VA. Streaming technology: from games to tele-ultrasound. *Digital Diagnostics*. 2022;3(2):131–140.

DOI: <https://doi.org/10.17816/DD100779>

Received: 15.02.2022

Accepted: 06.04.2022

Published: 05.06.2022

DOI: <https://doi.org/10.17816/DD100779>

直播技术：从游戏行业到远程超声检查

Kirill M. Arzamasov¹, Tatiana M. Bobrovskaya¹, Viktor A. Drogovoz²

¹ Moscow Center for Diagnostics and Telemedicine, Moscow, Russian Federation

² Scientific and Production Association "RusBITech", Moscow, Russian Federation

简评

论证。游戏产业的快速发展导致了许多具有独特特点的技术和技术工具的出现。其中一项在医学诊断中具有很大应用潜力的技术是流式传输（网络直播）。通过将超声波扫描仪连接到视频捕获系统，可以显著扩展诊断设备的功能。

目的是以远程超声检查为例，研究将游戏产业信息技术成果应用于远程医疗的可能性。

材料与方法。在这项研究中，使用专为游戏玩家设计的视频捕获系统记录了超声视频图像。视频图像是在对头臂动脉进行远程超声检查期间以下列模式获得的：灰度B型超声、彩超和脉冲多普勒模式。这项研究在一个视频流服务中实时播放。

结果。获得了视频图像的最佳指标，并确定了最小容许视频流设置，以便由超声专家进行充分的远程评估。建议在视频捕获自动化工位上使用以下设置：视频1280×720，每秒24帧，H. 264编码器，码率不低于 350Kbps。

结论。为游戏流传输开发的硬件和软件可以用于远程超声检查。

关键词：远程医疗；远程超声检查；超声检查；视频捕获；流式传输。

To cite this article

Arzamasov KM, Bobrovskaya TM, Drogovoz VA. 直播技术：从游戏行业到远程超声检查. *Digital Diagnostics*. 2022;3(2):131–140.

DOI: <https://doi.org/10.17816/DD100779>

收到: 15.02.2022

接受: 06.04.2022

发布日期: 05.06.2022

BACKGROUND

Tele-ultrasound is a new technique for ultrasound examination employing telemedicine. Digital ultrasound images from this examination are forwarded to an expert for remote evaluation. Applications for ultrasound systems with built-in remote consultation functionality are expanding constantly. However, updating the ultrasound diagnosis equipment remains an urgent challenge [1, 2].

A standard smartphone can be used to get a telemedicine consultation based on ultrasound findings, by sending an image or a cine-loop captured on the built-in camera [3–5]. However, because the message would contain personal data, this method is not always practical and quite risky.

The majority of ultrasound scanners older than 10–20 years have a video output for an external display and/or video printer. Gaming solutions (specific devices for in-game audio and video capture [6]) and live game streaming software may increase the functionality of outdated diagnostic equipment.

The aim of the study is to investigate the possibility of applying the gaming industry's information technology in telemedicine, like tele-ultrasound.

MATERIALS AND METHODS

The study subject was one of the authors who underwent ultrasound of the neck vessels in 2019. Greyscale B-mode, color duplex, pulse Doppler, and combinations thereof (greyscale B-mode + color duplex; greyscale B-mode + pulse Doppler) were the imaging modes that were used. Sequoia 512 Acuson ultrasound scanner was used. Images from the

ultrasound scanner were recorded using Ezcap 295 HD video capture system (<http://www.ezcap.com>).

OBS Studio 24.0.3 by Open Broadcaster Software (<http://www.obsproject.com>) was used for remote communication of the study findings. OBS Studio is a free open-source software for video recording and streaming. Twitch (<http://twitch.tv>) was used as a streaming service. A personal computer with the following characteristics was used as a video capture workstation: AMD Ryzen 5 3400G processor, 16 GB RAM, NVIDIA GeForce RTX 2070 graphics card, Windows 10 Pro 64-bit OS, LAN 100 Mbs, BenQ 21.5" IPS monitor, 1920 × 1080. An expert used a laptop with the following characteristics for remote evaluation: AMD E-450 APU, 8 GB RAM, Radeon HD7470 graphics card, Windows 7 64-bit OS, WiFi 72 Mbs, 15.6" monitor, 1366 × 768. Redmi Note 4 smartphone with the following characteristics was used as a mobile device: 3 GB RAM, 5.5" IPS monitor, 1920 × 1080, 401 ppi, 4G Internet. Prestige 338 video recorder, 1920 × 1080, 25 fps, webcam mode, was used for recording the findings of ultrasound examination.

The image quality was evaluated by three functional (ultrasound) diagnosis professionals with a combined experience of more than 10 yr. The quality of the study was considered sufficient if an expert could assess the segmentation of the intima-media complex correctly.

Microsoft Excel was used for statistical processing of the results. The measured parameters were presented as mean ± SD. The correlation of the parameters was assessed by the Spearman's rank correlation coefficient, since the data were nonparametric.

Figure 1 shows the flow chart of tele-ultrasound using streaming technology.

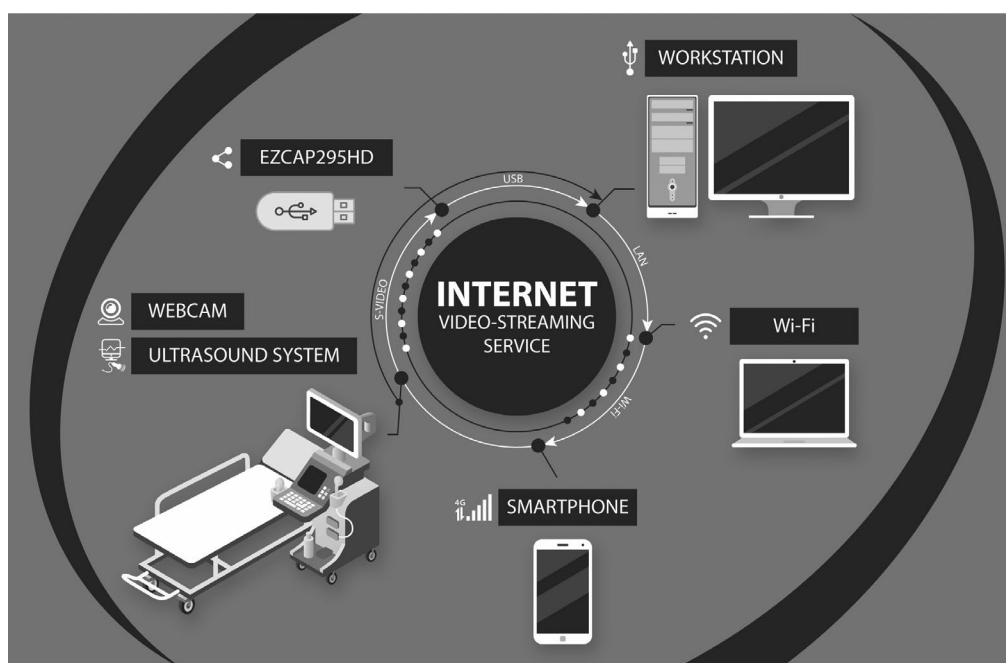


Fig. 1. Tele-ultrasound flow chart. The ultrasound system, to which Ezcap 295 HD (video capture device) is connected via S-Video (video output standard), which in turn is connected via USB to the workstation. The webcam is also connected to the workstation via USB. Video/audio streaming is performed via the video streaming service. The clients are a laptop connected to the Internet via Wi-Fi and a 4G-smartphone.

The expert opinion was based on a binary scale: If all three experts agreed that the server-side and client-side video quality were comparable, the evaluation was positive. If at least one expert concluded that the video quality did not match the original, the evaluation was negative. For the quality evaluation, each expert viewed the server-side and client-side image at the same time. The experts performed the quality evaluation independently.

RESULTS

The connection pattern was as follows: the ultrasound scanner's video output was connected to Ezcap 295 HD video capture board's input, which was then connected via USB to the video capture workstation with OBS Studio installed. An S-Video VCR output was used as the video output of the ultrasound scanner. On the video capture device, the corresponding video input was utilized. The maximum settings were set up by hardware: FULL-HD (1920 × 1080), 30 fps (the frame rate could not be changed and corresponded to the factory settings). Ezcap 295 HD was automatically detected on the video capture workstation once the video capture device driver was installed, and it was added as the video source in the OBS Studio. The image quality on the video capture workstation display was compared with the original quality on the ultrasound scanner display. Three experts evaluated the image, and they all came to the conclusion that the image quality on the video capture workstation display corresponds to that of the ultrasound scanner display.

Proper operation of tele-ultrasound requires two video streams (from the ultrasound machine and from the webcam pointed at the anatomical area under examination). These two video streams are merged in the video capture workstation and transmitted to a remote server. To test this feature, a webcam with 1920 × 1080 source image size was connected. To avoid interference, the image from the webcam was reduced to 640 × 360 by bicubic interpolation and superimposed on top of the image from the ultrasound scanner in the corner, outside the workspace.

The video capture device had a fixed resolution where the analog signal was digitized. The resolution of 1080p is unnecessarily large for the ultrasound scanner video output. As a result, bicubic interpolation the image size was used to reduced image size to 1280 × 720 by to save traffic during video streaming. The experts found no visual differences between the images on the video capture workstation display before and after interpolation.

The following step included configuring OBS Studio to stream video on Twitch and the streaming. The image quality was evaluated on remote devices (laptop and smartphone) connected to the video streaming web service. Nvidia NVENC hardware-based multithreaded encoder was used for video encoding in the video capture workstation. The video quality was set to maximum. These settings ensured CPU load not more than 15% and GPU load not more than 30%. The only

parameter that required adjustment was the video bitrate. A constant bitrate was selected to ensure uniform video quality.

In this study, we searched for the lowest possible video bitrate for reliable remote evaluation by an expert. We decided to begin the video stream at 3,000 Kbps, with a subsequent decrease of the bitrate to the minimum level, where, in the view of the expert, the ultrasound image quality would differ significantly from the original image. Each bitrate value was subjected to three measures, with a mandatory stop and restart of streaming in between each measurement. The stream contained cine-loops in greyscale B-mode, cine-loops in duplex mode (greyscale B-mode + color duplex or greyscale B-mode + pulse Doppler), and freeze frames, including those with ongoing measurements.

The expert opinion was based on a binary scale: The evaluation was positive if all three experts agreed that the server-side and client-side video quality was similar. The evaluation was negative if at least one expert concluded that the video quality did not match the original. For the quality evaluation, each expert viewed the server-side and client-side image at the same time. The experts performed the quality evaluation independently. Table 1 shows the results of tele-ultrasound system testing depending on bitrate settings.

The minimum bitrate of 200 Kbps resulted in a blurred image. The experts concurred that the image was not suitable for proper evaluation of ultrasound structures. Only freeze frames exhibited decent image quality at the 300 Kbps bitrate. According to the study, the ultrasound image was less clear when viewed on a laptop and more clear when viewed on a smartphone. For all devices and modes, the ultrasound image quality was satisfactory at 350 Kbps bitrate and above.

We also evaluated the time lag between server-side and client-side videos. Depending on the bitrate, the time lag was 3.94–4.92 s. As the bitrate decreased, so did the time lag (correlation coefficient: 0.82).

DISCUSSION

Currently, telemedicine research and consultations can be employed in areas where there is severe lack of medical professionals, particularly specialized ones, as well as in facilities with outdated equipment, as in the case of this study. There should also be consideration for the accessibility of mobile communications in our country. Therefore, using a smartphone is appropriate and enables speedy connection to a teleconference, particularly for remote counseling in case of emergency.

We were able to do an ultrasound with remote analysis by expert doctors using the Ezcap 295 HD, which the manufacturer markets as a video capture device for video games. This device provided high quality of video images required for efficient work of ultrasound diagnosis professionals.

Table 1. Results of remote testing of the tele-ultrasound system by experts

Video capture workstation	Remote evaluation of an ultrasound image by an expert				
Video bitrate. Kbps	Client type	Connection type	Input stream rate \pm SD. Kbps	Time lag \pm SD. s	Quality evaluation by experts
3000	Laptop	WiFi	456.80 \pm 76.28	4.92 \pm 0.24	+
	Smartphone	4G			+
2000	Laptop	WiFi	311.75 \pm 9.14	4.45 \pm 0.28	+
	Smartphone	4G			+
1000	Laptop	WiFi	153.92 \pm 19.56	4.64 \pm 0.49	+
	Smartphone	4G			+
500	Laptop	WiFi	110.00 \pm 2.24	4.24 \pm 0.54	+
	Smartphone	4G			+
350	Laptop	WiFi	89.00 \pm 4.85	3.94 \pm 0.36	+
	Smartphone	4G			+
300	Laptop	WiFi	83.67 \pm 1.15	4.03 \pm 0.31	-
	Smartphone	4G			+
200	Laptop	WiFi	70.00 \pm 0.9	4.11 \pm 0.38	-
	Smartphone	4G			-

We have chosen OBS Studio by Open Broadcaster Software as one of the well-liked free open-source streaming software tools for gaming. This software instantly detected and connected to Ezcap 295 HD. Twitch, which is marketed as a video game streaming service, was selected to test the streaming. In this study, we only used it to test the operability of the proposed system. Thus, the findings of this study only support the possibility of using the OBS Studio software for the purposes described above. It is possible to stream video to any video streaming platform with OBS Studio (according to the information on the site).

For the future implementation of tele-ultrasound, we advise using video streaming platforms that offer private streaming protected from unauthorized connection and viewing. The study did not assess such platforms. However, when it comes to remote research in general and tele-ultrasound in particular, information security is essential. Tele-ultrasound is used to stream two forms of confidential data. These are medical and personal data, the security of which must be guaranteed in accordance with the current rules and requirements of the Russian law. Private health information, such as medical data exchanged back and forth between the client and the server, should not be disclosed to third parties in any way. We advise that anonymized medical data (images from an ultrasound scanner) and associated medical documents (including personal data) should be transferred as two different streams using different security and encryption algorithms in order to increase the security of research. In the future, the transmission of anonymized ultrasound frames with a user identifier (UID) may be considered. The UID can be matched with the patient's name and other

personal data in the health information system database or using hardware/software security gateways (e.g., Vipnet Coordinator).

In this study, we assumed that the ideal bitrate for H.264 video streaming at 1280 \times 720 would be 3000 Kbps [7]. However, the tests revealed that the image quality did not change significantly when the bitrate was decreased down to 350 Kbps. This can be explained by the fact that most of the image streamed from the ultrasound scanner is static. According to a detailed analysis of the ultrasound scanner's image, the area of interest on the original image does not exceed 880 \times 822. After bicubic interpolation, the area of interest does not exceed 586 \times 548, which requires a three times lower bitrate. Furthermore, there are fewer bits needed to encode the ultrasound image because it is not in color. The color duplex mode has a limited color area/chart, which also ensures good performance at low bitrates.

We believe that we have selected the best possible video streaming settings for the study: 1920 \times 1080 and 25 fps for the input image from the ultrasound scanner; 1920 \times 1080 and 24 fps for the input image from the webcam; video output 1280 \times 720, 24 fps; H.264 encoder (Nvidia NVENC); and minimum bitrate of 350 Kbps.

In conclusion, it can be claimed that the suggested settings enable stable transmission of a high-quality video image from an ultrasound scanner to any client device, including a smartphone, with a cellular Internet connection. This enables the technology to be used for the streaming of ultrasound findings via VSAT space communication technologies. Tele-ultrasound cannot be negatively impacted by a video broadcasting delay of less than 5 s.

In the literature, there are reports on the use of platforms for mass communication (e.g., Voip), which are highly efficient when employed in tele-ultrasound [8]. For example, A.S. Liteplo et al. [3] compared the most widely used Voip platforms, Skype, and iChat. The authors concluded that iChat was superior to Skype. Later, it was demonstrated that Skype could be used effectively as well [4, 9]. Additionally, it has been demonstrated that using Apple FaceTime for tele-ultrasound can be a good option [10].

The aforementioned technologies require the installation of specialist software and make connecting clients much more challenging if there are several clients. Our findings show that ultrasound video streaming technology enables viewing the video on any Internet-connected device without the need for client-side installation of specialist software. The proposed technology allows an unlimited number of users to view the streamed data. This may be useful for multidisciplinary team meetings and consultations involving specialists and experts from various health facilities, including those in remote areas, as well as distance education of medical personnel. We can also assume that improved image quality on an ultrasound scanner will improve the image quality on a laptop or smartphone. Thus, we used video capture at 1080p, the highest resolution possible for a video capture device. Technically, an ultrasound machine with a digital video interface (HDMI, DVI-D, and DP) and high resolution (Full HD and higher) can be used together with the video capture device under consideration.

Furthermore, this study differs from similar ones in that it used software and technical solutions developed for the gaming industry, which are outside the scope of other researchers. Nonetheless, we were able to show that these solutions could be successfully applied to address medical issues.

Modern ultrasound scanners can transfer the research findings in digital format, and some models can perform tele-ultrasound without the use of additional devices; however, many devices still lack these capabilities and have lower ultrasound image quality. The methodology we describe may be appropriate for health facilities with low-cost or outdated equipment. The display resolution for ultrasound examination recommended by the American Association of Physicists in Medicine and the Society for Imaging Informatics in Medicine is 3 Mp (2048 × 1536) [11]. The described technique can be used with ultrasound scanners of a higher class when using video capture devices that support this resolution.

Study limitations

We can assume that this technical solution is also applicable to other ultrasound scanners with similar or different outputs supported by a video capture device although this study only evaluated one ultrasound scanner.

There has only been one video capture device tested. We believe that a video capture device with performance specifications non-inferior to those of the Ezcap 295 HD can produce a comparable result.

In this study, the quality of ultrasound images was evaluated solely based on subjective criteria. We accepted this limitation because all ultrasounds are a priori subjective and involve a human factor present at every stage, from ultrasound image display to assessment of ultrasound findings.

Finally, this study did not provide for testing of other video streaming platforms.

To date, numerous codecs (devices or software for data/signal conversion) have been developed, but in this work, we used H.264. Noise suppression, which is common in the H.264+, H.265, and H.265+ codecs, can negatively affect the ultrasound image quality, necessitating additional research to evaluate the changes made to the quality of transmitted ultrasound signal.

CONCLUSION

Video game streaming technologies can be used in telemedicine, for example, for on-site tele-ultrasound or mobile hospitals that have a portable ultrasound machine with a video output is available. The advantages of these technologies are their availability and high quality of the broadcast video image while using a minimum bandwidth of communication channels. In addition, this ultrasound technology can be used for distance learning or remote counseling.

Given that it is intended to transfer medical data for full-fledged work in a clinical setting, the issue of communication channel security from unauthorized access to transmitted medical information must also be addressed.

ADDITIONAL INFORMATION

Funding source. This study was not supported by any external sources of funding.

Competing interests. The authors declare that they have no competing interests.

Authors' contribution. All authors made a substantial contribution to the conception of the work, acquisition, analysis, interpretation of data for the work, drafting and revising the work, final approval of the version to be published and agree to be accountable for all aspects of the work. K.M. Arzamasov — research design development, volunteer during research; K.M. Arzamasov, T.M. Bobrovskaya — data analysis; K.M. Arzamasov, T.M. Bobrovskaya, V.A. Drogozov — data interpretation; K.M. Arzamasov, V.A. Drogozov — writing a manuscript.

Acknowledgments. The authors express their gratitude to the Head of the Department of Functional Diagnostics of the SCC of JSC "Russian Railways" S.V. Ivanov for his assistance in organizing and conducting the study on the basis of the SCC of JSC "Russian Railways", and also to the doctor of the Department of functional diagnostics of the SCC of JSC "Russian Railways" E.V. Andreeva for assistance in conducting the study. The authors express their gratitude to graphic designer T.A. Savosina for creating an illustration for the article, as well as M.V. Vlasova for the translation.

REFERENCES

1. Shchepin VO. Equipment and activity of ultrasound diagnostics units of medical organizations of the Russian Federation. *Bulletin of the N.A. Semashko National Research Institute Public Health*. 2014;(S):20–26. (In Russ).
2. Sterlikov SA, Leonov SA, Son IM, et al. Provision of diagnostic equipment for medical organizations providing outpatient care. *Health Care Manager*. 2016;(3):44–55. (In Russ).
3. Liteplo AS, Noble VE, Attwood BH. Real-time video streaming of sonographic clips using domestic internet networks and free videoconferencing software. *J Ultrasound Med*. 2011;30(11):1459–1466. doi: 10.7863/jum.2011.30.11.1459
4. Jensen SH, Duvald I, Aagaard R, et al. Remote real-time ultrasound supervision via commercially available and low-cost tele-ultrasound: a mixed methods study of the practical feasibility and users' acceptability in an emergency department. *J Digit Imaging*. 2019;32(5):841–848. doi: 10.1007/s10278-018-0157-9
5. Kim C, Cha H, Kang BS, et al. A feasibility study of smartphone-based telesonography for evaluating cardiac dynamic function and diagnosing acute appendicitis with control of the image quality of the transmitted videos. *J Digit Imaging*. 2016;29(3):347–356. doi: 10.1007/s10278-015-9849-6
6. Lomb B, Güneysu T. Decrypting HDCP-protected video streams using reconfigurable hardware. *Proc 2011 Int Conf Reconfigurable Comput FPGAs. ReConFig*. 2011. P. 249–254. doi: 10.1109/RECONFIG.2011.24
7. Aaron A, Li Z, Manohara M, et al. Per-title encode optimization. The Netflix Techblog, 2015. Available from: <https://netflixtechblog.com/per-title-encode-optimization-7e99442b62a2>. Accessed: 15.02.2022.
8. Carbone M, Ferrari V, Marconi M, et al. A tele-ultrasonographic platform to collect specialist second opinion in less specialized hospitals. *Updates Surg*. 2018;70(3):407–413. doi: 10.1007/s13304-018-0582-9
9. McBeth P, Crawford I, Tiruta C, et al. Help is in your pocket: the potential accuracy of smartphone- and laptop-based remotely guided resuscitative telesonography. *Telemed e-Health*. 2013;19(12):924–930. doi: 10.1089/tmj.2013.0034
10. Miyashita T, Iketani Y, Nagamine Y, Goto T. FaceTime for teaching ultrasound-guided anesthetic procedures in remote place. *J Clin Monit Comput*. 2014;28(2):211–215. doi: 10.1007/s10877-013-9514-x
11. College of radiology, American. ACR-AAPM-SIIM technical standard for electronic practice of medical IMAGING. 2017. Available from: <https://cdn.ymaws.com/siim.org/resource/resmgr/guidelines/elec-practice-medimag-2017.pdf>. Accessed: 15.02.2022.

СПИСОК ЛИТЕРАТУРЫ

1. Щепин В.О. Оснащенность и деятельность подразделений ультразвуковой диагностики медицинских организаций Российской Федерации // Бюллетень Национального научно-исследовательского института общественного здоровья имени Н.А. Семашко. 2014. № 5. С. 20–26.
2. Стерликов С.А., Леонов С.А., Сон И.М., и др. Обеспеченность диагностическим оборудованием медицинских организаций, оказывающих помощь в амбулаторных условиях // Менеджер здравоохранения. 2016. № 3. С. 44–55.
3. Liteplo A.S., Noble V.E., Attwood B.H. Real-time video streaming of sonographic clips using domestic internet networks and free videoconferencing software // J Ultrasound Med. 2011. Vol. 30, N 11. P. 1459–1466. doi: 10.7863/jum.2011.30.11.1459
4. Jensen S.H., Duvald I., Aagaard R., et al. Remote real-time ultrasound supervision via commercially available and low-cost tele-ultrasound: a mixed methods study of the practical feasibility and users' acceptability in an emergency department // J Digit Imaging. 2019. Vol. 32, N 5. P. 841–848. doi: 10.1007/s10278-018-0157-9
5. Kim C., Cha H., Kang B.S., et al. A feasibility study of smartphone-based telesonography for evaluating cardiac dynamic function and diagnosing acute appendicitis with control of the image quality of the transmitted videos // J Digit Imaging. 2016. Vol. 29, N 3. P. 347–356. doi: 10.1007/s10278-015-9849-6
6. Lomb B., Güneysu T. Decrypting HDCP-protected video streams using reconfigurable hardware // Proc 2011 Int Conf Reconfigurable Comput FPGAs. ReConFig. 2011. P. 249–254. doi: 10.1109/RECONFIG.2011.24
7. Aaron A., Li Z., Manohara M., et al. Per-title encode optimization. The Netflix Techblog, 2015. Режим доступа: <https://netflixtechblog.com/per-title-encode-optimization-7e99442b62a2>. Дата обращения: 15.02.2022.
8. Carbone M., Ferrari V., Marconi M., et al. A tele-ultrasonographic platform to collect specialist second opinion in less specialized hospitals // Updates Surg. 2018. Vol. 70, N 3. P. 407–413. doi: 10.1007/s13304-018-0582-9
9. McBeth P., Crawford I., Tiruta C., et al. Help is in your pocket: the potential accuracy of smartphone- and laptop-based remotely guided resuscitative telesonography // Telemed e-Health. 2013. Vol. 19, N 12. P. 924–930. doi: 10.1089/tmj.2013.0034
10. Miyashita T., Iketani Y., Nagamine Y., Goto T. FaceTime for teaching ultrasound-guided anesthetic procedures in remote place // J Clin Monit Comput. 2014. Vol. 28, N 2. P. 211–215. doi: 10.1007/s10877-013-9514-x
11. College of radiology, American. ACR-AAPM-SIIM technical standard for electronic practice of medical IMAGING. 2017. Режим доступа: <https://cdn.ymaws.com/siim.org/resource/resmgr/guidelines/elec-practice-medimag-2017.pdf>. Дата обращения: 15.02.2022.

AUTHORS' INFO

*** Kirill M. Arzamasov**, MD, Cand. Sci. (Med.);
address: Petrovka st. 24 bld, 1, Moscow, 127051, Russia;
ORCID: <http://orcid.org/0000-0001-7786-0349>;
eLibrary SPIN: 3160-8062; e-mail: k.arzamasov@npcmr.ru

Tatiana M. Bobrovskaya;
ORCID: <http://orcid.org/0000-0002-2746-7554>;
eLibrary SPIN: 3400-8575; e-mail: t.bobrovskaya@npcmr.ru

Viktor A. Drogozov, Cand. Sci. (Technical);
ORCID: <https://orcid.org/0000-0001-9582-7147>;
eLibrary SPIN: 1804-2636; e-mail: Vdrog@mail.ru

ОБ АВТОРАХ

*** Арзамасов Кирилл Михайлович**, к.м.н.;
адрес: Россия, 127051, Москва, ул. Петровка, д. 24 стр. 1;
ORCID: <http://orcid.org/0000-0001-7786-0349>;
eLibrary SPIN: 3160-8062; e-mail: k.arzamasov@npcmr.ru

Бобровская Татьяна Михайловна;
ORCID: <http://orcid.org/0000-0002-2746-7554>;
eLibrary SPIN: 3400-8575; e-mail: t.bobrovskaya@npcmr.ru

Дрогвоз Виктор Анатольевич, к.т.н.;
ORCID: <https://orcid.org/0000-0001-9582-7147>;
eLibrary SPIN: 1804-2636; e-mail: Vdrog@mail.ru

* Corresponding author / Автор, ответственный за переписку

DOI: <https://doi.org/10.17816/DD104865>

Килевидная деформация грудной клетки по «верхнему» типу (синдром Куррарино–Сильвермана): клинический случай

D. Mannatrizio¹, G. Fascia¹, G. Guglielmi^{1, 2}¹ Department of Clinical and Experimental Medicine, Foggia University School of Medicine, Фоджа, Италия² Radiology Unit, Barletta University Hospital, Барлетта, Италия

АННОТАЦИЯ

Преждевременное слияние некоторых центров окостенения грудины и сращение манубриостерального сочленения приводят к редкой форме деформации грудной клетки, называемую синдромом Куррарино–Сильвермана. У пациентов наблюдается аномально короткая грудина со смещением вперёд в области манубриостерального сочленения. Наиболее часто сочетается с сердечно-лёгочными заболеваниями и деформациями позвоночника. Подобную аномалию также ассоциируют с синдромами Нунан и Тернера.

В статье представлен случай 66-летней пациентки, обратившейся в клинику для прохождения повторной компьютерной томографии после операции и химиотерапии по поводу рака молочной железы, с жалобами на частые ежегодные эпизоды одышки, кашля, бронхита, более выраженные в детстве. Результаты компьютерной томографии показали отсутствие метастатических поражений и других сопутствующих заболеваний, за исключением редкой формы деформации передней грудной стенки, так называемой килевидной деформации верхней части грудной клетки (*pectus carinatum* — *верхний киль*) по хондроманубриальному типу. Угол в дорсальном направлении составлял 130°, длина грудины 9 см без вдавления в нижней трети.

Ключевые слова: килевидная деформация грудной клетки; компьютерная томография; грудина; деформация костей.

Как цитировать

Mannatrizio D., Fascia G., Guglielmi G. Килевидная деформация грудной клетки по «верхнему» типу (синдром Куррарино–Сильвермана): клинический случай // *Digital Diagnostics*. 2022. Т. 3, № 2. С. 141–148. DOI: <https://doi.org/10.17816/DD104865>

DOI: <https://doi.org/10.17816/DD104865>

“Superior Pectus Carinatum” (Currarino–Silverman Syndrome) in a 66-year-old woman: a case report

Domenico Mannatrizio¹, Giacomo Fascia¹, Giuseppe Guglielmi^{1, 2}

¹ Department of Clinical and Experimental Medicine, Foggia University School of Medicine, Foggia, Italy

² Radiology Unit, Barletta University Hospital, Barletta, Italy

ABSTRACT

The premature fusion of some of the sternal ossification centers and the obliteration of the manubrio-sternal joint caused a rare deformity called Currarino–Silverman syndrome. Patients present an abnormally short sternum with a forward angulation at the manubrio-sternal junction. Cardiopulmonary diseases and spinal deformities are the most frequent related disorders. It was also described as a component of Turner’s and Noonan’s syndromes.

Herein, we present the case of a 66-year-old woman who presented to our clinic for follow-up computed tomography after surgery and chemotherapy for breast cancer with frequent episodes of dyspnea, wheezing, bronchitis, and mild dyspnea annually, which was more frequent during childhood. Computed tomography showed the absence of metastatic lesions and other accompanying diseases, except for a rare deformity of the anterior chest wall, the so-called, a “superior” pectus carinatum, a chondromanubrial deformity with a dorsal-open angle of 130°, and a sternum body length of 9 cm, which is not depressed in the lower third.

Keywords: pectus carinatum; computed tomography; sternum; bone deformity.

To cite this article

Mannatrizio D, Fascia G, Guglielmi G. “Superior Pectus Carinatum” (Currarino–Silverman Syndrome) in a 66-year-old woman: a case report. *Digital Diagnostics*. 2022;3(2):141–148. DOI: <https://doi.org/10.17816/DD104865>

Received: 14.03.2022

Accepted: 06.06.2022

Published: 30.06.2022

DOI: <https://doi.org/10.17816/DD104865>

一例66岁女性“上部鸡胸” (Currarino-Silverman综合征) 病例

Domenico Mannatrizio¹, Giacomo Fascia¹, Giuseppe Guglielmi^{1,2}

¹ Department of Clinical and Experimental Medicine, Foggia University School of Medicine, Foggia, Italy

² Radiology Unit, Barletta University Hospital, Barletta, Italy

摘要

Currarino-Silverman综合征是一种罕见的畸形，由一些胸骨骨化中心过早融合和胸骨柄-胸骨关节闭塞导致。患者胸骨异常短小，胸骨柄-胸骨连接处成角向前突出。最常见的相关疾病有心肺疾病和脊柱畸形。还被描述为特纳综合征和努南综合征的组成部分。在此，我们介绍了1例66岁女性患者，其在因乳腺癌接受手术和化疗后到我们诊所进行计算机断层成像（CT）随访，其每年频繁出现呼吸困难、喘息、支气管炎和轻度呼吸困难，这些症状在儿童期更为频繁。CT显示无转移病灶和其他伴随疾病，仅发现罕见的前胸壁畸形，即“上部”鸡胸，其软骨柄畸形，背侧张开角130°，胸骨体长9cm，下三分之一处未凹陷。

关键词：鸡胸；CT；胸骨；骨畸形。

To cite this article

Mannatrizio D, Fascia G, Guglielmi G. 一例66岁女性“上部鸡胸”（Currarino-Silverman综合征）病例. *Digital Diagnostics*. 2022;3(2):141-148. DOI: <https://doi.org/10.17816/DD104865>

收到: 14.03.2022

接受: 06.06.2022

发布日期: 30.06.2022

BACKGROUND

The most common congenital chest wall malformations (CWMs) are pectus excavatum (PE) and pectus carinatum (PC). These anomalies present during the first years of life and occur during childhood. PC is less frequent than PE, and it affects 5%–15% of all patients with CWMs and occurs in approximately 1:1000 to 1:10000 of all live births, with a male predominance (4:1) (1) (2). The mild forms are more frequent than the severe forms of PC (3). The chondromanubrial type was first described by Guido Currarino and Frederic Silverman in 1958 (4).

The real etiopathogenesis of type 2 PC is still unknown, but the most plausible hypothesis is that the deformity is caused by an excessive growth of costal cartilage secondary to genetic factors, which results in a sternal deformity without sternal pathology (5).

A short, solid sternum with prominent outward protrusion and bilateral deformity of the second to fifth costal cartilages that form an acute intercostal angle is the pathognomonic aspect of this syndrome (5). The xiphoid process is usually directed forward, even if it can be also absent. In very rare cases, a “superior or chondromanubrial PC” has a normal length, and the sternum is not depressed in the lower third.

Degenerative changes in hyaline cartilages, atypical fibrils, reduced number of chondrocytes, and thin periosteum are observed microscopically (6).

DESCRIPTION OF THE CASE

A 66-year-old woman presented to our clinic to undergo a follow-up computed tomography (CT) after surgery and chemotherapy for breast cancer. She also reported 3–4 episodes of bronchitis, wheezing, and mild dyspnea annually, which was more frequent during her childhood.

She underwent CT of the chest and abdomen with contrast enhancement, which showed the absence of metastatic lesions and any other respiratory tract disorders but revealed a chondromanubrial deformity with a dorsal-open angle of 130° and a sternum body length of 9 cm, which was not depressed in the lower third. Dorsal kyphosis was also present.

During the anamnesis, her CWM was not evident because she was dressed up with a turtleneck sweater that covered her chest.

She reported having an unknown inborn CWM, which was first noted at the age of 3 and progressed until the age of 13 years, accompanied by dyspnea and wheezing that accentuated during exercise and recurrent respiratory infections.

Moreover, the aesthetic appearance of her chest had psychological implications in her childhood, such as having strange feeling among her schoolmates, insecurity, withdrawal, and avoidance of all sports activities that require

exposure of the chest. She has passed her childhood hiding her health problem.

DISCUSSION

The Currarino–Silverman (CS) syndrome is an extremely rare congenital deformity of the sternum.

It is also known by the terms “pouter pigeon chest,” “chondromanubrial deformity,” “type 2 pectus carinatum,” and “pectus arcuatum.” According to the original paper of Currarino and Silverman (4), this rare developmental anomaly is characterized by prominent sternal angulation with a decrease in length as a result of congenital complete non-segmentation or premature synostosis of the sternum.

The theory of a congenital etiology by gene downregulation is predominant (7–11). Essentially, a family history of CWMs is present in approximately 25% of the patients (1).

An abnormality of the differentiation of anterior segment mesenchymal cells and abnormal migration of mesenchymal cardiac precursors to the endothelial heart tube at the time of cardiogenesis may result in defects of endocardial cushion, sternum, and aortic arch derivatives (7). This syndrome is often combined with congenital heart defects and spinal abnormalities (kyphosis, scoliosis, and kyphoscoliosis), and it was also described as a component of Turner’s and Noonan’s syndromes (8).

Frequent confusion of CS syndrome with PE deformity is still an issue since one-third of patients present with concomitant mild to moderate depression of the lower third of the sternum (9).

Indeed, CS syndrome can be easily mistaken with PE, as both deformities appear in an almost similar fashion, but surgical approaches are very different. A distinctive feature of a PE deformity is the beginning of the sternal depression at the angle of Louis that becomes progressively deeper toward the xiphoid process with distorted and elongated cartilages (10). The angle of Louis must be less than 110° to be considered a true depression (5). Thus, confusion about classification is still an actual issue.

A uniform classification is a basis for surgical treatment and assessment of its short- and long-term results.

In 2006, Acastello classified CWMs based on the site of the defect’s origin (type 1, cartilaginous; type 2, costal; type 3, chondrocostal; type 4, sternal; type 5, clavicle-scapular) and attributed CS syndrome to the cartilaginous type 2 (superior) PC. Further, Torre *et al.* distinguished superior PC into two types:

- Type 1: The “inferior” or “chondrogladiolar” is the most frequent type, in which the sternal protrusion is located in the inferior or mid sternum and the last ribs can be slightly or severely depressed on lateral aspects.
- Type 2: The “superior” or “chondromanubrial” is the less frequent type, which has been further divided in



Fig 1. Sagittal whole body computed tomography scan showing an arching sternum and a chondromanubrial deformity with a dorsal-open angle of 130°.

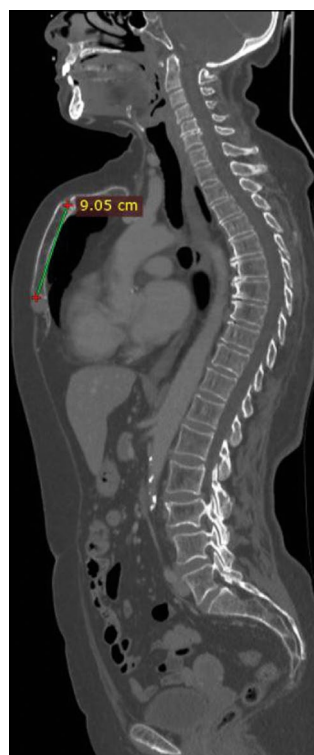


Fig 2. Sagittal whole body computed tomography scan showing a sternum body length of 9 cm and dorsal kyphosis.

two types depending on the external aspect. The first type is characterized by a superior PC with an inferior PE in which the sternum is S-shaped on a lateral view. This anomaly is classified as cartilaginous anomalies and called type II. Although this anomaly is considered a cartilaginous anomaly and a type II PC in the Acastello classification, Torre *et al.* classified it as part of sternal anomalies because of the sternal origin of the anomaly. The second type is a “superior PC” without the typical features of the CS syndrome. The sternum has a normal length and is not depressed in the lower third. This anomaly is probably due to a

cartilage anomaly similarly to inferior PC. Torre *et al.* proposed to use the term “superior PC” only for this type and to include this anomaly in the first category (cartilaginous anomalies) of CWM classification. This entity is extremely rare.

Most patients with CS syndrome are asymptomatic; therefore, surgical correction is optional, and different opinions exist about the ideal age for surgical correction. Asthma and chronic bronchitis, which occur in 16% of the patients, are the most common associated concomitant diseases, responsible for bronchial and pulmonary symptoms (11).



Fig 3. Lateral plain radiograph appearance of a type 2 pectus carinatum.

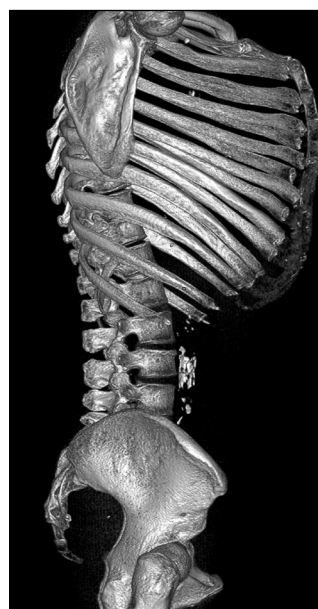


Fig 4. Computed tomography reconstruction of the rib cage showing that the sternum has a normal length and is not depressed in the lower third.

Kyphosis is present, to a greater or lesser degree, in almost all patients. Pain or tenderness at the protrusion site, decreased endurance, or palpitations can be present. Limitations at work and in sports and underachievement in school, in the absence of respiratory and heart diseases, should be attributed to emotional alterations.

A strong correlation of inborn cardiac pathology with CS syndrome has been reported, such as VSD, patent ductus arteriosus, atrial septal defect, tetralogy of Fallot, transposition of the great arteries, and coarctation of the aorta.

Chest CT with three-dimensional reconstruction, or magnetic resonance imaging in children with altered tissue density and radiation concern, is the best preoperative imaging for the evaluation of patients with CS. It allows the differential diagnosis with other pectus deformities, determination of the exact angles of the costal cartilages to the sternum, and enhances surgical planning.

In comparison to PE, several less invasive techniques have been developed for the correction of PC, including the Abramson procedure and its modifications, along with nonsurgical options such as observation, orthotic bracing, and dynamic compression (2) (12). However, due to the extreme rarity of the disease, challenging deformity, and variable anatomy of a fused sternum, there are no clear guidelines in the treatment approaches.

This unique growth pattern contributes to an almost universal failure of conservative treatment options, such as the vacuum bell or a compressive orthosis. The best surgical option remains the relatively aggressive Ravitch-type procedure with multi-level wedge osteotomy (12) (13), allowing for the achievement of a satisfactory outcome.

Given the rarity of the deformity, surgical correction should be completed by a multidisciplinary team, including thoracic reconstructive surgeons with experience in pectus

deformities. The preferred age for correction is late puberty or adulthood, as cartilage resection will be performed when the rib growth ends (1) (14) (15). It is important to keep in mind the potential for thoracic dystrophy should cartilage resection be performed at a young age or too extensively. Thus, other studies have reported the preferable age of 5–7 years or early adolescence (5) (16). Some patients who refused to undergo surgery turned to bodybuilding to improve and define the musculature around the CWM to minimize the appearance of protrusion. Even if this approach does not correct the abnormality, it can improve self-esteem and confidence. For female patients, one possibility to make protrusion less noticeable and improve the appearance of the chest is breast augmentation (17).

CONCLUSION

Although a rare condition, CS can be easily diagnosed through its typical radiological findings. Therefore, clinicians must be aware of and recognize this imaging pattern to make an accurate diagnosis and prevent further examination and aggressive treatment.

ADDITIONAL INFORMATION

Funding source. This study was not supported by any external sources of funding.

Competing interests. The authors declare that they have no competing interests.

Authors' contribution. All authors made a substantial contribution to the conception of the work, acquisition, analysis, interpretation of data for the work, drafting and revising the work, final approval of the version to be published and agree to be accountable for all aspects of the work.

Consent for publication. Written consent was obtained from the patient for publication of relevant medical information within the manuscript.

REFERENCES

1. Shamberger RC, Welch KJ. Surgical correction of pectus carinatum. *J Pediatr Surg*. 1987;22(1):48–53. doi: 10.1016/s0022-3468(87)80014-3
2. Muntean A, Stoica I, Saxena AK. Pigeon chest: comparative analysis of surgical techniques in minimal access repair of pectus carinatum (MARPC). *World J Pediatr*. 2018;14(1):18–25. doi: 10.1007/s12519-018-0121-2
3. Emil S. Current options for the treatment of pectus carinatum: when to brace and when to operate? *Eur J*. 2018;28(4):347–354. doi: 10.1055/s-0038-1667297
4. Currarino G, Silverman F. Premature obliteration of the sternal sutures and pigeon-breast deformity. *Radiology*. 1958;70(4):532–540. doi: 10.1148/70.4.532
5. Fokin A, Steuerwald NM, Ahrens WA, Allen KE. Anatomical, histologic, and genetic characteristics of congenital chest wall deformities. *Semin Thorac Cardiovasc Surg*. 2009;21(1):44–57. doi: 10.1053/j.semtcvs.2009.03.001
6. Fokin A. Pouter pigeon breast. *Chest Surg Clin N Am*. 2000;10(2):377–391.
7. Gabrielsen T, Ladyman G. Early closure of the sternal sutures and congenital heart disease. *Am J Roentgenol Radium Ther Nucl Med*. 1963;89:975–983.
8. Chidambaram B, Mehta AV. Currarino-Silverman syndrome (pectus carinatum type 2 deformity) and mitral valve disease. *Chest*. 1992;102(3):780–782. doi: 10.1378/chest.102.3.780
9. Regier DS, Oetgen M, Tanpaiboon P. Mucopolysaccharidosis type IVA. 2013 Jul 11 [updated 2021 Jun 17]. In: Adam MP, Ardinger HH, Pagon RA, et al., ed. GeneReviews [Internet]. Seattle (WA): University of Washington, Seattle; 1993–2022.
10. Martinez-Ferro M, Bellia-Munzon G, Schewitz IA, Toselli L. Pectus carinatum: when less is more. *Afr J Thorac Crit Care Med*. 2019;25(3):10.7196/AJTCCM.2019.v25i3.019. doi: 10.7196/AJTCCM.2019.v25i3.019

11. Lester C. Pigeon breast (pectus carinatum) and other protrusion deformities of the chest of developmental origin. *Ann Surg.* 137(4):482–489. doi: 10.1097/0000658-195304000-00008
12. Welch KJ, Vos A. Surgical correction of pectus carinatum (pigeon breast). *J Pediatr Surg.* 1973; 8(5):659–667. doi: 10.1016/0022-3468(73)90404-1
13. Coelho MS, Santos A, Pizarro L, et al. "Pectus excavatum/pectus carinatum": tratamento cirúrgico. *J Pneumol.* 1983;10(Suppl):47.
14. Ramadan S, Wilde J, Tabard-Fougère A, et al. Cardiopulmonary function in adolescent patients with pectus excavatum or carinatum. *BMJ Open Respir Res.* 2021;8(1):e001020. doi: 10.1136/bmjresp-2021-001020
15. Buziashvili D, Gopman JM, Weissler H, et al. An evidence-based approach to management of pectus excavatum and carinatum. *Ann Plast Surg.* 2019;82(3):352–358. doi: 10.1097/SAP.0000000000001654
16. Szafer D, Taylor JS, Pei A, et al. A simplified method for three-dimensional optical imaging and measurement of patients with chest wall deformities. *J Laparoendosc Adv Surg Tech A.* 2019;29(2):267–271. doi: 10.1089/lap.2018.0191
17. Geraedts TC, Daemen JH, Vissers YL, et al. Minimally invasive repair of pectus carinatum by the Abramson method: a systematic review. *J Pediatr Surg.* 2021;5:S0022-3468(21)00829-0. doi: 10.1016/j.jpedsurg.2021.11.028
18. Brichon PY, Wihlm JM. Correction of a severe pouter pigeon breast by triple sternal osteotomy with a novel titanium rib bridge fixation. *Ann Thorac Surg.* 2010;90(6):e97–99. doi: 10.1016/j.athoracsur.2010.08.068
19. Tarhan T, Meurer A, Tarhan O. Combined extra-/intrathoracic correction of pectus carinatum and other asymmetric chest wall deformities: A novel technique. *Oper Orthop Traumatol.* 2018;30(6):469–478. doi: 10.1007/s00064-018-0567-3
20. McHam B, Winkler L. Pectus Carinatum. 2021 Aug 9. In: StatPearls [Internet]. Treasure Island (FL): StatPearls Publishing; 2022.
21. Rea G, Sezen CB. Chest wall deformities. 2021 Aug 11. In: StatPearls [Internet]. Treasure Island (FL): StatPearls Publishing; 2022.
22. Ramadan S, Wilde J, Tabard-Fougère A, et al. Cardiopulmonary function in adolescent patients with pectus excavatum or carinatum. *BMJ.* 2021;8(1):e001020. doi: 10.1136/bmjresp-2021-001020

СПИСОК ЛИТЕРАТУРЫ

1. Shamberger R.C., Welch K.J. Surgical correction of pectus carinatum // *J Pediatr Surg.* 1987. Vol. 22, N 1. P. 48–53. doi: 10.1016/s0022-3468(87)80014-3
2. Muntean A., Stoica I., Saxena A.K. Pigeon chest: comparative analysis of surgical techniques in minimal access repair of pectus carinatum (MARPC) // *World J Pediatr.* 2018. Vol. 14, N 1. P. 18–25. doi: 10.1007/s12519-018-0121-2
3. Emil S. Current options for the treatment of pectus carinatum: when to brace and when to operate? // *Eur J.* 2018. Vol. 28, N 4. P. 347–354. doi: 10.1055/s-0038-1667297
4. Currarino G., Silverman F. Premature obliteration of the sternal sutures and pigeon-breast deformity // *Radiology.* 1958. Vol. 70, N 4. P. 532–540. doi: 10.1148/70.4.532
5. Fokin A., Steuerwald N., Ahrens W., Allen K. Anatomical, histologic, and genetic characteristics of congenital chest wall deformities // *Semin Thorac Cardiovasc Surg.* 2009. Vol. 21, N 1. P. 44–57. doi: 10.1053/j.semthor.2009.03.001
6. Fokin A. Pouter pigeon breast // *Chest Surg Clin N Am.* 2000. Vol. 10, N 2. P. 377–391.
7. Gabrielsen T., Ladyman G. Early closure of the sternal sutures and congenital heart disease // *Am J Roentgenol Radium Ther Nucl Med.* 1963. Vol. 89. P. 975–983.
8. Chidambaram B., Mehta A.V. Currarino-Silverman syndrome (pectus carinatum type 2 deformity) and mitral valve disease // *Chest.* 1992. Vol. 102, N 3. P. 780–782. doi: 10.1378/chest.102.3.780
9. Regier D.S., Oetgen M., Tanpaiboon P. Mucopolysaccharidosis type IVA. 2013 Jul 11 [updated 2021 Jun 17]. In: Adam M.P., Ardinger H.H., Pagon R.A., et al., ed. *GeneReviews* [Internet]. Seattle (WA): University of Washington, Seattle; 1993–2022.
10. Martinez-Ferro M., Bellia-Munzon G., Schewitz I.A., Toselli L. Pectus carinatum: when less is more // *Afr J Thorac Crit Care Med.* 2019. Vol. 25, N 3. P. 10.7196/AJTCCM.2019.v25i3.019. doi: 10.7196/AJTCCM.2019.v25i3.019
11. Lester C. Pigeon breast (pectus carinatum) and other protrusion deformities of the chest of developmental origin // *Ann Surg.* 1953. Vol. 137, N 4. P. 482–489. doi: 10.1097/0000658-195304000-00008
12. Welch K.J., Vos A. Surgical correction of pectus carinatum (pigeon breast) // *J Pediatr Surg.* 1973. Vol. 8, N 5. P. 659–667. doi: 10.1016/0022-3468(73)90404-1
13. Coelho M.S., Santos A., Pizarro L., et al. "Pectus excavatum / pectus carinatum": tratamento cirúrgico // *J Pneumol.* 1983. Vol. 10, Suppl. P. 47.
14. Ramadan S., Wilde J., Tabard-Fougère A., et al. Cardiopulmonary function in adolescent patients with pectus excavatum or carinatum // *BMJ Open Respir Res.* 2021. Vol. 8, N 1. P. e001020. doi: 10.1136/bmjresp-2021-001020
15. Buziashvili D., Gopman J.M., Weissler H., et al. An evidence-based approach to management of pectus excavatum and carinatum // *Ann Plast Surg.* 2019. Vol. 82, N 3. P. 352–358. doi: 10.1097/SAP.0000000000001654
16. Szafer D., Taylor J.S., Pei A., et al. A simplified method for three-dimensional optical imaging and measurement of patients with chest wall deformities // *J Laparoendosc Adv Surg Tech A.* 2019. Vol. 29, N 2. P. 267–271. doi: 10.1089/lap.2018.0191
17. Geraedts T.C., Daemen J.H., Vissers Y.L., et al. Minimally invasive repair of pectus carinatum by the Abramson method: a systematic review // *J Pediatr Surg.* 2021. Vol. 5. P. S0022-3468(21)00829-0. doi: 10.1016/j.jpedsurg.2021.11.028
18. Brichon P.Y., Wihlm J.M. Correction of a severe pouter pigeon breast by triple sternal osteotomy with a novel titanium rib bridge fixation // *Ann Thorac Surg.* 2010. Vol. 90, N 6. P. e97–99. doi: 10.1016/j.athoracsur.2010.08.068
19. Tarhan T., Meurer A., Tarhan O. Combined extra-/intrathoracic correction of pectus carinatum and other asymmetric chest wall deformities: a novel technique // *Oper Orthop Traumatol.* 2018. Vol. 30, N 6. P. 469–478. doi: 10.1007/s00064-018-0567-3
20. McHam B., Winkler L. Pectus Carinatum. 2021. In: StatPearls [Internet]. Treasure Island (FL): StatPearls Publishing; 2022.
21. Rea G., Sezen C.B. Chest wall deformities. 2021 Aug 11. In: StatPearls [Internet]. Treasure Island (FL): StatPearls Publishing; 2022.
22. Ramadan S., Wilde J., Tabard-Fougère A., et al. Cardiopulmonary function in adolescent patients with pectus excavatum or carinatum // *BMJ.* 2021. Vol. 8, N 1. P. e001020. doi: 10.1136/bmjresp-2021-001020

AUTHORS' INFO

*** Giuseppe Guglielmi**, MD, Professor;
address: Viale L. Pinto 1, 71121 Foggia, Italy;
ORCID: <http://orcid.org/0000-0002-4325-8330>;
e-mail: giuseppe.guglielmi@unifg.it

Domenico Mannatrizio, MD;
ORCID: <http://orcid.org/0000-0003-3365-7132>;
e-mail: dr.mannatrizio@gmail.com

Giacomo Fascia, MD;
ORCID: <http://orcid.org/0000-0001-5244-5093>;
e-mail: giacomo.fascia@unifg.it

ОБ АВТОРАХ

*** Guglielmi Giuseppe**, MD, Professor;
адрес: Viale L. Pinto 1, 71121, Фоджа, Италия;
ORCID: <http://orcid.org/0000-0002-4325-8330>;
e-mail: giuseppe.guglielmi@unifg.it

Mannatrizio Domenico, MD;
ORCID: <http://orcid.org/0000-0003-3365-7132>;
e-mail: dr.mannatrizio@gmail.com

Fascia Giacomo, MD;
ORCID: <http://orcid.org/0000-0001-5244-5093>;
e-mail: giacomo.fascia@unifg.it

* Corresponding author / Автор, ответственный за переписку

DOI: <https://doi.org/10.17816/DD106050>

Уролимфатические фистулы, выявленные по данным компьютерной томографии на фоне почечной колики

П.Б. Гележе^{1, 2}, К.М. Горячева³¹ Научно-практический клинический центр диагностики и телемедицинских технологий, Москва, Российская Федерация² Европейский медицинский центр, Москва, Российская Федерация³ Первый Московский государственный медицинский университет имени И.М. Сеченова (Сеченовский Университет), Москва, Российская Федерация

АННОТАЦИЯ

В работе представлены два клинических наблюдения уролимфатических фистул, диагностированных методом компьютерной томографии. В обоих случаях пациенты поступили в клинику с симптоматикой почечной колики. Уролимфатические фистулы являются редким состоянием, обусловленным формированием связи между мочевыделительной и лимфатической системами. Как правило, состояние вызвано обструкцией лимфатических сосудов на фоне паразитарной инвазии. Иными причинами могут быть лучевая терапия, травма забрюшинного пространства, прорастание опухоли. В эру до антибиотиков были распространены инфекционные процессы, такие как ксантогранулематозный пиелонефрит и туберкулёз почек.

Представляем клинические случаи уролимфатических фистул, сформированных на фоне уролитиаза.

В представленных клинических случаях моча напрямую поступала в лимфатические сосуды через уролимфатический свищ, обнаруженный на компьютерных томограммах с контрастным усилением. Уролимфатические фистулы, вызванные нарушением оттока мочи из-за блока мочевыводящих путей, выявляются редко по причине того, что диагностическим методом выбора при почечной колике является ультразвуковое исследование брюшной полости. В подавляющем большинстве случаев уролимфатические фистулы лечатся консервативно и не требуют оперативного вмешательства. Как правило, сформированные соустья перестают существовать при успешном лечении состояния, которое вызвало свищ.

Ключевые слова: уролимфатическая фистула; уретеролитиаз; почечная колика; компьютерная томография.

Как цитировать

Гележе П.Б., Горячева К.М. Уролимфатические фистулы, выявленные по данным компьютерной томографии на фоне почечной колики // *Digital Diagnostics*. 2022. Т. 3, № 2. С. 149–155. DOI: <https://doi.org/10.17816/DD106050>

DOI: <https://doi.org/10.17816/DD106050>

Computer tomography of uro-lymphatic fistulas associated with renal colic

Pavel B. Gelezhe^{1, 2}, Kristina M. Goryacheva³

¹ Moscow Center for Diagnostics and Telemedicine, Moscow, Russian Federation

² European Medical Center, Moscow, Russian Federation

³ The First Sechenov Moscow State Medical University (Sechenov University), Moscow, Russian Federation

ABSTRACT

This article presents two clinical observations of uro-lymphatic fistulas diagnosed by computed tomography. In both cases, the patients were admitted with symptoms of renal colic. Uro-lymphatic fistulas are a rare condition caused by the formation of a connection between the urinary and lymphatic systems, which is caused by, as a rule, lymphatic vessel obstruction due to parasitic infestation. Other causes may be radiation therapy, retroperitoneal trauma, and tumor sprouting. In the era before antibiotics, infectious processes such as xanthogranulomatous pyelonephritis and renal tuberculosis were common. Cases of uro-lymphatic fistulas formed against urolithiasis background are presented below. In the clinical cases presented, urine directly entered the lymphatic vessels through a uro-lymphatic fistula detected on contrast-enhanced computed tomography. Uro-lymphatic fistulas caused by impaired urine outflow due to blocked urinary tract are rarely detected since abdominal ultrasound is the diagnostic method of choice in renal colic. In the vast majority of cases, uro-lymphatic fistulas are treated conservatively and do not require surgical intervention. As a rule, the formed fistulas cease to exist when its root cause is successfully treated.

Keywords: uro-lymphatic fistula; ureterolithiasis; renal colic; computed tomography.

To cite this article

Gelezhe PB, Goryacheva KM. Computer tomography of uro-lymphatic fistulas associated with renal colic. *Digital Diagnostics*. 2022;3(2):149–155.

DOI: <https://doi.org/10.17816/DD106050>

Received: 07.04.2022

Accepted: 26.05.2022

Published: 05.06.2022

DOI: <https://doi.org/10.17816/DD106050>

以肾绞痛为背景的计算机断层扫描显示的泌尿淋巴瘘管

Pavel B. Gelezhe^{1,2}, Kristina M. Goryacheva³

¹ Moscow Center for Diagnostics and Telemedicine, Moscow, Russian Federation

² European Medical Center, Moscow, Russian Federation

³ The First Sechenov Moscow State Medical University (Sechenov University), Moscow, Russian Federation

简评

本文介绍了计算机断层扫描诊断的泌尿淋巴瘘的两个临床观察结果。在这两个病例中，患者都因肾绞痛症状入院。泌尿淋巴瘘是一种罕见的疾病，是由于泌尿系统和淋巴系统之间形成了连接。这种情况通常是由淋巴管在寄生虫害的背景下阻塞引起的。其他原因可能包括放射治疗、腹膜后间隙创伤、肿瘤萌发。在出现抗生素之前，黄色肉芽肿性肾盂肾炎和肾结核等感染过程很常见。

我们介绍了在尿石病背景下形成的泌尿淋巴瘘的临床病例。

在所提出的临床病例中，尿液通过泌尿淋巴瘘直接进入淋巴管，这是在对比增强计算机断层扫描中检测到的。由于尿路堵塞导致尿液异常流出而引起的泌尿淋巴瘘，很少被发现，这是因为超声检查是肾绞痛的首选诊断方法。在绝大多数情况下，泌尿淋巴瘘是保守治疗的，不需要手术干预。通常情况下，当引起瘘管的疾病被成功治疗后，已形成的吻合将不再出现。

关键词：尿淋巴瘘；输尿管结石；肾绞痛；CT扫描。

To cite this article

Gelezhe PB, Goryacheva KM. 以肾绞痛为背景的计算机断层扫描显示的泌尿淋巴瘘管. *Digital Diagnostics*. 2022;3(2):149–155.

DOI: <https://doi.org/10.17816/DD106050>

收到: 07.04.2022

接受: 26.05.2022

发布日期: 05.06.2022

BACKGROUND

An abnormal connection between the urinary system and lymphatic vessels is known as urolymphatic fistula (ULF), which is a rare disorder. In most cases, such fistulas are clinically associated with chyluria [1]. ULF is usually caused by parasitic infections of the kidneys or lymphatic system, including filariasis, echinococcosis, cysticercosis, ascariasis, malaria, and renal tuberculosis [2, 3]. The ULF, however, is rarely associated with renal colic. Only isolated cases are reported in world literature [3].

We present two cases of ULF associated with renal colic.

CLINICAL CASES

Clinical case No. 1

At approximately 3 am, a 65-yr-old male patient woke up with a dull, aching pain in his left iliac region [visual analogue scale (VAS) score: 3–4]. The pain intensity remained the constant both at rest and on movement. The antispasmodic the patient took had no effect. To relieve the condition, he came to the clinic.

Clinical examination revealed a stable and closer to satisfactory condition. There were no respiratory or hemodynamic disorders. The respiration rate was 18/min. The pulse was 74/min. The abdomen was unswollen, soft, and sensitive in the left iliac region. There were no peritoneal signs were observed. Auscultation of bowel sounds was done. Flatus was passing. There is no dysuria. The right

costovertebral angle tenderness was positive. There were no abnormalities in urinalysis. Blood tests revealed leukocytosis with left shift.

The left renal colic was suggested in the emergency room. The patient was referred for an intravenous contrast-enhanced computed tomography (CT) of the abdomen and kidneys to confirm that diagnosis and exclude a sigmoid diverticulitis.

At 15 min, the CT revealed a small peripelvic contrast extravasation (urinoma) (during the delayed phase). In addition, the retrograde contrast enhancement of lymphatic vessels was observed along the left renal vein during the excretory phase. These signs are typical for ULF. The examination showed the calculus at the left ureteric orifice, left ureteropyelocalicoectasia, left peripelvic urinoma, and right renal calculus (Figure 1).

The left ureteric calculus had urodynamic effects on the left upper urinary tract resulting in high risk of purulent-septic complications, so the left contact lithotripsy was initiated.

Surgery Report Summary. Ureteroscope No. 7 was freely passed through the urethra into the bladder. The ureteric orifices were slit-shaped and typically located. A large black calculus protruded from the left ureteric orifice into the bladder. For safety, a core wire was guided to the left ureteric orifice. The calculus was also moved into the ureter. The ureteroscope was inserted into the left ureter. Laser lithotripsy was performed. Calculus fragments were removed. Over the previously inserted wire, stenting catheter

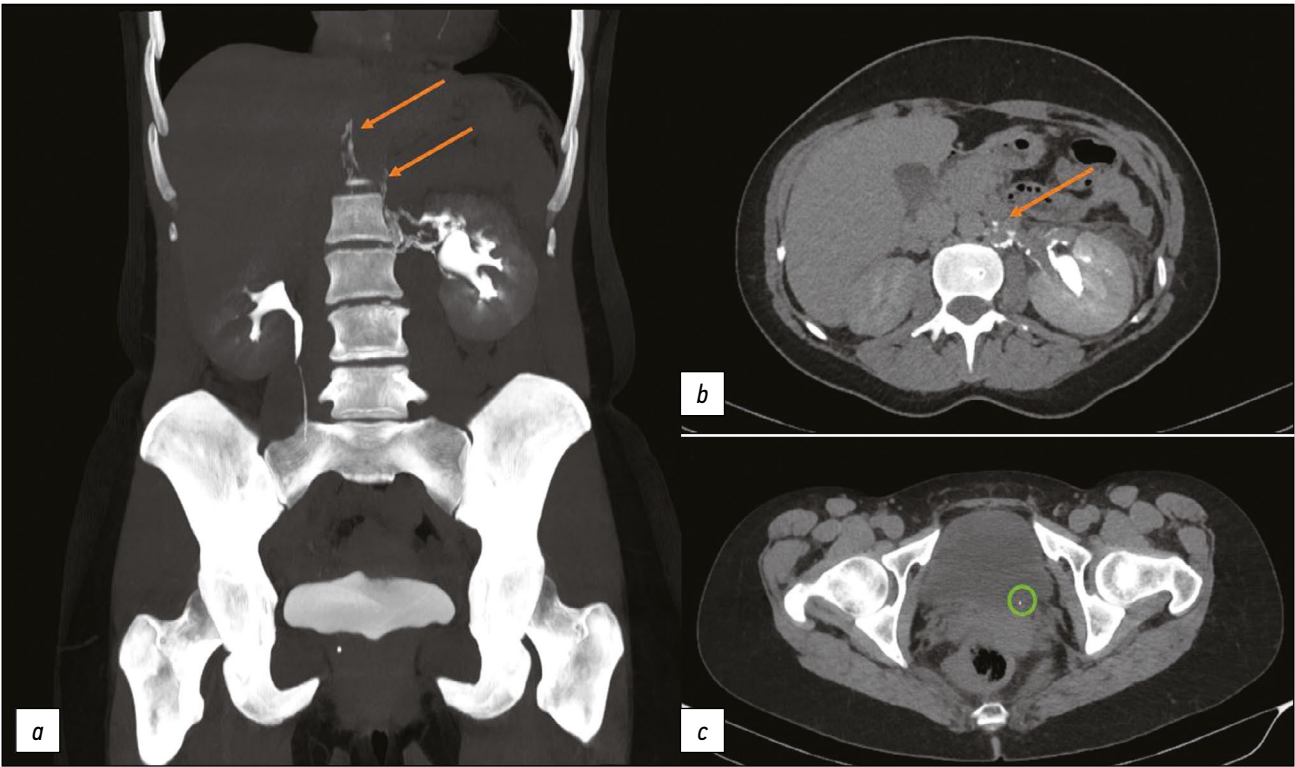


Fig. 1. Computed tomography of the abdomen with intravenous contrast enhancement. The excretory phase: (a, b) Orange arrows show the contrast spreading along lymphatic vessels; (c) A green circle highlights a calculus at the left ureteric orifice.

No. 6 was guided from the left side, having the proximal end folded in the pelvis and the distal one in the bladder.

The patient was discharged the next day for further outpatient treatment and follow-up.

Clinical case No. 2

The previous, a 38-yr-old female patient complained gradually increasing lumbar pain (VAS score: up to 3). Clinical examination revealed that the general condition was relatively satisfactory. The abdomen was soft and painless. There were no peritoneal signs observed. The right costovertebral angle tenderness was positive. Complete blood count was normal. The left renal colic was suspected in the emergency room. To confirm the diagnosis, a contrast-enhanced CT of the abdomen and pelvis was recommended.

The CT showed a contrast extravasation in the left kidney lymphatic ductus up to the thoracic lymphatic duct (typical for ULF). A calculus at the left ureteric orifice with ureteropyelocaliectasis and signs of urinary tract obstruction, as well as a calculus at left middle calix, were found during the examination (Figure 2).

The patient refused hospitalization and was referred to a third-party hospital for further treatment.

DISCUSSION

Fistulas of the urinary system can communicate with the intestines, skin, blood and lymphatic vessels, and thoracic cavity (pleura, bronchi) [3]. Urinary fistulas can

be divided into two: those that communicate with renal collecting tubules via the renal parenchyma and those that communicate directly with the renal pelvis. The relatively abundant lymphatic vessels of the renal pelvis eventually communicates with the retroperitoneal lymphatic system via the peripelvic system [4, 5].

In developed countries, most cases of fistulas involving the kidney are caused by iatrogenic trauma, such as percutaneous nephrostomy or nephrolithotomy guidewire insertion, extracorporeal shock wave lithotripsy, and abdominal surgery. Other causes include radiation therapy, penetrating trauma, and neoplastic invasion. Chronic infections commonly associated with calculi formation (xanthogranulomatous pyelonephritis) and tuberculosis have become less common causes due to development of next generation antibiotics [3].

In our clinical cases, urine directly entered the lymphatic vessels through the ULF detected by contrast-enhanced CT. Following the obstruction of the urinary system, the ULF developed (Figure 3). The reported cases are relatively unique because most ULFs are caused by obstruction of lymphatic vessels. The ULF is often followed by chyluria caused by lymphatic fluid penetration into the urinary system [1]. In our cases, no chyluria was detected, possibly as a result of the directed urine flow from the urinary system to lymphatic vessels in the setting of increased pressure in the urinary system [6].

Since most cases of renal colic are diagnosed using abdominal radiography and ultrasound, urolithiasis-related

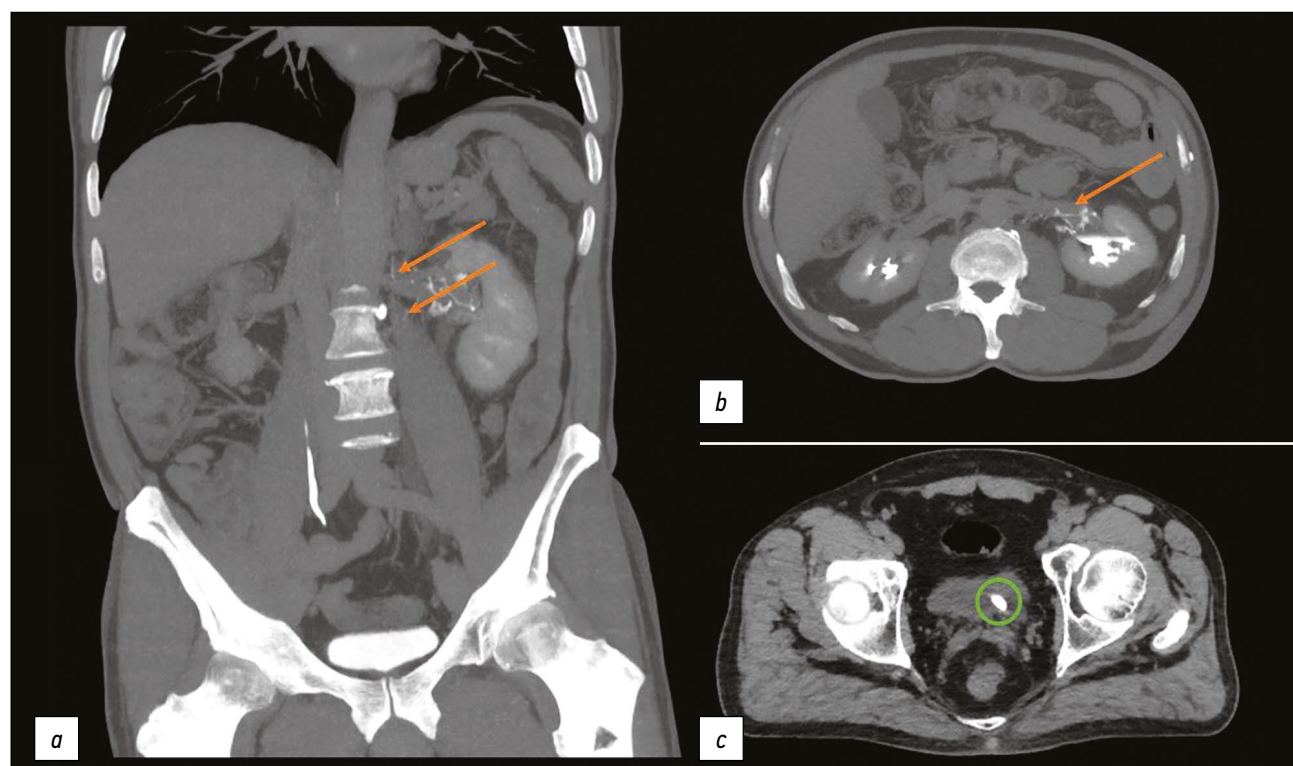


Fig. 2. Computed tomography of the abdomen with intravenous contrast enhancement. The excretory phase: (a, b) Orange arrows show the contrast spread along lymphatic vessels; (c) A green circle highlights a calculus at the left ureteric orifice.

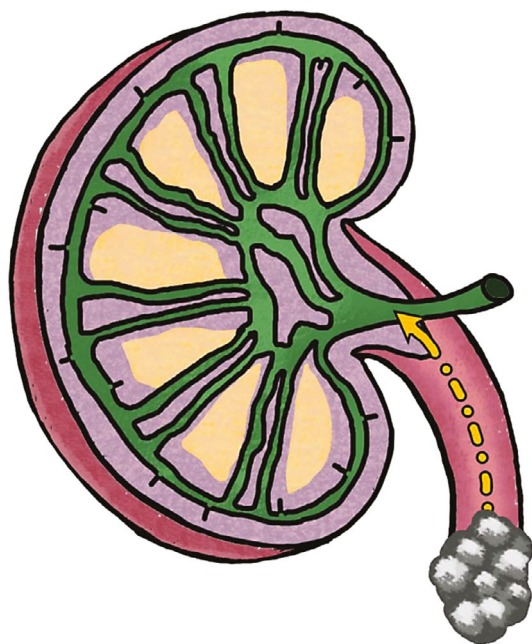


Fig. 3. A schematic shows the mechanism of urolymphatic fistula formation associated with impaired urine outflow due to the ureteral calculus (yellow arrow).

ULFs are rarely detected [3, 7]. The excretory phase CT is advised if the urinary and lymphatic systems are still connected after the ureteral obstruction. In other causes of the lymphatic system occlusion, it is possible to perform lymphography[8].

In most cases, ULFs are treated conservatively [8, 9]. Fistulas usually close after the treatment of the underlying condition.

The reported cases have some limitations. The fistulas described could theoretically exist before the current attack of renal colic. The first patient did not have a CT scan of the urinary system after the treatment, so we do not know whether the fistula persisted after lithotripsy and ureteral stenting.

CONCLUSION

As a result, these ULFs were detected as a part of examination due to renal colic attacks and were confirmed by contrast-enhanced CT. Despite the direct urine penetration into lymphatic vessels, no significant clinical changes were observed.

Further research is required to determine clinical consequences of this disorder.

ADDITIONAL INFORMATION

Funding source. This study was not supported by any external sources of funding.

Competing interests. The authors declare that they have no competing interests.

Authors' contribution. All authors made a substantial contribution to the conception of the work, acquisition, analysis, interpretation of data for the work, drafting and revising the work, final approval of the version to be published and agree to be accountable for all aspects of the work. P.B. Gelezhe — selection and analysis of literary data, writing the text of the article, illustrations creating; K.M. Goryacheva — illustrations creating.

REFERENCES

1. Stainer V, Jones P, Juliebo SO, et al. Chyluria: what does the clinician need to know? *Ther Adv Urol*. 2020;(12):1756287220940899. doi: 10.1177/1756287220940899
2. Roffi F, Eiss D, Petit F, et al. Pyelolymphatic fistula in a patient with lymphatic filariasis: a case report. (In French). *J Radiol*. 2007;88(12):1896–1898. doi: 10.1016/s0221-0363(07)78369-5
3. Yu NC, Raman SS, Patel M, et al. Fistulas of the genitourinary tract: a radiologic review. *Radiographics*. 2004;24(5):1331–1352. doi: 10.1148/rg.245035219
4. McIntosh GH, Morris B. The lymphatics of the kidney and the formation of renal lymph. *J Physiology*. 1971;214(3):365–376. doi: 10.1113/jphysiol.1971.sp009438
5. Skandalakis JE, Skandalakis LJ, Skandalakis PN. Anatomy of the Lymphatics. *Surg Oncol Clin N Am*. 2007;16(1):1–16. doi: 10.1016/j.soc.2006.10.006
6. Diamond E, Schapira HE. Chyluria — a review of the literature. *Urology*. 1985;26(5):427–431. doi: 10.1016/0090-4295(85)90147-5
7. Rajaonarison N, Ahmad A, Cucchi JM, et al. Reversible uro-lymphatic fistula. *Clin Imaging*. 2012;36(1):72–74. doi: 10.1016/j.clinimag.2011.04.012
8. Graziani G, Cucchiari D, Verdesca S, et al. Chyluria associated with nephrotic-range proteinuria: pathophysiology, clinical picture and therapeutic options. *Nephron Clinical Practice*. 2011;119(3):248–253. doi: 10.1159/000329154
9. Kim RJ, Joudi FN. Chyluria after partial nephrectomy: case report and review of the literature. *Sci World J*. 2009;(9):1–4. doi: 10.1100/tsw.2009.5

СПИСОК ЛИТЕРАТУРЫ

1. Stainer V., Jones P., Juliebo S.O., et al. Chyluria: what does the clinician need to know? // *Ther Adv Urol*. 2020. N 12. P. 1756287220940899. doi: 10.1177/1756287220940899
2. Roffi F., Eiss D., Petit F., et al. [Pyelolymphatic fistula in a patient with lymphatic filariasis: a case report. (In French)] // *J Radiol*. 2007. Vol. 88, N 12. P. 1896–1898. doi: 10.1016/s0221-0363(07)78369-5

3. Yu N.C., Raman S.S., Patel M., et al. Fistulas of the genitourinary tract: a radiologic review // Radiographics. 2004. Vol. 24, N 5. P. 1331–1352. doi: 10.1148/rg.245035219
4. McIntosh G.H., Morris B. The lymphatics of the kidney and the formation of renal lymph // J Physiology. 1971. Vol. 214, N 3. P. 365–376. doi: 10.1113/jphysiol.1971.sp009438
5. Skandalakis J.E., Skandalakis L.J., Skandalakis P.N. Anatomy of the Lymphatics // Surg Oncol Clin N Am. 2007. Vol. 16, N 1. P. 1–16. doi: 10.1016/j.soc.2006.10.006
6. Diamond E., Schapira H.E. Chyluria — a review of the literature // Urology. 1985. Vol. 26, N 5. P. 427–431. doi: 10.1016/0090-4295(85)90147-5
7. Rajaonarison N., Ahmad A., Cucchi J.M., et al. Reversible uro-lymphatic fistula // Clin Imaging. 2012. Vol. 36, N 1. P. 72–74. doi: 10.1016/j.clinimag.2011.04.012
8. Graziani G., Cucchiari D., Verdesca S., et al. Chyluria associated with nephrotic-range proteinuria: pathophysiology, clinical picture and therapeutic options // Nephron Clinical Practice. 2011. Vol. 119, N 3. P. 248–253. doi: 10.1159/000329154
9. Kim R.J., Joudi F.N. Chyluria after partial nephrectomy: case report and review of the literature // Sci World J. 2009. N 9. P. 1–4. doi: 10.1100/tsw.2009.5

AUTHORS' INFO

*** Pavel B. Gelezhe**, MD, Cand. Sci. (Med.);
address: 24-1 Petrovka street, 127051 Moscow, Russia;
ORCID: <https://orcid.org/0000-0003-1072-2202>;
eLibrary SPIN: 4841-3234; e-mail: gelezhe.pavel@gmail.com

Kristina M. Goryacheva;
ORCID: <http://orcid.org/0000-0003-1221-9694>;
eLibrary SPIN: 2722-6891; e-mail: cristina.imago27@yandex.ru

ОБ АВТОРАХ

*** Гележе Павел Борисович**, к.м.н.;
адрес: Россия, 127051, Москва, ул. Петровка, д. 24, стр. 1;
ORCID: <https://orcid.org/0000-0003-1072-2202>;
eLibrary SPIN: 4841-3234; e-mail: gelezhe.pavel@gmail.com

Горячева Кристина Михайловна;
ORCID: <http://orcid.org/0000-0003-1221-9694>;
eLibrary SPIN: 2722-6891; e-mail: cristina.imago27@yandex.ru

* Corresponding author / Автор, ответственный за переписку

DOI: <https://doi.org/10.17816/DD107983>

Об особенностях этической экспертизы в исследованиях с применением технологий и систем искусственного интеллекта на базе Государственного бюджетного учреждения здравоохранения города Москвы «Научно-практический клинический центр диагностики и телемедицинских технологий Департамента здравоохранения города Москвы» (ГБУЗ НПКЦ ДиТ ДЗМ)

О.И. Пчелинцева, О.В. Омелянская

Научно-практический клинический центр диагностики и телемедицинских технологий, Москва, Российская Федерация

АННОТАЦИЯ

Вопросы этики медицинских испытаний поднимались многократно. Этическое сопровождение исследований с участием человека в качестве субъекта исследований законодательно закреплено и требует особого внимания.

Особое место этические вопросы занимают при проведении клинических исследований лекарственных средств, где невозможно заранее и точно спрогнозировать эффективность и безопасность нового препарата на живой организм. В настоящее время при проведении экспертизы клинических исследований внимание уделяется качеству жизни пациентов, вопросам соблюдения прав пациентов, а также соблюдению правил надлежащей клинической практики и действующего законодательства. Благодаря техническому развитию увеличивается количество исследований не только лекарственных средств, но и медицинских изделий, использующих в том числе специализированные медицинские технологии и программное обеспечение.

Автоматизация, развитие, совершенствование, структуризация задействованных процессов обуславливают применение всё более технических устройств, использующих в своей работе не только программы, но и системы. Особое место в развитии медицинской науки занимает программное обеспечение с использованием систем искусственного интеллекта.

Искусственный интеллект, который ещё лет 50–80 назад был областью научной фантастики, сейчас прочно вошёл в нашу обычную жизнь. Внедряя возможности искусственного интеллекта в медицинское программное обеспечение, применяя его в составе медицинского оборудования, разрабатывая медицинские изделия с системами искусственного интеллекта, получаем продукт, требующий тщательного изучения и дальнейшего развития, которое включает в себя комплекс работ по проведению научных исследований, регистрации и поддержанию подобных систем и комплексов. Все работы регулируются законодательством в сфере обращения медицинских изделий и требуют глубокого системного и научного подхода, в том числе с привлечением этики для контроля соблюдения прав и безопасности не только участников исследования, но и их медицинских данных.

Этический комитет является независимым органом, контролирующим соблюдение прав и требований законодательства, проводящим этическую и научную экспертизу документации исследований. Этические вопросы при планировании любых исследований с участием человека или его данных должны подробно обсуждаться и рассматриваться. Следует обращаться в этические комитеты не только на этапе одобрения материалов исследования, но и при планировании дизайна, разработке документации исследования и материалов для пациентов, а также регулярно на всех этапах проведения исследования.

Ключевые слова: искусственный интеллект; клинические исследования; этика; надлежащая исследовательская практика.

Как цитировать

Пчелинцева О.И., Омелянская О.В. Об особенностях этической экспертизы в исследованиях с применением технологий и систем искусственного интеллекта на базе Государственного бюджетного учреждения здравоохранения города Москвы «Научно-практический клинический центр диагностики и телемедицинских технологий Департамента здравоохранения города Москвы» (ГБУЗ НПКЦ ДиТ ДЗМ) // *Digital Diagnostics*. 2022. Т. 3, № 2. С. 156–161. DOI: <https://doi.org/10.17816/DD107983>

Рукопись получена: 17.05.2022

Рукопись одобрена: 06.06.2022

Опубликована: 15.06.2022

DOI: <https://doi.org/10.17816/DD107983>

Features of conducting ethical review of research on artificial intelligence systems on the basis of the research and practical clinical center for diagnostics and telemedicine technologies of the Moscow Health Care Department, Moscow, Russian Federation

Olga I. Pchelintseva, Olga V. Omelyanskaya

Research and Practical Clinical Center for Diagnostics and Telemedicine Technologies, Moscow, Russian Federation

ABSTRACT

The ethics of medical tests have been raised many times. Ethical support of research involving a human subject is legally fixed and requires special attention.

Ethical issues occupy a special place when conducting clinical trials of medicines, where it is impossible to predict in advance and accurately the effectiveness and safety of a new drug on the human body. Currently, during clinical trial examination, attention is paid to patients' quality of life, and issues of compliance with patients' rights, as well as compliance with the rules of good clinical practice and current legislation. Thanks to technological development, the number medical studies and devices using, among other things, specialized medical technologies and software is increasing.

Automation, development, improvement, and structuring of the processes involved cause an increase in the use of technical devices that use not only programs but also systems in their work. Artificial intelligence system software have a special place in medical science development.

Artificial intelligence, which was the field of science fiction 50–80 years ago, is now firmly embedded in our everyday life. By introducing artificial intelligence's capabilities into medical software, using it as part of medical equipment, and developing medical devices with artificial intelligence systems, we get a product that requires careful study and further development, which includes a complex of works on conducting scientific research, and registration and maintenance of such systems and complexes. All work is regulated by legislation in the field of circulation of medical devices and requires a deep systematic and scientific approach, including involving ethics to monitor compliance with the rights and safety of study participants and their medical data.

The Ethics Committee is an independent body that monitors compliance with the rights and requirements of legislation and conducts ethical and scientific examination of research documentation. Ethical issues when planning any research involving a person or his/her data should be discussed and considered in detail. The ethics committees should be contacted not only at the stage of approving research materials, but also when planning the design and developing research documentation and materials for patients, as well as regularly at all stages of the study.

Keywords: artificial intelligence; clinical trials; ethics; good research practice.

To cite this article

Pchelintseva OI, Omelyanskaya OV. Features of conducting ethical review of research on artificial intelligence systems on the basis of the research and practical clinical center for diagnostics and telemedicine technologies of the Moscow Health Care Department, Moscow, Russian Federation. *Digital Diagnostics*. 2022;3(2):156–161. DOI: <https://doi.org/10.17816/DD107983>

Received: 17.05.2022

Accepted: 06.06.2022

Published: 15.06.2022

DOI: <https://doi.org/10.17816/DD107983>

关于基于莫斯科市国家预算医疗保健机构“莫斯科市卫生管理局诊断和远程医疗技术科学与实践临床中心”应用人工智能技术和系统的研究中的伦理鉴定的特征

Olga I. Pchelintseva, Olga V. Omelyanskaya

Research and Practical Clinical Center for Diagnostics and Telemedicine Technologies, Moscow, Russian Federation

简评

关于医学试验的伦理问题已被多次提出。对涉及人作为研究对象的研究的伦理支持是立法规定的，且需要特别注意。

伦理问题在药物的临床试验中特别重要，因为不可能事先准确地预测一种新药对活体的疗效和安全性。目前，临床试验鉴定的重点在于患者的生活质量、患者的权利问题，以及对适当临床实践规则和现行法律的遵守。技术的发展不仅导致了对药品研究的增加，也导致了对医疗设备研究的增加，包括使用专门的医疗技术和软件。

相关流程的自动化、开发、改进和结构化导致了越来越多的技术设备的应用，这些设备在工作中使用系统，而不仅仅是软件。在医学科学的发展中，应用人工智能系统的软件占据了一个特殊的位置。

人工智能在50-80年前还是科幻小说的范畴，现在已经牢牢地融入了我们的日常生活。通过将人工智能的能力引入医疗软件，将其作为医疗设备的一部分，开发带有人工智能系统的医疗产品，我们得到了一个需要仔细研究和进一步开发的产品，其中包括对此类系统和综合体的科学研究、注册和维护等一系列工作。所有这些工作都受医疗器械流通领域的立法监管，需要深入的系统和科学态度，其中包括伦理，以监测不仅是研究参与者的权利和安全，也包括其医疗数据。

伦理委员会是一个独立的机构，负责监督对法律权利和要求的遵守情况，对研究文件进行伦理和科学鉴定。在计划任何涉及个人或其数据的研究时，应详细讨论和考虑伦理问题。伦理委员会不仅应在研究材料的批准阶段联系，而且在研究设计的规划、研究文件和患者材料的制定以及研究的所有阶段都要定期与伦理委员会接触。

关键词：人工智能；临床研究；伦理；适当的研究实践。

To cite this article

Pchelintseva OI, Omelyanskaya OV. 关于基于莫斯科市国家预算医疗保健机构“莫斯科市卫生管理局诊断和远程医疗技术科学与实践临床中心”应用人工智能技术和系统的研究中的伦理鉴定的特征. *Digital Diagnostics*. 2022;3(2):156-161.

DOI: <https://doi.org/10.17816/DD107983>

收到: 17.05.2022

接受: 06.06.2022

发布日期: 15.06.2022

SCIENTIFIC STUDIES: GOALS, STAGES, AND MARKETING AUTHORIZATION

An ethical review is mandatory for all scientific studies involving human subjects or their health-related data. The objective of the ethical review is to protect rights and confidentiality of study subjects while ensuring compliance that all legal requirements are met.

Not only drug products are subject to *in vitro* and *in vivo* research. Studies with medical devices are also increasingly involving human subjects or their health information.

Toxicological tests, technical tests, and other stages of research are mandated by law before medical devices can be registered. But what about software?

The software shall undergo evaluation by certain types of studies that the regulator (Federal Service for Supervision in Healthcare of Russia) uses to decide whether to approve or refuse a marketing authorization. A regulatory dossier includes a Clinical Study Report. Clinical trials of medical devices are performed mainly in special healthcare institutions and involve patients as study subjects. As we all recall, human research participation is possible only if there are document for the planned study, which is considered by the Ethics Council with granting permission for conducting the study based on council's approval.

THE SIGNIFICANT ROLE OF ETHICS COMMITTEES AS IN THE CASE STUDY OF THE INDEPENDENT ETHICS COMMITTEE OF THE MOSCOW ORGANIZATION OF THE RUSSIAN SOCIETY OF ROENTGENOLOGISTS AND RADIOLOGISTS

A local (independent) ethical committee (IEC) of a study site reviews all materials when obtaining the study permission. Studies are typically prospective in design, and ethical committees play the significant role in conducting such studies. Based on the study results, the IEC may refuse to approve the study. For example, if there are patient safety risks, based on interim safety reports, the national ethics committee has the right to suspend the study in the site.

Studies using artificial intelligence (AI) systems are included in separate dossier block. For most AI-based studies, it is acceptable to use a retrospective design with existing databases.

Ethical issues are not clearly regulated in AI-based studies, but ethical committees are usually aware of planned retrospective studies. Although this approach does not violate any applicable laws and regulations, it involves some risks that are better to be minimized. When dealing with a patient database, it is necessary to anticipate risks of data leak and

personal patient identification, as well as to obtain sufficient high-quality data for further analysis.

In Russia, not all ethical committees review AI-based studies. However, in 2019, the Scientific and Practical Clinical Center for Diagnostics and Telemedicine Technologies of the Moscow Health Care Department (SPCCDTT) hosted an independent ethics committee of the Moscow Regional Branch of the Russian Society of Roentgenologists and Radiologists (RSRR MRB IEC) with the primary goal to implement good research practices for AI-based studies.

The RSRR MRB IEC has reviewed 45 studies; 60% of them were initially did not receive approval due to design errors. In just 3 yr, we managed to reduce the number of refusals to 10% using an individual approach to each application and standardizing documents and processes consistently and systematically.

Each IEC expert has more than 5 yr of research experience and has received training in good clinical practice. We evaluate study designs, including those that are retrospective, paying close attention to data security issues, data use, and possible risks, the process of obtaining data, and their storage and processing.

Due to the rapid scientific progress and wide opportunities for AI system application, the deeper approaches should be used when planning such studies for ethical analysis and assessment of potential risks. In SPCCDTT, all studies are initially (at the planning stage) considered by an IEC, regardless their design. Information on study progress is submitted at least once a year. The study is supervised by the Principal Investigator, who is also considered by the IEC.

In addition to reviewing studies, the ethics committee is responsible for peer review of scientific work of SPCCDTT members. For each paper, the IEC prepared a review and a list of recommendations, assisting authors in avoiding errors before submitting the manuscripts for publication. Therefore, the IEC is an additional scientific supervisory body, which helps authors to improve the quality of their publications for top-rated journals.

The world's leading scientific journal do not consider manuscripts without the approval of the ethical committee. The modern scientific world places high priority on protecting patient rights, data security, confidentiality, and legitimacy of materials submitted for publication. Not only researchers are responsible for data accuracy, but also ethical committees that approve studies and review manuscripts.

The RSRR MRB IEC experts thoroughly check all documents provided by applicants. Our researchers request that we review and approve their studies. We carefully analyze documents, including at least a study plan, informed consents of patients, and curriculum vitae of the principal investigator. To avoid possible errors when conducting the study and interpreting results, we check each document and, together with the applicant, adjust the work plan.

In most documents submitted, we note the lack of the randomization process description or the lack of

randomization step in controlled trials, as well as the small size of population and incorrect patient selection criteria. Special attention is paid to an informed consent because its content directly affects the rate of enrollment.

Our help is requested by graduate students and candidates for degrees. A potential thesis is comprehensively analyzed. We take into account the study's abstract, scientific content, originality, and practical relevance. We check if the research plan reflects study goals and methods. We analyze patient data, its storage and transfer, its confidentiality, and the protecting rights of study subjects.

When reviewing documents for AI-based studies, we carefully check reference data sources, processing algorithms, and ways of health information storage and transfer. We also consider potential risks for patients and study integrity in case of partial or complete loss of data.

CONCLUSION

In addition to the comprehensive analysis of documents submitted, the ethics committee give advice on improving manuscripts for their subsequent publication in top-rated journals.

AUTHORS' INFO

* **Olga I. Pchelintseva**, Cand. Sci. (Biol.);
address: Petrovka st. 24 bld 1, Moscow, 127051, Russia;
ORCID: <https://orcid.org/0000-0002-6442-1360>;
eLibrary SPIN: 2528-5803; e-mail: ethics@npcmr.ru

Olga V. Omelyanskaya;
ORCID: <https://orcid.org/0000-0002-0245-4431>;
eLibrary SPIN: 8948-6152; e-mail: o.omelyanskaya@npcmr.ru

The main principle of the IEC is to comply with good research practices at each stage of the study.

The IEC provides ethical support for scientific and clinical trials of drug products and medical devices.

We are open for collaboration with candidates, graduate students, researchers, and third-party applicants.

We are always ready to help in conducting high-quality clinical and scientific studies.

ADDITIONAL INFORMATION

Funding source. This study was not supported by any external sources of funding.

Competing interests. The authors declare that they have no competing interests.

Authors' contribution. All authors made a substantial contribution to the conception of the work, acquisition, analysis, interpretation of data for the work, drafting and revising the work, final approval of the version to be published and agree to be accountable for all aspects of the work.

O.I. Pchelintseva — literature review, analysis of literary sources, writing of the text of the article

O.V. Omelyanskaya — literature review, analysis of literary sources, correcting the article

ОБ АВТОРАХ

* **Пчелинцева Ольга Игоревна**, к.б.н.,
адрес: Россия, 127051, Москва, ул. Петровка, д. 24, стр. 1;
ORCID: <https://orcid.org/0000-0002-6442-1360>;
eLibrary SPIN: 2528-5803; e-mail: ethics@npcmr.ru

Омелянская Ольга Васильевна;
ORCID: <https://orcid.org/0000-0002-0245-4431>;
eLibrary SPIN: 8948-6152; e-mail: o.omelyanskaya@npcmr.ru

* Corresponding author / Автор, ответственный за переписку